ELECTRICAL COMMUNICATION

Technical Journal of the
International Telephone and Telegraph Corporation
and Associate Companies

•

Volume 27   **MARCH, 1950**   **Number 1**

ELECTRICAL COMMUNICATION

Volume 27	March, 1950	Number 1

CONTENTS

DeHavilland "Comet," the first 500-mile-an-hour jet-propelled airliner now undergoing final tests, is capable of flying 36 passengers across the Atlantic at an altitude of 40,000 feet. The very-high-frequency radiotelephone apparatus installed in this pioneer air transport is the *STR-12A* equipment built by Standard Telephones and Cables, Limited, London, England. A view of this set appears on page 6.

Remote Control of 1500-Volt Traction Supply

A SUPERVISORY remote-control system was recently installed on the Liverpool Street–Shenfield section of the British Railways. The electric trains on this section operate from power obtained by making contact with a 1500-volt direct-current overhead line. Previous traction supervisory installations in Great Britain have been limited to 600-volt systems utilizing third- or fourth-rail power circuits. (Equipment for an overhead system has, however, been supplied in India for the Bombay–Baroda Railway.)

The control station is at Chadwell Heath in a building especially constructed for it. The control desk and diagram, shown in Figure 1, are in the main control room; the associated relays, switches, and batteries are in two adjacent rooms.

Considerable attention has been given to the appearance and operational aspects of the control

Figure 1—Control room at Chadwell Heath. The mimic diagram is just back of the curved control desk.

equipment. Keys and indicators are arranged conveniently to the operator and colour schemes and lighting are pleasing, all of which aid in reducing fatigue and in maintaining the vigilance of the operator.

For supervisory signalling, the remote stations are connected to the control station by multi-conductor cables. There are eight party networks, four to stations east and four to those west of the control room. Each network serves up to six stations and consists of two pairs of conductors, one being a spare. Two metering pilots, each using one pair of wires, serve all stations to the east, and two similar channels serve all stations to the west. The system now controls seven substations and four track-sectioning cabins but is capable of being expanded to handle 36 such units, the maximum number that may be required on the section.

Unlike previous systems having one set of control-station equipment for each substation, this modern common-equipment system needs

but one set of control-room apparatus regardless of the number of substations. This common equipment is switched to any controlled station at a master control panel. Although a single operator could supervise the entire system, two separate sets of common equipment are provided to permit faster operation under emergency conditions and to ensure uninterrupted control of the network even if a major fault were to occur in one of the common equipments.

The following operations may be performed from the control desk.

Check the condition of all circuit breakers.

Open and close circuit breakers supplying power to the rectifiers.

Open and close circuit breakers between rectifiers and tracks.

Open and close simultaneously four chosen track circuit breakers at any station.

Obtain two indications simultaneously of rectifier outputs in amperes or of busbar voltages either in one or in two substations.

Miscellaneous alarm indications.

Standby pilot-line switching.

Selective telephony to all parts of the network.

Since the master-control panels are used for all substations, they cannot maintain a continuous record of the circuit-breaker conditions at any one station. To provide this information a mimic diagram is mounted behind the desk in full view of both operators. It shows the main electrical system with each circuit breaker and rectifier represented by a lamp signal, the colour of which indicates its operating condition. The mimic diagram is manually dressed on information supplied by the master-control panels.

Telephone-type apparatus is used exclusively for switching. By means of constant-total signal checking, maloperation is prevented as any corrupt codes are rejected. Either the system does the right thing or nothing at all.

To facilitate maintenance and inspection, the apparatus is mounted on Post Office type jack-in panels. A faulty panel may be replaced by another in a moment and repairs made later. Figure 2 shows the apparatus normally installed at a substation.

Figure 2—Supervisory apparatus of the type installed in substations. Jack-in panels permit rapid replacement of a faulty unit with a spare known to be in operating condition.

Since the substations are connected to the control station only when being controlled by it special provision is made for them to call the control station in the event of a fault or unauthorized change in a circuit-breaker position, such as tripping on overload. An alarm bell sounds in the control room and the lamp corresponding to the calling substation is lighted. The operator switches the common equipment to that substation and presses the "check" key, whereupon the positions of all circuit breakers are reported. This operation takes only 10 or 12 seconds.

Among the important benefits of the common-equipment system is a great saving in control-room space and the ease and simplicity with which additional substations may be included in the installation. Such additions may be made without disturbing the regular operation of the existing networks.

This system was designed, manufactured, and installed by Standard Telephones and Cables, Limited, London, England.

Recent Telecommunication Development

Etchings of Faraday

THE MOST-RECENT ETCHING in the series being published by the International Telecommunications Union is of Michael Faraday.

Michael Faraday (1791–1867) first won renown for his chemical researches on the liquification of gasses and on the development of steel alloys and optical glasses. Turning to electricity, he produced rotary movement around each other of magnets and conductors carrying electric currents. He then discovered that an electric current can be induced in one circuit by an electric current flowing in another circuit. He showed also that any electric charge is related to an equivalent charge of opposite polarity and measured the difference in the specific inductive capacitance of various dielectrics.

He demonstrated that polarized light and magnetic fields were interrelated, and his work on magnetism indicated that wherever a magnetic field exists there is matter.

The Faraday portrait is the fifteenth in a series that started in 1935. Each etching is on a good grade of paper and with margins measures 9 by $6\frac{5}{8}$ inches (23 by 17 centimeters). All of the portraits are still available at 3 Swiss francs each from Secrétariat général de l'Union internationale des télécommunications, Palais Wilson, 52, rue des Pâquis, Genève, Suisse. The etchings are of Ampère, Baudot, Bell, Erlang, Faraday, Ferrié, Gauss and Weber, Hertz, Hughes, Marconi, Maxwell, Morse, Popov, Siemens, and Tesla.

Radio Equipment on the "Comet"

THE FIRST commercial airliner propelled solely by jet engines to be extensively test flown is the new "Comet," introduced at the Society of British Aircraft Constructors Exhibition at Farnsworth, England, by the DeHavilland Aircraft Company. With a cruising speed of 500 miles per hour and a service ceiling of 40,000 feet, the craft will accommodate 36 passengers.

Very-high-frequency radiotelephone equipment was installed in the Comet by Standard Telephones and Cables, Limited, of London. Their type *STR-12A* set is used and includes a crystal-controlled transmitter and receiver com-bined in a single remotely located unit operating in conjunction with a control box containing the frequency-determining circuits mounted in the pilots' compartment. Band-pass circuits enable any one of 23 carrier frequencies to be selected by a single switching operation.

The transmitter has an output power of $3\frac{1}{2}$ watts. During a recent test flight to Libya, communication was maintained with London even when the airplane was flying over the outskirts of Paris at an altitude of 35,000 feet.

Similar equipment has been fitted in a number of aircraft of British European and British Overseas Airways Corporations.
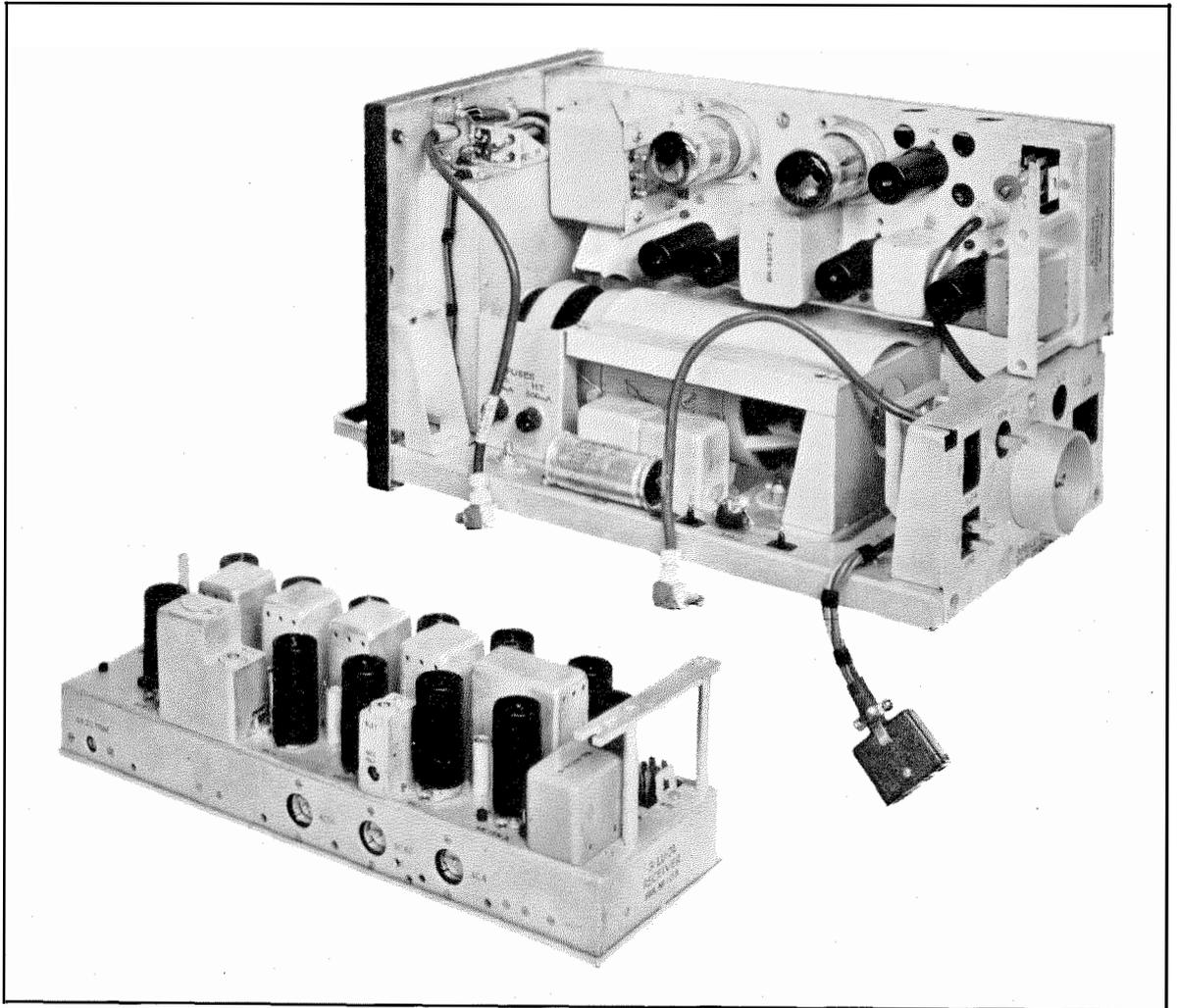
STR-12A aircraft radiotelephone equipment with outer cover removed. The receiver (at lower left) has been dismounted from the chassis for this photograph. The transmitter is mounted on its side at the top of the set and the power unit is at the bottom. Both are easily removable. The control box is not shown.

Mathematics in Engineering*

By SIDNEY FRANKEL

Federal Telecommunication Laboratories, Incorporated, Nutley, New Jersey

AS FAR AS the engineer is concerned, mathematics is merely a tool to help him organize his thinking.

When man manipulates and attempts to control physical forces in a haphazard fashion, using only trial and error to obtain a lucky, hoped-for result, the process may be called "tinkering." When he attempts to order his manipulations into a more or less logical procedure, his efforts may be termed "engineering." The dividing line between tinkering and engineering is rarely sharp and distinct. On the one hand, it is virtually impossible for anyone but an idiot or an infant to manipulate physical things without doing some reasoning about it. On the other hand, important discoveries are sometimes accidentally made by random tinkering during the course of an engineering investigation. But, in general, we can say that manipulation of physical things can be called engineering only when the major portion of the effort involved is carried on in a logical planned manner, and where the amount of careful reasoning involved is restricted only by the law of diminishing returns.

The latter statement implies that a fair ability at reasoning is involved. The amount of useful thinking that a well-trained engineer can apply to a specific technical problem is far greater than the amount of reasoning that could be applied usefully by, say, a shepherd.

Granting, then, that a certain amount of reasoning is economically desirable in engineering work, we are faced with the problem of determining the quantity and quality of reasoning that will yield a maximum economic return in any given situation.

It is clear, of course, that this statement implies that there is at least a partial alternative to reasoning that at some point becomes more economical than reasoning itself. This alternative is, of course, experimentation.

The meaning of the term "quantity of reasoning" is fairly clear. It specifies how much reasoning shall be done.

The term "quality of reasoning" requires some discussion. It seems to imply that reasoning need not be precise to be acceptable. This, indeed, is one of the implications and its meaning will be explained shortly. But the term "quality" implies not only degree of precision, but degree of elaboration as well.

There are various kinds of situations in which it is fairly obvious that precise reasoning is unjustified, i.e., where there is no justification in attempting to predict exactly what will happen under certain circumstances. Broadly they may be classed as follows:

A. Situations where it doesn't matter whether or not you know exactly what is happening.

Copyright, Keuffel & Esser Co.
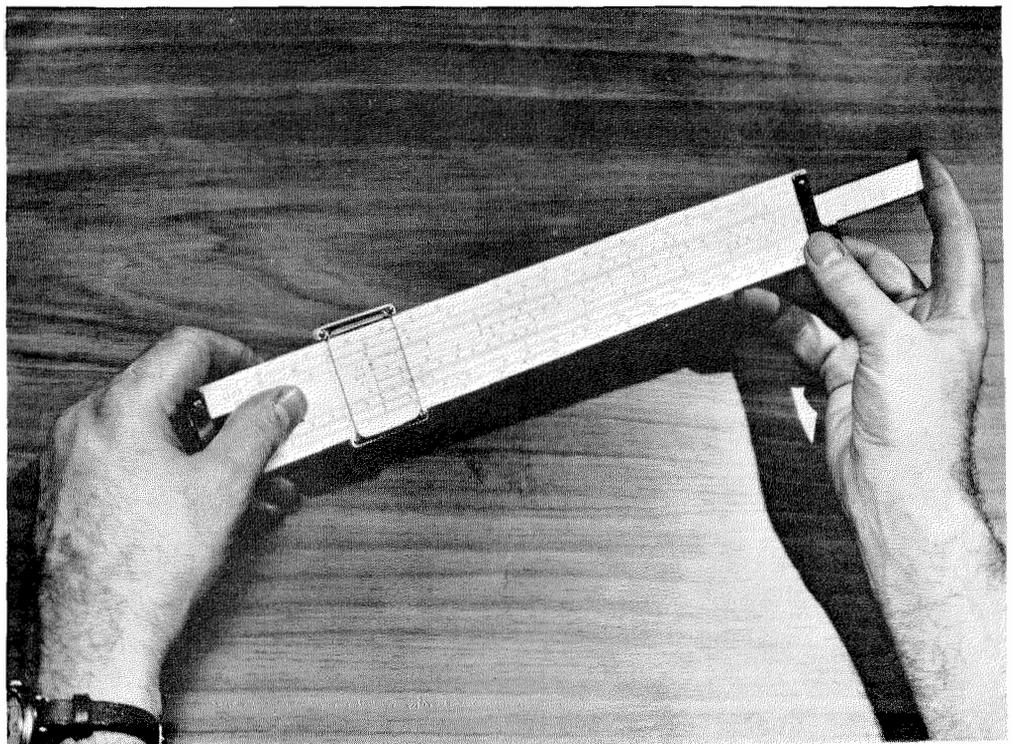
For example, in the bypass capacitor of a radio-frequency amplifier, it does not make any serious difference if the radio-frequency voltage across the capacitor is 1 percent of the plate voltage or 2 percent of the plate voltage, although these figures differ by 100 percent. As another example, as far as transmission of power is concerned, it usually doesn't matter if the characteristic impedance of a transmission line is known with an accuracy within no better than 10 percent.

In such cases, it is a waste of time to attempt to predict behavior within an accuracy of, say, 0.1 percent.

B. Situations where physical quantities are n•t known with sufficient accuracy to justify precise calculations based on them.

For example, in predicting the value of capacitance required to resonate an inductor at a specified frequency, there is no point in designing the capacitor within an error of 1 percent if the value of inductance is known only within 25 percent.

C. Situations in which the actual physical system under consideration is so complicated that quantitative reasoning about it is beyond the ability of any scientist.

In such cases, one "simplifies" the problem; i.e., one substitutes another problem that looks very much like the original problem, for which one expects for one reason or another the predicted behavior to be very much the same as the original system, and about which one can reason with some facility. For example, if the model shop prepares a hollow metallic object that is supposed to be a perfect right circular cylinder capped at the ends, but has the normal imperfections to be expected in machining, we acknowledge that it would be a waste of time to predict, exactly, the resonant frequencies of this cavity. Instead we simplify the problem by computing the resonant frequencies of the nominal cavity that the shop was supposed to try to build. We expect the actual frequencies to be pretty close to those predicted.

Sometimes, this process of substitution can be carried too far. Consider, for example, the operation of a class-C amplifier. When properly operated, the tube acts in a fashion similar to a resistive switch that opens and closes periodically. From a knowledge of the amount of drive applied to the grid of the tube, one can make a fair guess at a fixed value of resistance to be used in series with the switch, and proceed by conventional analytical means to predict the power output obtainable from such an amplifier. Thus, for the complex system of nonlinear tube characteristics associated with a resonant circuit we substitute a resonant circuit periodically shock-excited through a resistor.

This procedure might even be justified in attempting to predict the second-harmonic voltage produced across the tuned circuit. It would be completely out of line to attempt to predict the tenth harmonic, which varies strongly with the nonlinearities in the tube characteristics. An attempt to predict the tenth harmonic by this method would be a waste of time. An attempt to predict even the fifth harmonic by the more-direct attack on the tube characteristics would also be a waste of time since the tube characteristics are usually not known with the required accuracy.

The question of calculations that are too elaborate is a little more delicate. These are the calculations that obtain far more information than is needed, usually as a by-product of the process used in obtaining needed information.

To cite an extreme example, suppose we have a resonator made of a coaxial line capped at the ends. From measurements, we have determined that it resonates at a certain frequency. To be specific, let us suppose that it resonates at 500 megacycles per second. Suppose we ask, "How shall we change the dimensions of the cavity to make it resonate at 1000 megacycles?" The average engineer will tell us without hesitation to cut the length in half. The quick, almost instinctive, method of reasoning used here is the method of dimensional analysis, plus the knowledge that the resonant frequency is independent of cross-sectional shape. In external appearance, at least, it is the simplest form of reasoning that is sufficiently quantitative to be termed mathematical.

On the other hand, if the theory of resonant transmission lines were not known, one might be tempted to start with the engineering differential equations of the line, proceed to integrate them, insert boundary conditions, etc. Eventually, this process leads to the same conclusion as above, but with less economy of time, therefore money. True, additional knowledge has been gained as a

result of the analysis. Voltage and current distributions are known. Power required to maintain a given degree of excitation is an easy by-product of the calculation. But this additional information, which was of no immediate use, has had to be paid for on a project that perhaps could ill afford it.

The situation might be even worse than this. One might be tempted to start with Maxwell's equations to obtain the desired result. Here the by-products are even more extensive. One obtains a picture of electric and magnetic field distributions in minute detail. Such information can be very useful—to some other project that needs the information and can afford to pay for it.

So much for the negative side of mathematics in engineering. What are the advantages of accurate analysis that should be stressed in the solution of engineering problems?

Frequently, situations arise in which there is no question in anybody's mind that the cost of appeal to experiment is, or could readily become, prohibitive. Some of these situations are introduced in the form of terse questions below.

Possible or Impossible?

Is it possible to design a network to transform an unbalanced input voltage to a balanced output voltage for any balanced load? Can such a network be a pi network? What are the minimum number of meshes such a network must have? If two sources are to excite a common load at the same frequency without reacting on each other, what must be the minimum insertion loss of the coupling network? Can an isotropic radiator be constructed? Can mass be converted into energy? These are some of the questions that are more readily answered, at least in part, by analysis rather than experiment.

In obtaining answers to questions of this sort, one must be very careful to interpret the results correctly. The analysis will state that results are possible or impossible *within the limitations imposed at the start of the analysis*. A result that is possible (or impossible) under certain conditions may be impossible (or possible) under others. The first law of thermodynamics states that it is possible to convert heat into mechanical energy. The second law of thermodynamics states that

it is impossible to convert heat into mechanical energy without at the same time dumping heat into a cold reservoir. It is impossible to increase the bandwidth of an amplifier greatly without reducing its gain; but it is possible to increase the bandwidth without reducing the gain by adding enough amplifier stages,—provided you don't increase the bandwidth too much!

These ifs, ands, and buts of the possible and the impossible remind me of a little incident, which occurred to me when I was fresh out of college with a degree in mathematics and looking for a job. I met the chief engineer of one of our local radio stations. Like many engineers with not too much training in mathematics, he was overly impressed with the efficacy of this powerful tool in the hands of a tyro. But after a few sessions with me, in which we tried to find analytical solutions for some of his problems, he effected quite a rapid cure. Showing me to the door one day at the conclusion of an interesting, if somewhat fruitless, session he murmured with a sigh of regret, "We would make a wonderful team, I think, were it not for one thing. I'm afraid that if I worked with you for any length of time I would discover that most of the things I've been doing are impossible."

Many years later, I appreciated the importance of this remark. When a person constitutes himself as engineer and mathematician rolled into one, there is not often any serious problem of coordination of ideas between engineer and mathematician. If he asks a question and gets a negative answer, he backs up automatically to the starting point, finds what group of assumptions are leading to the negative result and, if the assumptions have been made purely for convenience (as they frequently are), he modifies them in order that his analysis may yield a more-favorable result. When, however, the functions of engineer and mathematician are separated into two highly specialized personalties, the utmost in patience and insight is frequently required on the part of both in order that they may function successfully as a team.

How?

It is not possible to ask mathematically "How shall I build a gadget to produce a certain result?" At least it is not possible to get an answer

to such a broad question. But it is sometimes surprising how vaguely a question may be stated and yet lead to analysis that yields at least one constructive result. For example, within certain limitations one is permitted to ask, "How shall I construct a linear, passive, lumped-constant two-terminal pair network to yield a specified frequency response?" and expect to obtain a whole class of solutions satisfying his requirements. One may ask "Given a certain type of message and a certain type of interference added to it, what kind of filter shall I construct in order that its output may be as nearly like the message as possible?" One may ask this question and obtain a positive answer.

This process of starting an investigation by stating a desired result and from it evolving a design configuration is called synthesis. It is a more-advanced approach than straightforward analysis and is usually invoked only when previous experience fails to indicate a good starting point for analysis, or where the amount of trial and error involved might be less economical than direct synthesis.

How Much?   How Many?   How Big?

Probably the vast majority of problems fall in this category. Through past experience or through inventiveness, we become convinced (at least temporarily) that our design should take a certain qualitative form. We know the schematic diagram of a power supply, an audio-frequency amplifier, a Wheatstone bridge, but what shall be the values of the components to yield specified voltage, hum, transients, distortion, sensitivity, etc.? By the same token that most of the effort is applied in this field, the required design formulas exist to answer most of the questions. Here, care is required to see that formulas are not employed beyond the limitations within which they were derived.

Which One?

Sometimes our inventiveness is so great that we find ourselves faced with a choice of possible solutions. As a simple example, there is an infinite number of possible combinations of inductance and capacitance that will resonate at the same frequency. When this happens one or more additional restrictions must be imposed, and some-times the restrictions are such that the solution can be found by analytical means. In production work, an additional restriction is frequently obtained by specifying that the total cost shall be a minimum. Frequently, in airborne designs, the additional restriction may be minimum weight or size. At other times, solutions must be nonmathematical, even nontechnical, and must involve such annoying considerations as ease of procurement.

Early in this paper it was indicated that the engineer is frequently faced with the problem of deciding how much analysis should be applied to a problem. The answer to this question usually involves, not merely the nature of the technical problem itself, but the nature of the analytical abilities at the disposal of the engineer, either within himself or among his associates. In general, the greater the available analytical talents, the more stress should be laid on analytical solutions.

But, —

If you are inclined to be analytical, don't be impatient with experimenters who prefer to get their answers in the laboratory. Ninety-nine times out of a hundred, they are choosing the method that will bring *them* the quickest results.

And if you are experimentally inclined, don't fall into one of two common errors. The first of these, which is more annoying but less dangerous, is to sneer at "pencil pushers." The more-dangerous not-at-all-annoying attitude reminds me of a facetious remark I heard from an engineer years ago to the effect that "nobody believes experimental data except the man who takes it, but everybody believes the results of a theoretical analysis except the man who makes it." The grain of truth in this remark stems from the awe with which theoretical work is viewed by some engineers. To get a result, analysts sometimes make assumptions that are not in accord with fact. If your intuition (born of experience) warns you that something is fishy about certain analytical conclusions, smoke the irritation out. You may be wrong or the analyst may be wrong; he may have committed a blunder or you may be unduly prejudiced by too-narrow experiences; but you have to meet each other on common ground and agree in your final conclusions.

Low-Frequency Radiotelegraph Transmitter for Arctic Use

By H. P. MILLER, Jr.

Federal Telephone and Radio Corporation, Clifton, New Jersey

DESPITE the trend toward higher and higher frequencies, there are still important uses for low-frequency radio-communication facilities. A definite advantage is that in regions of extreme magnetic storms, the lower frequencies permit reliable communication over considerable distances when high-frequency signals would fade out. Since these magnetically unstable regions are in the arctic and are characterized by low temperatures, storms, and difficult transportation problems, they impose a number of special requirements on the equipment used. For instance, the low temperatures make water cooling undesirable and transportation difficulties dictate that the equipment be made in units that are readily transportable by air.

The transmitter equipment described herein was designed to meet these requirements. Known as the *TLA* equipment, it was originally so designated by the Civil Aeronautics Administration and was used for point-to-point communication in collecting weather information throughout Alaska. Later it was used by the Royal Canadian Air Force, as the *GT-28*, to insure reliable communication between airport stations. Due to the urgency required in establishing the latter communication facilities, much of this equipment was transported by air to the points of use. These transmitters have also been used in an experimental *Consol* long-range navigational system.

1. General Description

The *TLA* and *GT-28* transmitter equipment is capable of delivering 10 kilowatts of continuous-wave power into a 70-ohm transmission line, and originally operated only on frequencies between 80 and 200 kilocycles per second. In later equipments, the frequency range was 200 to 300 kilocycles. Provisions are included for disconnecting the final amplifier stage and supplying 500 watts from the exciter unit directly to the transmission line.

The output of the transmission line is connected to an antenna system through suitable coupling and loading circuits in the antenna-tuning house. The amount of power delivered to the antenna depends on the type of antenna,
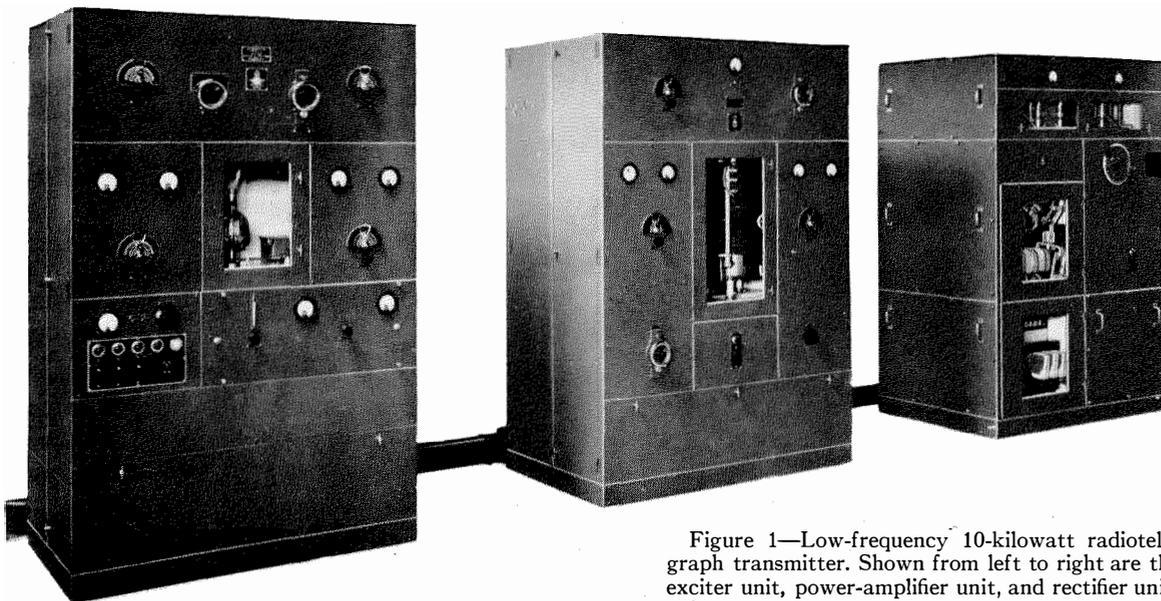
Figure 1—Low-frequency 10-kilowatt radiotelegraph transmitter. Shown from left to right are the exciter unit, power-amplifier unit, and rectifier unit.

11

operating frequency, and length of transmission line. Tuning-house efficiencies of at least 70 to 80 percent are obtainable. Harmonics in the antenna are at least 75 decibels below the level of the fundamental frequency.

Single-frequency operation with on–off keying is normally used, but special provisions can be made for modulated-continuous-wave signals at a small reduction in output power. The operating frequency of the exciter can be changed from the front of the panel by replacing a crystal and retuning.

The power amplifier is continuously adjustable over a frequency range of 1.4 to 1. For wider ranges, it is necessary to change coil taps and several mica padding capacitors in the amplifier.
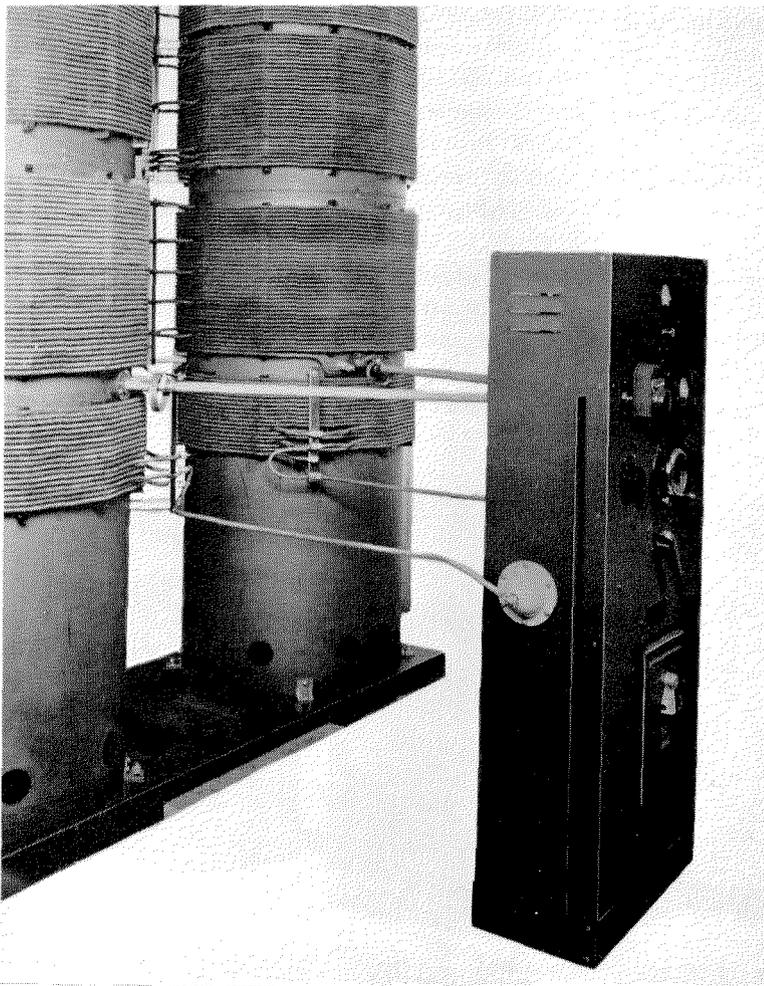
The range of adjustments possible in the antenna-tuning house depends on the antenna used. The antenna for which the equipment was designed has a capacitance ranging between 0.0025 and 0.00175 microfarad and a total resistance between 1.5 and 6 ohms. Some variations beyond these limits are permissible. In cases where the operating frequency and the antenna capacitance are both low, additional inductive loading must be used.

The transmitter proper, as shown in Figure 1, consists of an exciter, power amplifier, and high-voltage rectifier. Tuning-house equipment for operation at the lowest frequencies is shown in Figure 2. It consists of a combined coupling and tuning cabinet and two loading inductors. The upper sections of the loading inductors are removed when operating at the higher frequencies.

The manner in which the units are interconnected is shown in the block diagram of Figure 3. Power for the exciter and power amplifier is supplied through the high-voltage rectifier (not shown) from a 220-volt, 3-phase, 60-cycle line. Connections for remote keying and stop–start control are made to the exciter. Radio-frequency connection between the exciter and power amplifier is made with a 70-ohm dual-conductor shielded transmission line. Between the power amplifier and the tuning-house cabinet, a 70-ohm coaxial cable (*RG-35/U*) is used. Switching facilities are provided in the power amplifier so that the exciter can be used alone.

Power and control interconnections are made through sheet-metal ducts located above the floor in the rear of the units; these may be seen in Figure 1. The transmitter units and the antenna-tuning cabinet are of aluminum-frame

Figure 2—Antenna-tuning-house equipment. Power from the transmitter is supplied through a 70-ohm coaxial line to the cabinet at the right. The loading inductors are in the background.
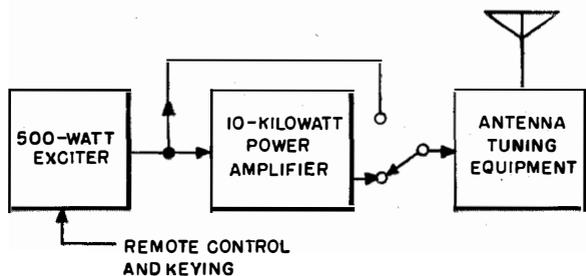
Figure 3—Components of the equipment. The antenna may be supplied directly from the exciter unit. A rectifier power supply connects to both exciter and power amplifier.

construction and have aluminum panels and shelves. Interlocked doors are provided where access to inside components is necessary during routine maintenance.

2. Exciter Unit

The low-power stages include a crystal-controlled oscillator, buffer, and intermediate power amplifier. A tube provides on–off keying by opening the cathode circuit of the buffer. These tubes are all of the *807* type, and are mounted with their associated circuits in a tray that is removable from the front of the cabinet. Two crystals with a selector switch are contained in an oven mounted on the tray. Provisions have also been made for substituting an external signal source for the crystals. Inductive interstage coupling is used for the radio-frequency circuits in the tray. The inductors used in the outputs of the oscillator and buffer are iron cored, and are tapped so that the proper inductance can be obtained for each operating band. Taps are selected by a band-change switch on the front of the tray.

The driver stage (500-watts output) is of the single-ended type using a *450TH* tube with conventional tuned grid and plate circuits. The output link is inductively coupled to the plate circuit and is series tuned. In each tuned circuit, a variometer wound with litzendraht cable is used for tuning. In addition, taps on some inductors and steps of capacitance are provided for band changing. These are simultaneously selected by five band-change switches operated by a single control on the front of the unit.

Three power supplies utilizing tube rectifiers are part of the exciter unit and include a 125-volt bias supply for all tubes except the oscillator, a

500-volt plate and screen supply for the *807* tubes in the tray, and a 3000-volt supply for the *450TH* driver stage.

The general arrangement of the equipment can be seen from the side view shown in Figure 4. The components of the output circuit appear on the top shelf. Below this is a shelf on which are mounted the *450TH* tube with its associated grid- and plate-tuning circuits. Under this shelf on the far side is the removable tray. On the same level with the tray is the 125-volt bias supply (foreground), and a fan that draws air into the unit through a filter. The other two power supplies are mounted on the base of the unit. Terminals for external connections are shown in the lower left-hand corner.
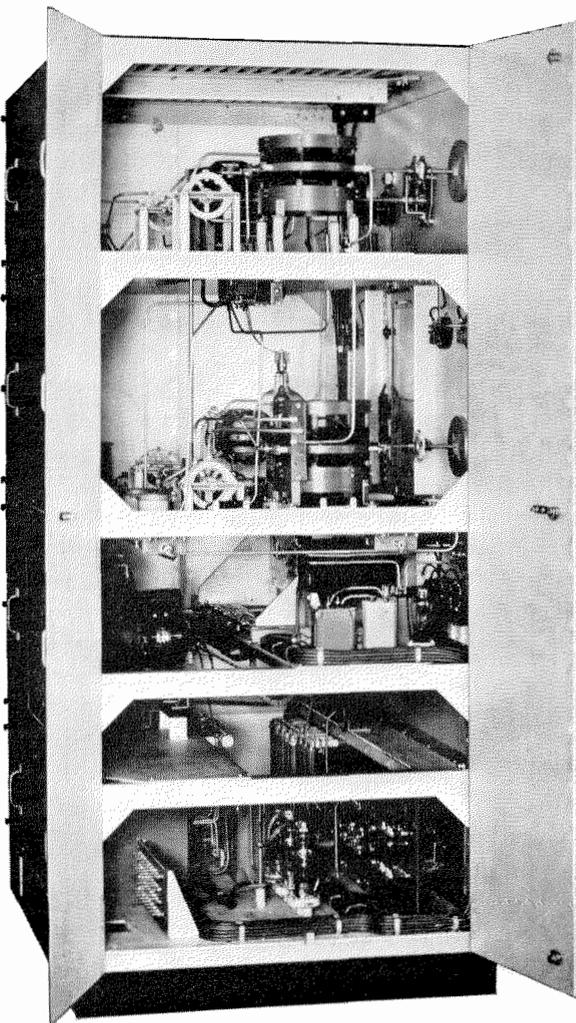
Figure 4—Exciter unit viewed through doors in the left side of the cabinet.
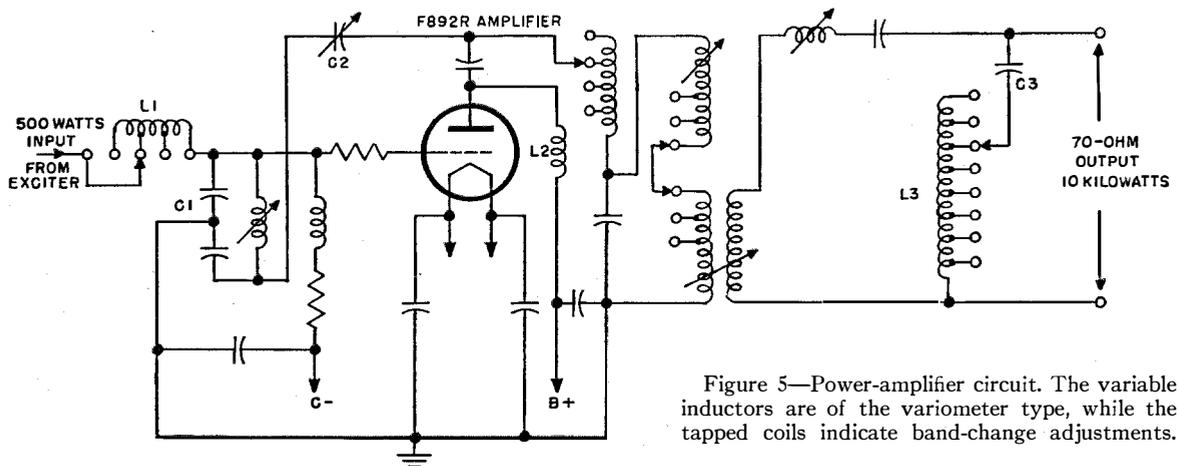
Figure 5—Power-amplifier circuit. The variable inductors are of the variometer type, while the tapped coils indicate band-change adjustments.

3. Power Amplifier

The power amplifier is also a conventional tuned-grid tuned-plate amplifier using a single *F892R* air-cooled tube. Details of the circuit are shown in Figure 5.

For the fixed tuning adjustments of the power amplifier, the frequency range of 80 to 200 kilocycles has been divided into five overlapping bands with center frequencies at 91, 107, 130, 150, and 168 kilocycles. In shifting from one band to another, inductance is varied by taps and capacitance by replacing or interchanging fixed mica capacitors.

The inductor *L3* of Figure 5 requires most frequent changing in a given band since it is part of a harmonic-suppressing circuit. This must be adjusted so that with *C3* it series-resonates at approximately the second harmonic of the operating frequency, helping to keep this frequency out of the antenna system. At the fundamental frequency, the reactance of the shunt circuit is high compared with the 70-ohm output circuit, and very little of the fundamental frequency is bypassed.

It will be seen that the grid tank circuit is roughly balanced with respect to ground, and that the end away from the grid furnishes a neutralizing voltage through the capacitor *C2*.

An interesting feature of the grid circuit is the tapped inductor *L1*. This inductor, together with a part of the capacitance of *C1*, forms an *L* network that matches the 70-ohm line from the exciter to the grid of the *F892R* tube. The taps on *L1* are selected so that when the grid circuit is tuned for maximum grid current, the line from

the exciter is terminated in an effective impedance of between 65 and 75 ohms, and the line current is low. It is possible to match the line to the grid without *L1* by the use of a capacitance voltage divider, but this results in considerable difficulty in obtaining the correct tuning adjustment: The length of the line between amplifier and exciter is such a small fraction of a wavelength that it can readily become a part of the tuned circuits, rather than act as a transmission line. Without *L1*, it is possible to tune the grid circuit to obtain either high or low current in the transmission line, and in the absence of a line ammeter it is sometimes difficult to distinguish between these two conditions. With *L1* in use, and properly tapped, there is never any question as to the correct tuning adjustment for low line current.

Another interesting feature of this unit is the parallel-feed plate choke *L2*, which may be seen in Figure 6. The problem here was to construct a choke that would carry 2 amperes of plate current, have a high effective parallel resistance between 80 and 200 kilocycles, and be as small as possible. The final design, shown in Figure 6, consisted of 10 pie windings of No. 18 single-cotton-covered enameled copper wire on a 3-inch-diameter ceramic tube 10-inches long. The number of turns in the pies varied according to the position, those in the center having fewer turns than the rest, the advantages of which arrangement have already been described.[1]

---

[1] H. P. Miller, Jr., "Multi-Band R-F Choke Coil Design," *Electronics*, v. 8, p. 254; August, 1935.

Inside of the ceramic tube, a large number of powdered-iron-dust cores $\frac{3}{8}$-inch in diameter by $\frac{9}{16}$-inch long were mounted in such a way that the inductance of each pie was increased without an appreciable increase in the coupling between pies.

The solid-line curve of Figure 7 shows the variation with frequency of the effective parallel resistance of the choke. It will be seen that between 80 and 350 kilocycles the effective parallel resistance is over 500,000 ohms. The low point at about 385 kilocycles is still high enough (120,000 ohms) to avoid excessive heating due to the third harmonic when the operating frequency is near 128 kilocycles.

As a matter of interest, the dotted curve has been added in Figure 7 to show the characteristics of the choke without the iron-dust cores. From this it is seen that the main effect of the cores is at the lower frequencies where the choke is substantially a pure inductance.

A single-phase rectifier using two *5Z3* tubes in parallel provides a fixed bias of 250 volts for the *F892R* amplifier tube.
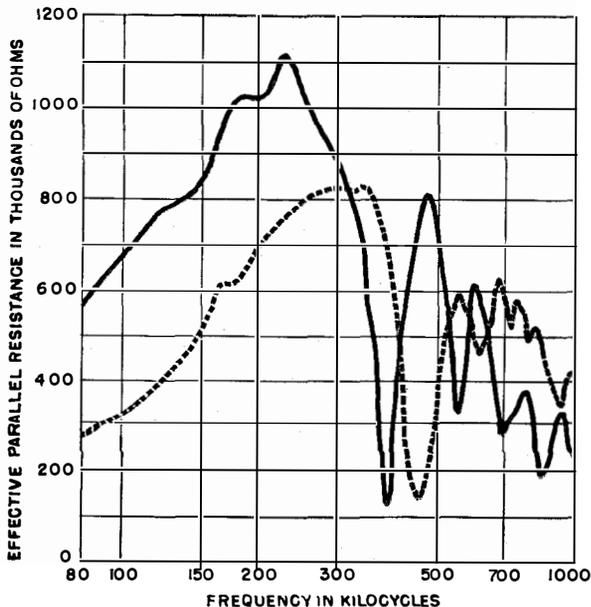
Figure 7—Parallel-resistance characteristics of shunt plate-feed inductor with (solid line) and without (dotted line) iron-dust cores.

Figure 6—Isometric cut-away view of the shunt plate-feed inductor for the power amplifier. Iron-dust cores are placed to increase inductance of individual pies without increasing coupling between pies.

Each access door in the power-amplifier unit is provided with an interlock to disconnect the high-voltage bus when the door is open. The removable panels in the rear are not interlocked, but two red lights inside the top of the unit serve as a warning when it is operated for testing with the panels removed.

The general arrangement of the power-amplifier cabinet can be seen from the rear view, Figure 8. The input and grid circuits are in the middle compartment on the right, the *F892R* tube is in the center, and the plate-circuit inductor is on the left. The neutralizing capacitor, with two variable plates that are

operated like the pages of a book, is at the bottom right, while the output circuit is at the top right. A blower for the power tube and a fan for compartment cooling draw air from the rear of the unit through dust filters that are not shown.

4. High-Voltage Rectifier Unit

High-voltage plate supply for the power-amplifier tube is furnished at 9400 volts by a 3-phase full-wave rectifier using six *872A* mercury-vapor tubes.

Adjustment of the output voltage from 65 to 105 percent of rated voltage is obtained by means of a manually operated 7-position tap switch in the primary circuit of the plate transformer. It is also possible to reduce the voltage by remote control to obtain half-power operation. Control circuits are arranged so that the rectifier is always started on the half-power primary tap and is automatically shifted to the higher voltage after a delay of a few seconds.

The output of the rectifier is smoothed by a single-section choke-input filter. A 500-ohm resistor is connected in series with the filter capacitor to limit the current through the rectifier tubes when starting. The ripple measured in the output of the rectifier is less than 1 percent.

The general arrangement of the components in the high-voltage-rectifier unit can be seen from the rear view of the cabinet shown in Figure 9. The plate transformer occupies most of the lower part of the frame with the bleeder resistors directly above it. In front of the resistors and protected from their heat by metallic shields are the filament transformers and filter choke. The rectifier tubes, which are not visible in the figure, are accessible through a door on the front of the unit. Directly beneath the tubes are two strip heaters for warming the mercury-vapor tubes when the ambient temperature is low. For shipment, the plate transformer can be removed through the rear of the unit. In case the transformer is to be shipped by air, the noninflammable oil in it can be removed and the case filled with a dry inert gas under pressure.

5. Antenna-Tuning House

The antenna-tuning equipment is intended for use in a building located close to the ground end
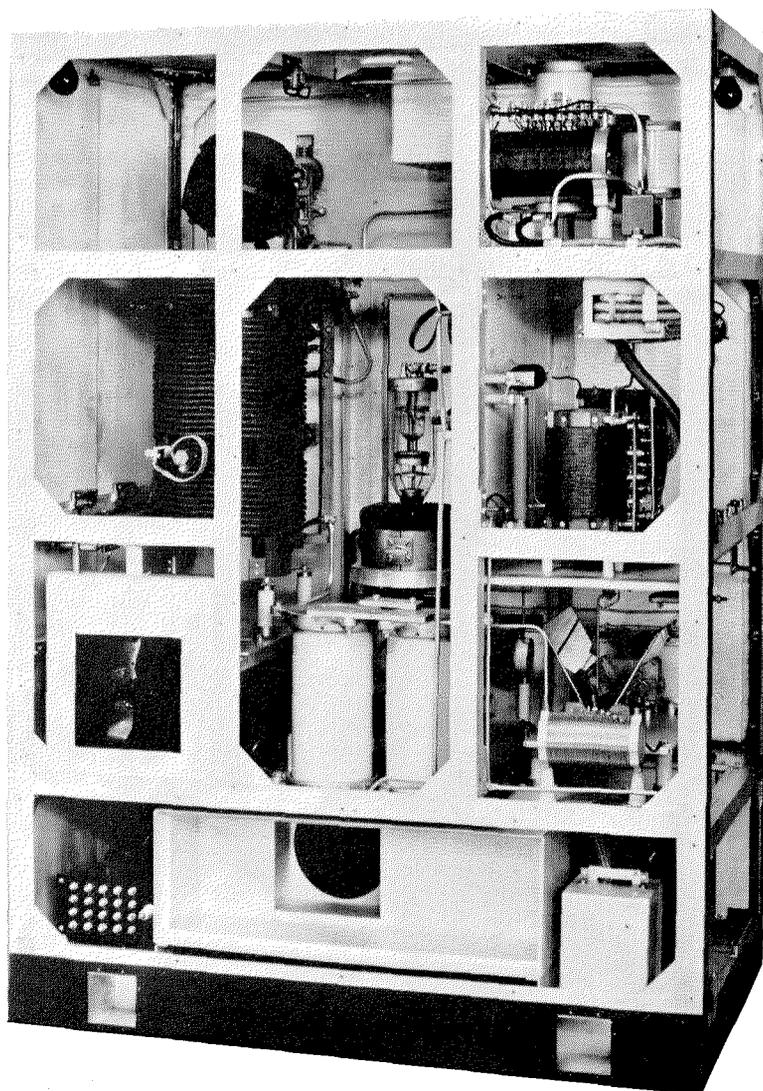
Figure 8—Rear view of power-amplifier unit. The back panels have been removed for this photograph.

of the antenna down-lead. The circuit arrangement is shown in Figure 10.

Fundamentally, the 70-ohm transmission line from the amplifier is terminated in a capacitance C, across which is the tuned antenna circuit. This capacitance can be varied in steps by a series of switches until the line is properly terminated. Since the normal procedure in tuning an antenna circuit is for maximum antenna current, the resultant line termination is slightly capacitive. This capacitive reactance is balanced out by a small tapped inductor $L1$ inserted in series with the line.

It will be noted from Figure 10 that the coupling capacitance C is connected in series with only one ($L2$) of the two antenna-tuning inductors. Since the inductance of $L2$ is the same as that of $L3$, the currents in the two inductors will be practically the same. The effective resistance of the circuit to the right of C will, therefore, be four times the resistance of the antenna circuit. The reactance of C is small compared to the reactance of $L2$, and when combined with the circuit to the right, provides the proper termination for the 70-ohm transmission line.

The circuit used for antenna tuning was the result of a number of practical considerations. Under certain operating conditions, the current at the base of the antenna down-lead will be 80 amperes and the antenna voltage as high as 90 kilovolts root-mean-square. This requires large inductors with widely spread electric fields. Since the inductors are housed in a special heat-insulated building, special care must be taken to minimize the amount of building space required. This was accomplished through the use of two inductors connected effectively in parallel, and
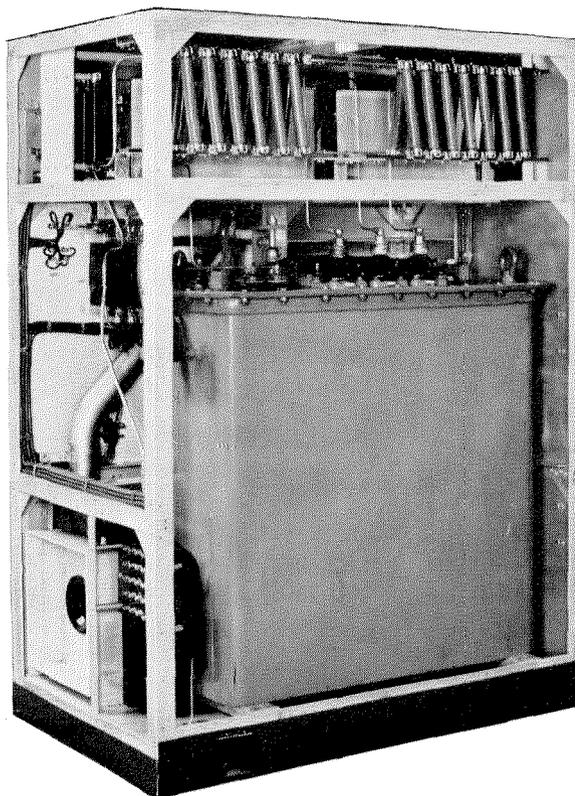
Figure 9—Rear view of high-voltage-rectifier unit.

wound in opposite directions. By placing the two inductors close together, as shown in Figure 2, the aiding fields resulting from the opposed windings were kept as high as possible, and the fields extending out toward the building walls were minimized. This, together with a Faraday shield and protective features incorporated in the building plans, which are described below, permit the use of a frame building 14 feet square with an average ceiling height of about 10 feet.
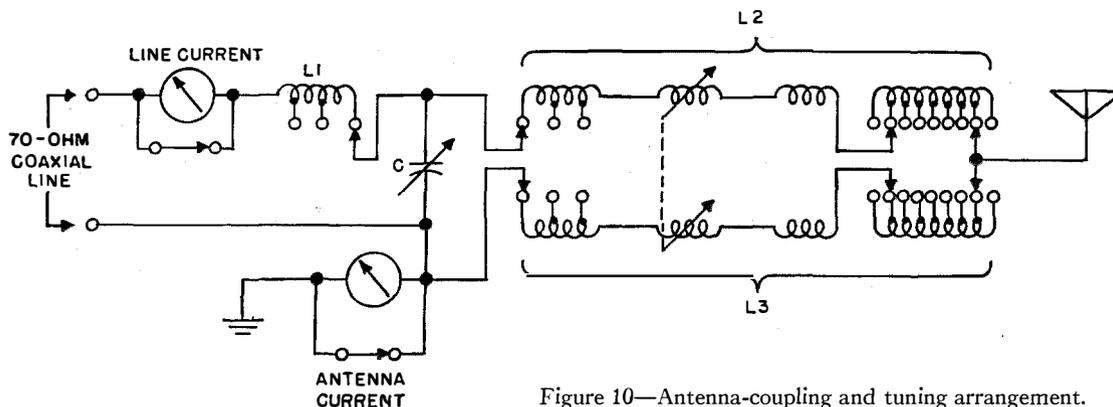
Figure 10—Antenna-coupling and tuning arrangement.
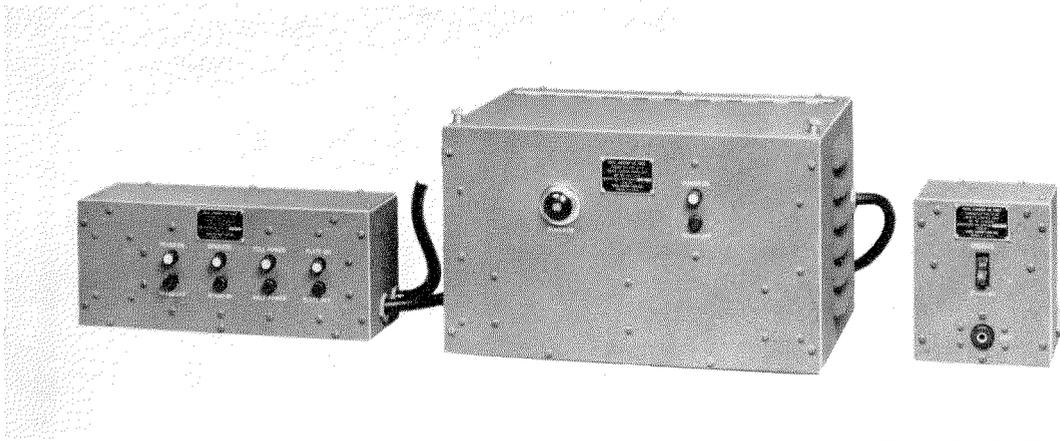
Figure 11—Remote-control units. At the left is the transmitter-control box. Center and right—a selenium-rectifier unit and a control unit for high-speed remote keying.

As shown in Figure 2, the inductor windings are of litzendraht cable and are supported on ribs of glass-bonded mica attached to bakelite tubes 29 inches in diameter. The lower inductor, containing a variometer, has a height of over 5 feet. The upper inductor, which is used only when additional loading is needed, is over 3-feet high. The over-all assembled height including the wooden base is 8 feet, 7 inches. Bakelite screws and pins are used for fastening the inductors together, and where metallic bolts and nuts must be used on terminal strips, they are made of copper or Everdur.

The rotor in each of the lower inductors is connected by a bakelite rod to the tuning-house control unit. A small handwheel on the front of this cabinet permits simultaneous rotation.

One of the economic results of using two inductors was that it reduced the size of the litzendraht cable and permitted using the same cable for the tuned plate circuit in the power amplifier. With a maximum antenna current of 80 amperes, the current through each antenna inductor will be about 40 amperes. This is slightly less than the maximum current in the plate circuit. The Q of these inductors is about 1500.

Since the antenna-tuning house is usually in an isolated location and unattended, it is not always practicable to keep it at normal room temperature during cold weather. The procedure that has been followed is to use a heat-insulated house and to install electrically operated room heaters of sufficient size to keep the temperature from going too low. For this purpose, a thermostat with contactors for turning the heaters on and off is mounted in the cabinet. The temperature maintained in the building depends on the outside temperature and may be as low as 0 degrees centigrade.

The type of antenna lead-in insulation used in the house depends on the antenna characteristics and the voltages that may be expected. For low-capacitance low-resistance antennas, where the antenna potentials may reach 90 kilovolts root-mean-square, a plate-glass window 3-feet square has been used. In the center of the glass, a pair of steatite bowl insulators are placed to support the feed-through conductor. Such a window requires a protective hood on the outside of the building to minimize flashovers in stormy weather. The window frame and the inside of the hood are covered with thin sheet copper to cut down losses in the building and to prevent fires that might be caused by concentrated electric fields. This copper sheet is grounded by connection to a Faraday shield covering the inside of the building. For cases where the antenna capacitance and resistance are both high, with resulting low antenna potentials, suitable porcelain entrance insulators are obtainable.

The Faraday shield consists of a network of wires supported on the inside walls and arranged so that there are no short-circuited turns. A 10-gauge tinned-copper wire is fastened to the side walls 12 inches off the floor, and securely connected to the antenna-grounding system. Vertical 14-gauge enameled wires spaced 12 inches apart are soldered to the 10-gauge wire and

tacked to the walls for a height of 5 feet. Above this level, they are supported on insulated screw eyes. On the front and back walls, the vertical wires are terminated at the ceiling, but on the side walls they are extended almost to the center of the ceiling. It was found that the potentials build up on the ends of the ceiling wires where they came close together above the inductors are sufficient to require the use of corona shields. As an additional protection, the use of iron and steel nails and bolts in the assembly of the building was avoided above the floor level. Either copper or brass was used in their place, in order to minimize heating due to the strong magnetic fields.

6. Control Facilities

Either local or remote control can be selected by means of a switch on the front of the exciter unit. In the local position, individual switches are used for starting to facilitate tuning and checking the operation of the equipment. In the remote position, starting is sequential and circuits are interlocked to insure correct starting. Functions that may be remotely controlled are:

Start–stop
Operate–standby
Power-amplifier plate voltage, on–off
Full power–half power

Two-wire controls, with a common return, are provided for each of these functions. If the control point is at some distance from the transmitter, it is preferable to use telephone-dial-controlled relays that are mounted adjacent to the transmitter equipment. With the control point close to the transmitter, a small control unit, similar to that shown at the left of Figure 11 can be used. In this unit, a push-button switch is provided for each of the above functions.

7. Keying Facilities

Control of keying can also be either local or remote. On local control, a hand key mounted on the exciter unit may be used for testing and local keying. On remote control an external source of 100 volts is used to change the bias on the keyer tube. Speeds up to 200 words per minute are readily obtained under these conditions. The 100 volts needed for this purpose can be obtained from a selenium rectifier in a unit similar to the center unit in Figure 11. The right-hand unit in this photograph is used at a remote-keying position. It contains an operate–standby switch and a key jack.
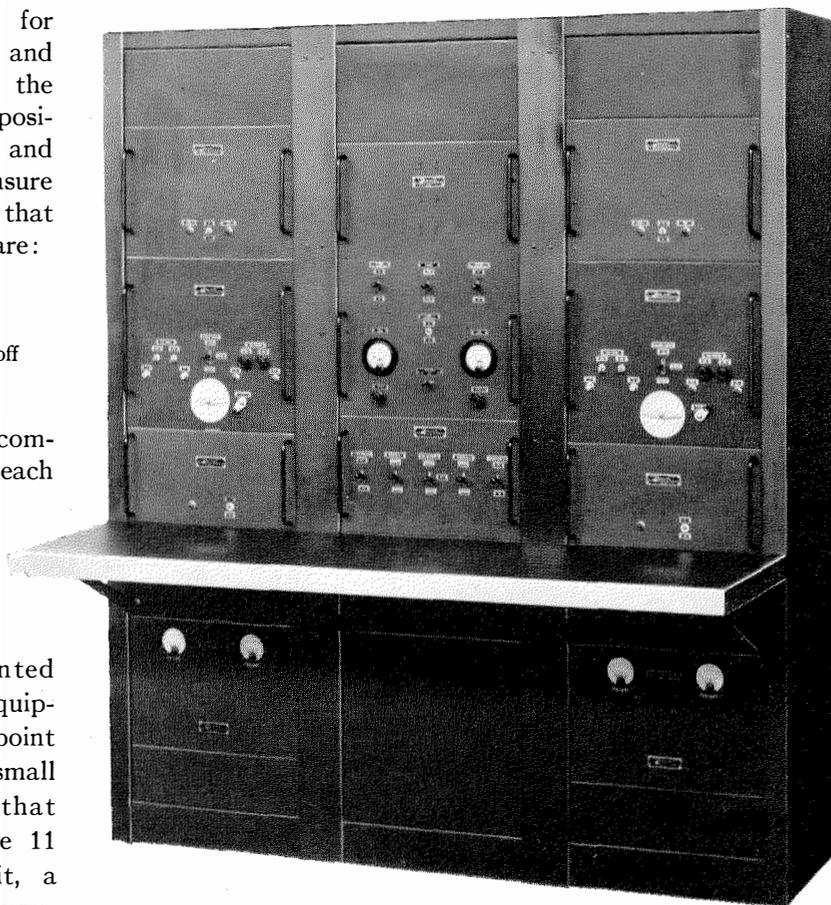
Figure 12—Master-oscillator and phasing unit with remote-control equipment for two transmitters. Used with the experimental *Consol* long-range radio-navigational system developed for the U. S. Air Force.

8. Remote Frequency Control

As indicated above, provisions have been made in some transmitters for remote frequency control. These transmitters are used in an experimental *Consol* long-range navigational system with the control rack shown in Figure 12. This rack combines centralized controls for duplicate transmitters as well as duplicate master oscillators. The latter are the second units above the operating shelf in the two outside bays. The signal from the oscillator in use is at times keyed and at other times shifted in phase in accordance with the requirements of the navigational system.

9. Transportation by Airplane

A number of these transmitters have been delivered to their stations in the far north by air. By removing the high-voltage transformer from the rectifier unit and by temporarily removing the oil, it is possible to keep the shipping weight of any one unit under 1900 pounds.

Improved Equipment Practice Reduces Size of Telephone Transmission Systems

By F. FAIRLEY, R. J. M. ANDREWS, and A. C. DELAMARE

Standard Telephones and Cables, Limited, London, England

IT IS NOW 26 YEARS since telephone wire transmission equipment was first mounted on 19-inch panels. Although some advance in design occurred in 1932,[1,2] it was not so radical a change as has been brought about by the new practice to be described. This change can be compared only with that which took place in 1923 when the old framework construction for repeater equipment gave place to the 19-inch steel panel.

1. History

The rapid increase in long-distance telephone facilities, which took place in the early thirties, created a critical situation in the demand for building space. This situation became more acute when, after 1935, a trend to cable-carrier operation for long-distance circuits began. The new development tended to simplify and reduce the size of external plant, but to increase the volume of equipment installed at the terminals and main switching centres.

A review of the then-existing practice was therefore begun to discover means of reducing the volume of equipment without sacrificing performance. Another aspect of the problem was to provide a more-fully standardised type of construction that would permit an increase in the quantity manufactured in existing plants. Yet another facet was the general awakening to the need for improvements in the aesthetic appeal of industrial designs.

The outbreak of the second World War in 1939 interrupted the work, but in retrospect it can be seen now that this suspension was completely effective only for the first year. At the outbreak of war, carrier operation of military lines had only just been introduced. The equipment supplied closely followed the design of civil-type equipment, but was mounted on short racks. The experience of the first year of operations showed that these were too heavy and radical

Two 9-foot bay-sides in the new practice installed in the Salisbury repeater station of the British Post Office. In the background are the corresponding 10½-foot bays in the older practice.

[1] J. A. H. Lloyd, W. N. Roseway, V. J. Terry, and A. W. Montgomery, "New Voice Frequency Telegraph System," *Electrical Communication*, v. 10, pp. 184–199; April, 1932.

[2] J. S. Lyall, "New Standard Repeater Equipment," *Electrical Communication*, v. 11, pp. 66–73; October, 1932.
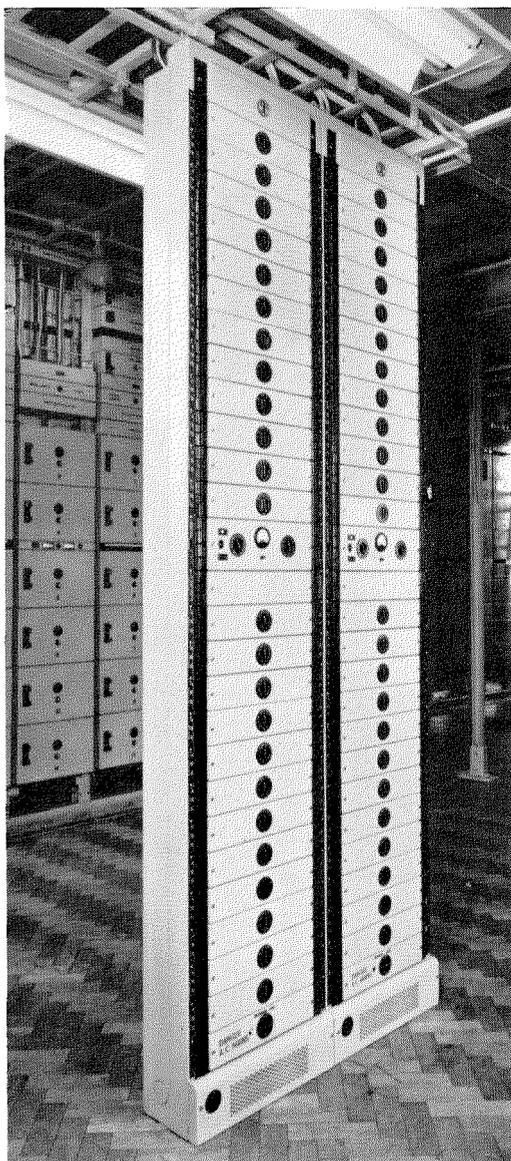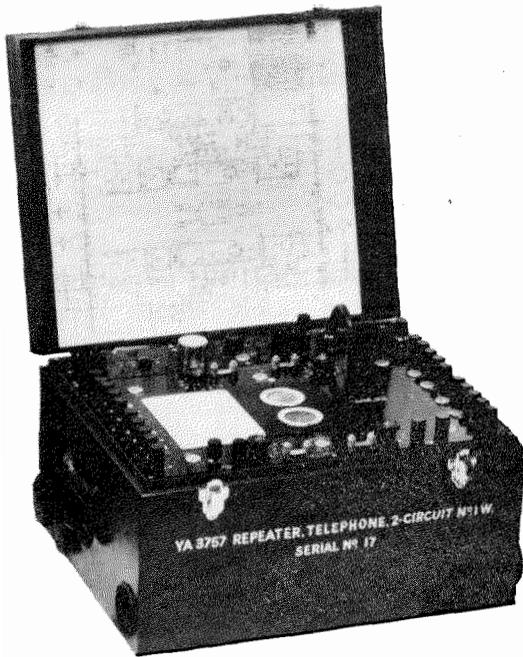
Figure 1—Early type of 2-circuit repeater
developed for the army.

re-design was necessary. The history of this de-
sign work has an important bearing on the evolu-
tion of the new practice and falls historically
into three periods.

1.1 Development of New Military Systems

The larger part of the existing rack-type equip-
ment had had to be left on the Continent in 1940,
and the Army was as short of communications
equipment as it was of weapons. The first war-
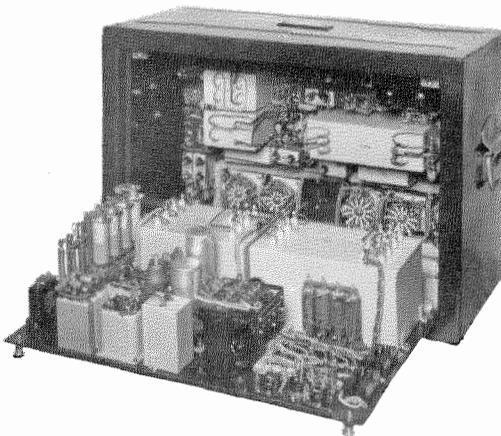
Figure 2—Portable single-channel carrier telephone
equipment with rear door open.
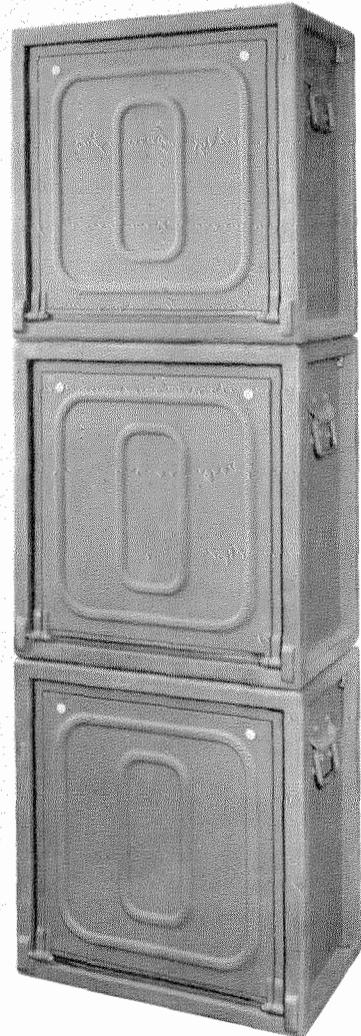
Figure 3—Stack of portable equipments.

time designs of military equipment were there-
fore carried out under extreme pressure. A simple,
folded metal box construction was used. This
radical departure from standard equipment prac-
tices resembled more the construction of portable
test sets. Figure 1 shows the first type of two-
circuit audio-frequency repeater developed for
the Army. Later developments reverted some-
what to standard practices by using a folded box
construction of a slightly different form, giving
increased accessibility. A portable single-channel
carrier telephone equipment may be seen in
Figure 2.

These later designs fall into the second period. The types of equipment (carrier telephone and telegraph) required the extensive use of filters and initiated the first step towards component container design.

In the third phase of war-time development, a reversion was made to the panel type of construction. This was to break up the equipment into convenient sub-assemblies to accelerate production and to provide easier maintenance in the field. New designs of filters replaced the older wax-filled types. The equipment cases were standardised in dimensions and provided with securing bolts for fastening each one to its neighbour. A stack of such units is shown in Figure 3. Thus at stations where a large amount of portable equipment was concentrated, the advantages of bay construction could be obtained without sacrificing portability.

1.2 POST-WAR RECONSIDERATION

At the end of the war, heavy demands for civil-type equipment arose. The building situation had worsened in every country in Europe and had remained practically without improvement elsewhere.

Development both on the equipment mounting and on the components has taken place since then. The mechanical features of the folded metal military boxes have been retained, and folded metal frameworks have been built to match the dimensions of the racks formerly used. The use of folded metal frameworks for 19-inch apparatus panels was not new. Such frameworks had been used for some years prior to the war for studio equipment and for housing the crystal drive equipment for broadcasters. But the close packing of components in the new apparatus

units involved a greater concentration of weight than in the earlier folded metal structures, and steps had to be taken to strengthen the construction.

There was however a notable advance in equipment design during this period. This was the abandonment of panel construction in favour of mounting frames, and the arrangement of these frames as plug-connected units in the equipment bay.

2. *Development of Cabinet-Type Bay and Panel Frame*

The development of the new bay can be said to have sprung from the third phase of the de-
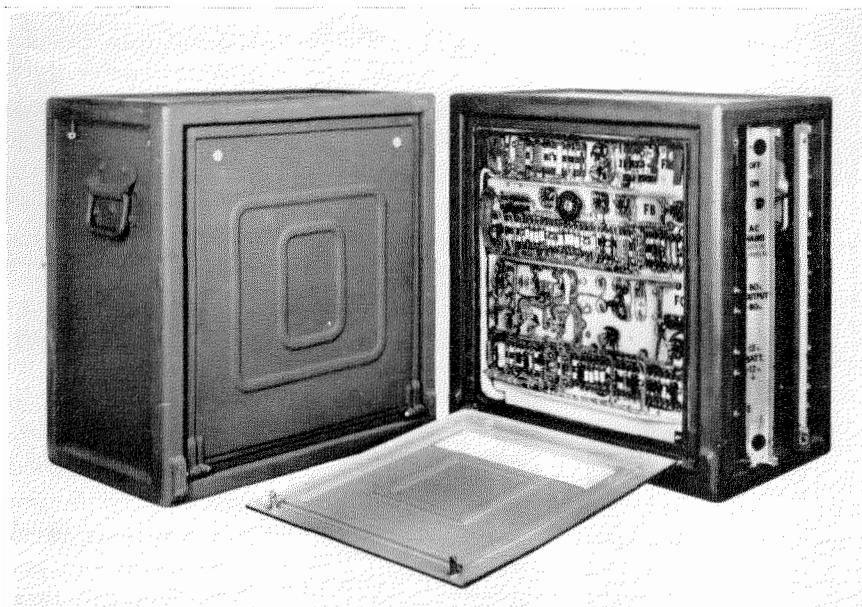
Figure 4—Later type of military equipment.

velopment of military systems, described above. In this construction (Figure 4) the mounting of the apparatus was on 19-inch panels of lighter weight than the standard type. The panels were mounted on hinged frames, and the apparatus was arranged so that access to the back of the frames was only necessary for valve replacements. Access to the front of the panels for setting up adjustments could be obtained by opening a shower-proof door.

At the end of the war, this system was one of the alternatives presented as a basis for the

development of a new equipment practice. The other was an adaptation of the 1932 equipment practice by mounting the apparatus in two layers. This was abandoned on account of inaccessibility and of the difficulty of keeping all controls in the front.

The first ideas on the form of a cabinet based on the third phase of the military-equipment
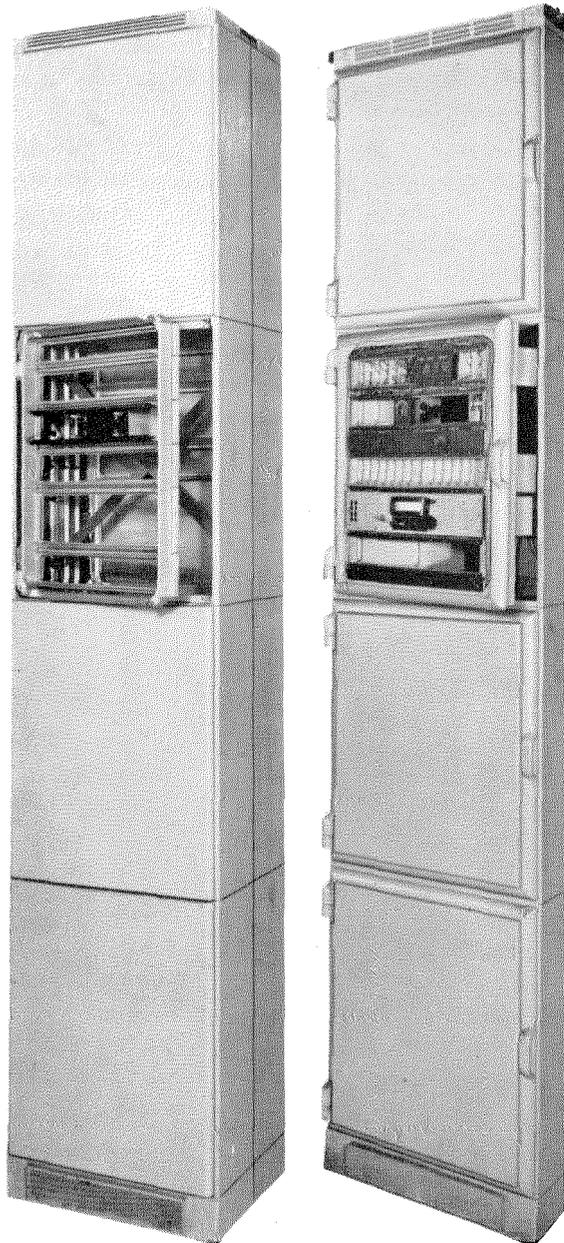
▲ Figure 5—Experimental models of stacked construction. The bay at the left has internal hinges on the apparatus frames.

design naturally turned to an arrangement whereby the boxes of equipment could be stacked and bolted together as shown in Figure 5. The idea of units with hinged doors was at first sight attractive. But the difficulty of manoeuvring the doors in the confined space between suites of bays, and the limitations imposed on design by the stereotyped containing units resulted in this proposal being abandoned. Time and effort had not, however, been expended in vain, for in the model of this system that was constructed were introduced frame-type panels in place of the old-style mounting plates. To the back of these frames, which may be seen in Figure 6, were attached the canned units containing filters and coils, and in front there was space for the mounting of the smaller components. The panel terminals were soldered to a cableform provided with a "swan neck" to enable the frame to be swung open.

The frame-type mounting for apparatus offered undoubted advantages. It eliminated the drilling of each mounting plate in a manner peculiar to the apparatus to be mounted on it, and made possible the bulk ordering of frames for all types of panel.

Consideration was next given to the design of connections between panels and the bay. The idea of plug-in units had always been attractive from the maintenance point of view, and the technique with automatic exchange equipment was well established. But previous experience with such connections when used for the very small currents involved in many instances in transmission equipment had never been good. There had also been difficulties when the connector had the dual function of mechanically locating the apparatus unit as well as of making the electrical connection. For the latter reason it was decided to make the electrical connections by means of plugs, recent development work having given promise that such connections could be made reliable, and to arrange for the mechanical location of the panels by means of die-cast locators secured to the bay framework.

The abandoned design of bay, which consisted of stacked units on the lines of the military-equipment boxes, had been based on the units being die-cast. The possibility of making a die-cast frame for a complete bay was investigated but abandoned on account of the cost. Experi-
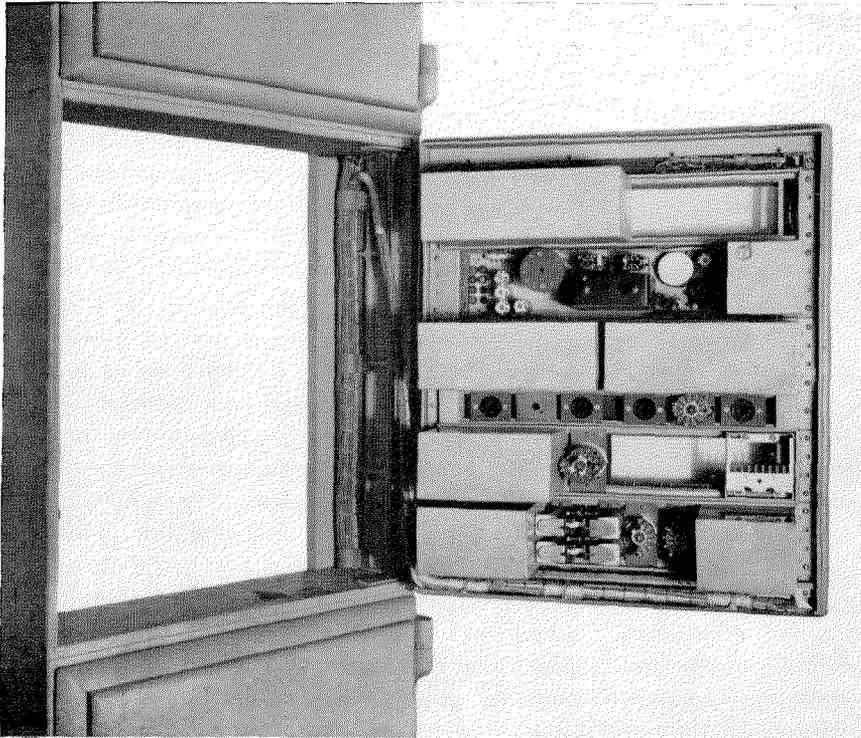
Figure 6—Gate-type apparatus frame.

In view of the heavy concentration of equipment, the height of the new bays was limited to 9 feet (2·74 metres), and to permit installation in stations designed for bays of the older types, the width and depth from front to back were adjusted to correspond with those of the old-style equipment.

2.1 DEVELOPMENT OF PANEL FRAME

In the abandoned "stacked" design, a cast-aluminum panel frame had been proposed. It was found that this construction occupied excessive space. However, the need for each end of the panel to be fitted with a locating device to engage with corresponding means on the bay framework suggested die-casting as a means of accurately manufacturing these parts without resort to machining operations. The final design of panel frame was provided with die-cast ends connected by pressed-steel longitudinal members.

The sizes of the panel frames had next to be standardised. Their width had, of course, been determined by the overall width of the bay and by the requirements of the locating members. For 26 years, the basic unit of height of panels had been $1\frac{3}{4}$ inches (44 millimetres). The origin of this unit is obscure, but it is probably related to the minimum space required for relay mounting. Some advantage in equipment calculations might have resulted from the selection of an integral number of inches or centimetres for the unit of panel height in the new practice, but custom is a powerful factor, and the old unit was retained. However, $1\frac{3}{4}$ inches was too small for the height of a single panel, although such panels had been employed in the 1932 equipment

ence had already been gained in the manufacture of pressed steel cabinets for the master oscillator and test bays of broadcasting transmitters and for other types of equipment. But in nearly every case these cabinets had been used to mount single-sided equipment panels and required access to the rear. The new bays would be required to carry a much greater weight of equipment and would need additional stiffening. To avoid the introduction of encumbering bracing members, bays were made single sided, requiring front access only. Thus a stiffening rib could be introduced down the back edge of each bay member and would serve to bolt two single-sided bays together. A rigid structure was thus secured, and flexibility obtained because pairs of single-sided bays could be assembled or separated at will, depending on requirements. In the 1932 equipment practice, the panels mounted on the front and back of any framework were assembled and wired in the factory and could not be separated later. Another advantage was that a suitable mounting was available when rear access was impossible.

practice, and the height of the smallest panel was fixed at $3\frac{1}{2}$ inches (89 millimetres). On this size of panel, economical packing resulted in a weight for a complete panel of around 20 pounds (9·1 kilograms), considered to be near the upper limit for handling as a removable unit.

However, two additional sizes were included to cater for assemblies which, though light in themselves, were rather bulky. They were $5\frac{1}{4}$ inches (133 millimetres) and 7 inches (178 millimetres) respectively.

The three standardised sizes of panel framework are illustrated in Figure 7. The die-cast end members house the socket blocks that provide the plug connections with the bay wiring. These members are connected by longitudinal "side-plates" of pressed steel. To each side-plate is welded a steel channel member, which provides additional stiffness and affords a means for securing the canned apparatus units with clips at the back of the frame. A series of holes in the front edge of the side-plates provide fixing for smaller apparatus elements and control units that are mounted on the front of the panel frame. Tinned earthing tags are provided at frequent intervals on the side-plates. There are thus only five standardised parts necessary for building panel frames of all three sizes:—two sizes of end die-castings, a die-cast strip (for 7-inch frame), and two types of longitudinal side-plates. Figure 8 shows the simplicity with which a panel of equipment may be removed for replacement by another.

A feature, standardised on all panel frames, is a plastic moulded terminal strip, running the full length of the panel at the front edges of the upper and lower side-plates. Each terminal is integral with a test socket, which is accessible from the front of the strip, the corresponding wiring terminal projecting into the wiring space of the panel. The socket terminals may be inserted in any of the 18 positions available on each strip. The sockets may be used as measuring points, or they may be used to give facilities for temporarily disconnecting some part of the circuit of the panel. In such cases, a simple U-link is supplied for normally bridging the points at which a break may be required to be made. The wiring tags are accessible from the front of the panel so that soldered connections may be made in parallel with the U-links should such duplication be considered desirable. The terminals, apart from the sockets, also provide convenient points for suspending in the front space small circuit elements such as rod-type resistors. The tags are split for this purpose, so that the wiring to the component and the component itself may be attached to the separate portions.

It was clearly desirable to allow for as many connections to each end of a panel as possible. Preliminary considerations of length of leakage paths and a requirement for a minimum breakdown voltage of 2000 volts between contacts showed that it would be possible to provide fifteen contacts at each end of a $3\frac{1}{2}$-inch high panel. In the next size of panel ($5\frac{1}{4}$ inches) two moulded blocks each providing 10 contacts are fitted to each end; and in the 7-inch panel, which consists of two $3\frac{1}{2}$-inch panel assemblies, there are 30 contacts at each end.
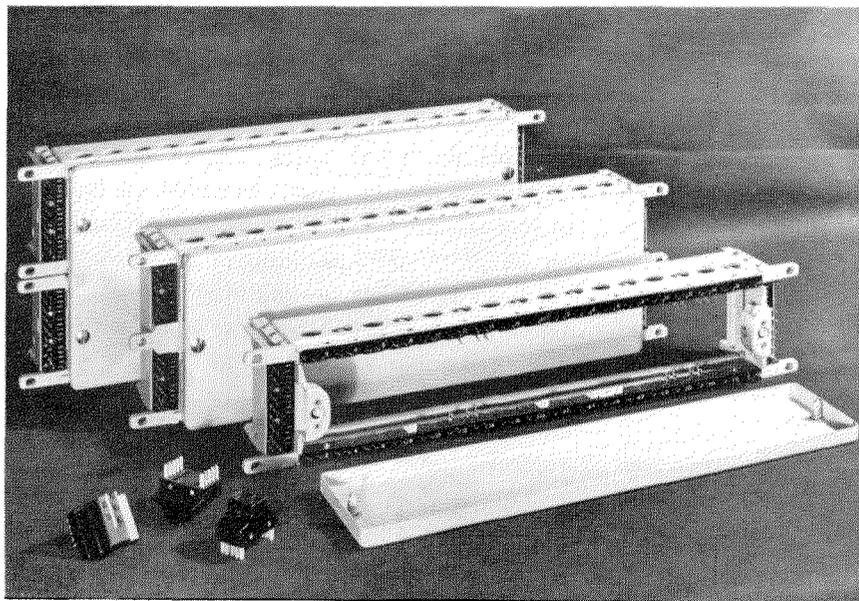
Figure 7—Three standard sizes of panel frames.

Every care has been taken to ensure the reliability of these contacts, and preliminary experience with new equipments in the field has fully justified the reliance placed in them. In their design, there has been no attempt, as has happened so frequently in the past, to combine the functions of mechanical pressure and electrical conductivity in the same material, and to use this material for the contact sockets. Instead, steel springs have been used for the pressure-exerting elements, and silver-plated nickel-silver punchings, for the contacts. Each contact element is integral with a soldering tag, which projects backwards into the panel for connection with the panel wiring, and forwards into the space alongside the socket block, there to provide means for bridging the plug connection if desired with a soldered strap. The sockets and their springs are identical both in the panel blocks and in the connector blocks equipped on the bay framework, and all tags for soldered connections are hot tinned.

For high-frequency currents, special sockets providing coaxial connections have been designed. They are shown, with their associated
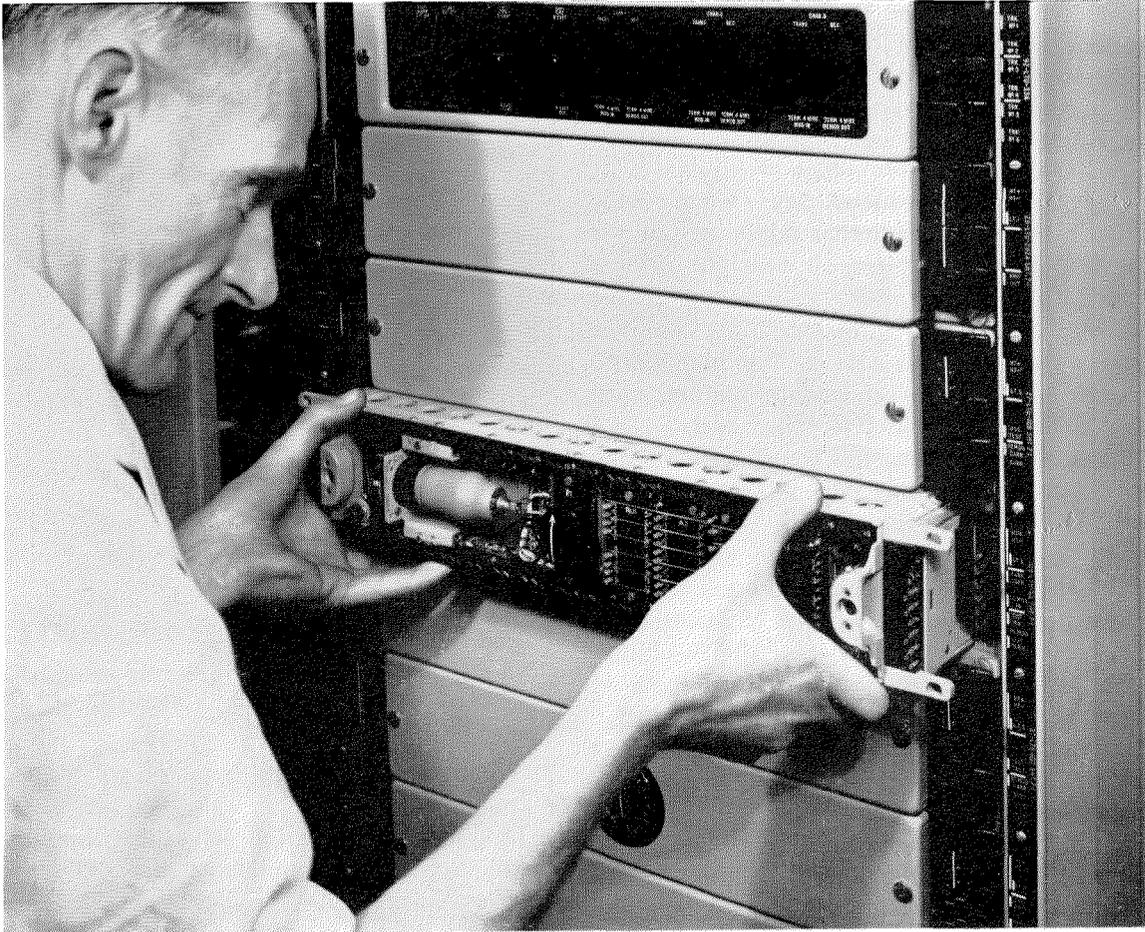
Figure 8—Removal of apparatus panel from bay.

ductivity in the same material, and to use this material for the contact sockets. Instead, steel springs have been used for the pressure-exerting elements, and silver-plated nickel-silver punchings, for the contacts. Each contact element is integral with a soldering tag, which projects backwards into the panel for connection with the panel wiring, and forwards into the space alongside the socket block, there to provide means for bridging the plug connection if desired with a soldered strap. The sockets and their springs are connecting plug, in Figure 9. The coaxial sockets are interchangeable with the normal sockets used on panel ends. For the $3\frac{1}{2}$-inch panel, the socket blocks provide three coaxial connections in place of 10 of the normal 15 plain connections, and in the $5\frac{1}{4}$-inch panel, a three-socket coaxial block can replace each of the two 10-contact blocks otherwise used. There is no design at present for enabling coaxial circuits to be interrupted for testing on the longitudinal strips on the panel side-plates.

The wiring of the panels and of the bays is carried out in tinned copper wire insulated with a thin coating of polyvinyl-chloride. The use of textile-covered wire has been eliminated. Although the polyvinyl-chloride-insulated wire shows an insulation resistance lower than textile-covered wire under dry atmospheric conditions, the improvement in insulation resistance under conditions of extreme humidity over textile-covered wire is very marked. Owing to the stronger resistance to electrical breakdown at high voltage, thinner coverings suffice with the plastic-insulated wire, and there is now no need for an enamel covering, which was a frequent cause of defectively soldered joints when textile insulation was used. Another advantage of the polyvinyl-chloride covering is that the colours obtained are brighter than with waxed textile covering, which assists identification. Another factor contributing to this is that the plastic covering has a smoother surface texture, with consequently less liability to collect dirt.

The only disadvantages of the plastic covering are that its fairly low melting point requires additional care in soldering, and that it is slightly subject to "cold flow" so that pressure on the wires due to the tight lacing of cable forms or other causes must be avoided. Special stripping tools have been developed and enable the insulation to be neatly removed without any danger of nicking the wire.

Screened pairs for low-frequency connections are formed of two plastic-insulated conductors, twisted together and covered with a lapped screen of tinned copper wire. The whole is covered with a polyvinyl-chloride sheath. The advantage of a lapped screen is that it can be easily stripped back, and may be twisted up to form the actual screen connection.

For higher frequencies, polythene-insulated wire is used. Wires with polythene insulation are made up into screened pairs with a lapped screen and covered overall with a polyvinyl-chloride sheath. However, the majority of high-frequency circuits are unbalanced and are carried in coaxial cables with polythene insulation. The outer conductor is braided, because a lapped screen would give rise to an excessive impedance in the return conductor. The need for a braided screen having a soldered connection close to the polythene insulation of the inner conductor set a difficult prob-
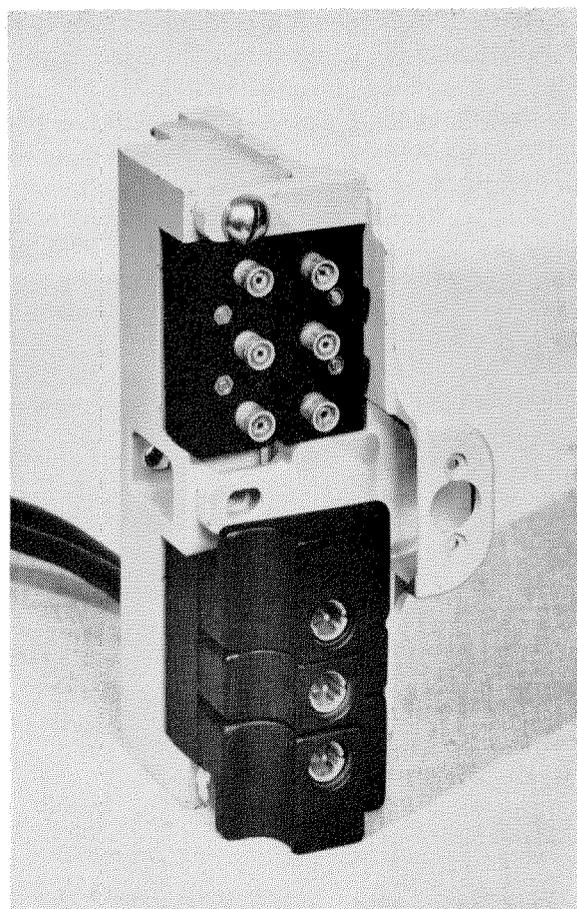
Figure 9—Bay-to-panel coaxial connectors assembled in die-castings for $5\frac{1}{4}$-inch panels.

lem, because the melting point of polythene is sharp and fairly low.

This problem has been solved by slipping a thermo-setting plastic moulded thimble over the polythene insulation and under the braided outer conductor, thus introducing a heat-resisting barrier between them. The screen is clamped tightly over the thimble by a thin tinned copper band, the two ends of which are drawn together and clenched with pliers forming an "ear" for soldering to the screen connection. The band is soldered all round the screen. If, by any chance, the polythene insulation melts due to extra long application of the soldering iron, the moulded thimble prevents contact between the inner conductor and the screen. At the end of the thimble is a small terminal that reinforces mechanically the fine inner conductor at the point of attachment. High-frequency terminals on apparatus elements

are arranged with lugs to engage with the "ears" formed at the ends of the coaxial-cable connections.

Cableforms for panels are generally simple, consisting of one or more main arms running across the panel and accommodated in the channels above the can-mounting studs. Separate arms from the main form feed the terminals of the canned units and the apparatus units on the front of the panel. The arms for the latter are left sufficiently long for individual units to be removed for examination without disconnection.

A cover in the form of a shallow pressed-steel tray protects the whole of the front of each panel, except for the ends where the panel-to-bay connections are made. The covers are fixed to the die-castings at the ends of the panel by coin-operated quick-release fasteners. Only three sizes of cover are required, corresponding with the three standardised panel sizes. They are pierced as required to expose any controls and meters to which access is required for the normal adjustments of the equipment. The panel cover is therefore the only component that is peculiar to a panel assembly and requires special treatment.

2.2 APPARATUS UNITS

The principle of grouping together in a sealed container the elements of networks and filters was extended in the new design to all circuit elements that, when properly protected against climatic conditions, remain stable and have a long life. Most coils, capacitors, and resistors fall into this class. Those elements that can be regarded as variable due to changing circuit conditions or as the result of aging, or which may need periodical replacement or adjustment during normal service, generally are mounted individually in the space between

the panel frame members and immediately beneath the front cover, where they are instantly accessible.

The design of the canned units combines the high electrical stability given by hermetic sealing, with the mechanical stability needed for satisfactory shipment and long service. Much space is, of course, saved by sealing the elements in groups instead of individually. Despite the wide variety of circuit arrangements required by modern telephone transmission systems, it has been possible to simplify manufacture by constructing the units, like the panel frames, from a small number of standardised parts.

Figure 10 shows a group of assemblies that represent the different stages in the evolution of the canned unit. On the left, is the early type of bitumen-filled unit. In the centre, is the air-filled unit developed for military systems. In this type, the circuit elements were grouped in accordance with their position in the electrical circuit, were separately tested as units, and were then assembled and wired together to form a complete filter. This method of construction was found at once to be a great improvement, but it was still necessary to dismantle the filter to remove a faulty component in the middle of the assembly.

In the new units, the individual mounting-plate arrangement for component groups was
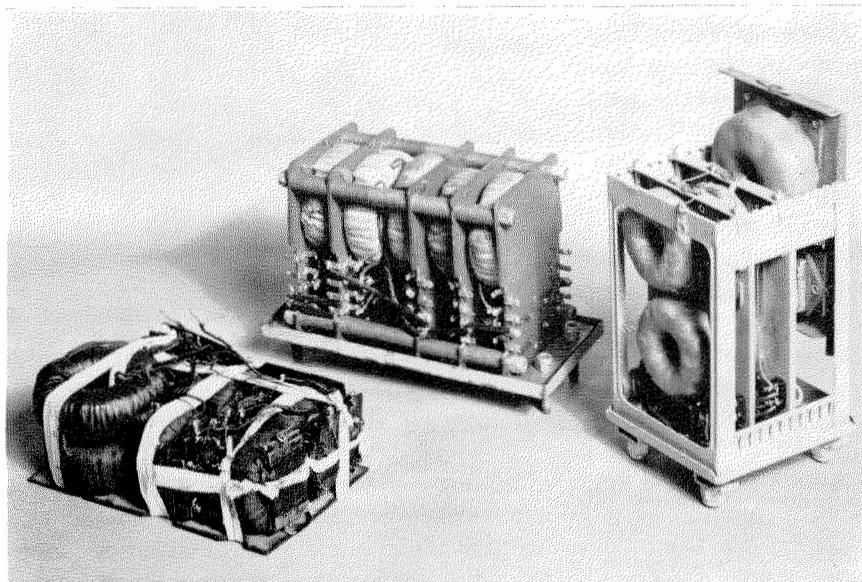
Figure 10—Development of potted filters. The early type at the left is bitumen filled. The other two are the military and new types and are both air filled.

retained, and a slotted frame designed to enabled these assembled plates to be spaced apart. This construction is illustrated in the right-hand unit of Figure 10.

The can assemblies are produced in a restricted range of sizes and have a number of common parts. All cans have the same depth of $5\frac{1}{4}$ inches (133 millimetres) corresponding with the depth available in the bay from the back of the mounting channels on the panel side-plates to the flange at the back of the bay-side. There are three heights of can assembly corresponding with the three standardised panel frame sizes, and for each of these heights the length of the can can vary in steps of $\frac{1}{4}$ inch (6 millimetres) from $1\frac{5}{16}$ to $7\frac{9}{16}$ inches (33 to 192 millimetres).

Inside a can, the basic structure consists of a rigid but light framework in which are mounted the small apparatus plates each carrying a wired assembly of circuit elements. The framework is an open structure made up by spot-welding indented ribbed steel strips, known as "combs," between two formed-up sheet-steel end-plates. The end-plates conform in height with the three heights of can, and in depth with the standard depth. Only three sizes are therefore required for all varieties of can. The combs are the same for all cans, except that they vary with the length of the can. The pitch of the teeth is $\frac{1}{4}$ inch and therefore corresponds with the $\frac{1}{4}$-inch increments in the lengths of the cans. The apparatus plates are located in the framework in suitable positions by special bolts.

The framework is mounted by four stout studs inside a shallow steel tray with drawn-up edges, which may be regarded as the lid of the can. The studs carry the special clips that clamp the canned unit to the channels attached to the side-plates of the panel framework. The weight of the components is therefore transferred by the studs directly to the panel frame, and the lid serves only as part of the hermetic sealing. The studs are sealed by copper brazing where they pass through the lid, and on the latter are mounted the hermetic-seal terminals that carry the connections from the panel wiring to the can elements. The framework does not fit tightly inside the lid, but forms a trough with the drawn-up edges of the latter in which the cover of the can is subsequently located and soldered to complete the sealing of the whole unit.

The apparatus plates carrying the circuit elements are either of light-gauge sheet steel, blanked and formed, or, where close proximity of a metal plate may affect the electrical performance of the circuit elements, the plates may be of synthetic-resin-bonded fabric. Only three sizes of plates are required, corresponding with the three heights of can. The plates are jig-drilled with the holes necessary for mounting the various components, but a measure of rationalisation has
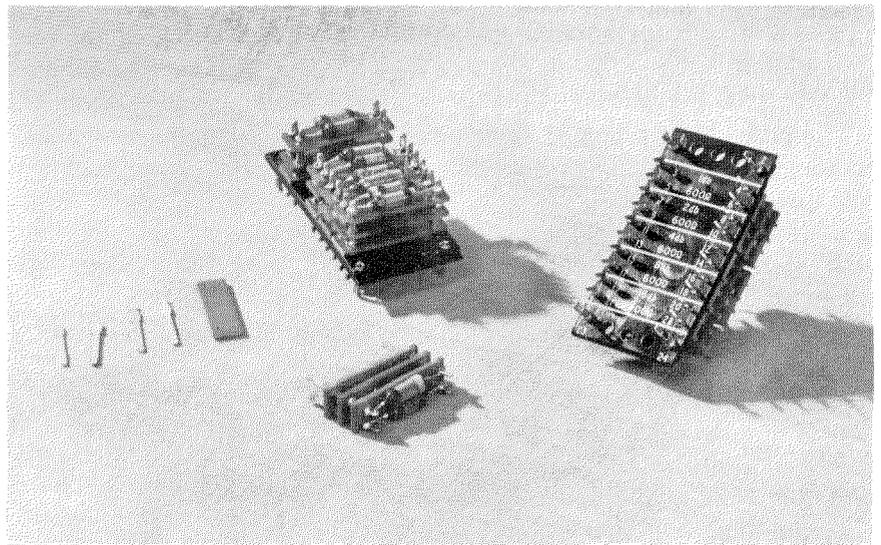
Figure 11—Typical assemblies of resistance attenuator units and their components.

been achieved by using one drill jig to cover the drillings for a number of components, although all the components in the combination may not be used on a given plate. Components are firmly secured to the plates either by eyeletting or by screws with self-locking nuts.

All wiring among components on a plate is carried out before assembly in the can frame-

work, any leads that require to be connected to other plates in the same can or to the seal terminals being soldered to small terminals mounted down the edges of the plate. These terminals are accessible for wiring after the assembly of the plates in the framework.

The hermetic-seal terminals on the can lid are of the matched-expansion metal-glass type (Cinseals), individually soldered to the lid. They are reasonably robust and simple to wire, and they provide a complete barrier to the entrance of water vapour.

The second category of circuit elements, which have been broadly classified as those that require periodical adjustment or replacement, are, in general, suitable for use under all climatic conditions without hermetic sealing. These components are assembled on a small number of basic mountings, each of which is required in large quantities in its primary form, but which can be modified by the addition of special drillings, for example, to extend their application to other purposes. Examples of such mountings are attenuator networks, modulators, multi-position rotary switches, valves, and relays.

Fixed attenuator pads are used in great numbers in transmission systems. The resistors used in the new practice are generally of the high-stability rod type with wire terminals. They are assembled in groups of up to four on small standardised plates of insulating material as shown in Figure 11. The plates are pierced to carry four terminal punchings, and the latter are held in place by the wiring of the resistors. The frontal area of a complete four-terminal pad, shown in front in Figure 11, is $1\frac{3}{8} \times \frac{3}{8}$ inch (35×10 millimetres). To mount these pads on the panel, use is made of a plastic moulded plate with slots down each side through which the terminals of the pads may be passed and secured in place by twisting. The pads are mounted behind the plate with the twisted wiring tags on the front, and the assembly is fixed to the front of the panel frame by small brackets screwed to the holes provided in the side-plates. Any pad can be removed at any time by untwisting the terminals and drawing the pad out from the back of the plate. The moulded plates are available in two sizes for the $3\frac{1}{2}$- and $5\frac{1}{4}$-inch panels respectively, the smaller plate accommodating 5 and the larger, 10 pads. Since the 7-inch panel is

effectively two $3\frac{1}{2}$-inch panels, the smaller size of moulded plate may be used in either half of the panel frame.

The moulded plates, described above, are also used for mounting modulator assemblies in which the modulator elements are in the form of wire-ended capsules. The associated balancing voltage divider is accommodated, when necessary, by providing an additional drilling on the plate. Small fixed and variable capacitors can also be mounted on these plates. For high-frequency applications, screening covers can be fitted over the resistor networks at the back of the plates and over the terminals at the front.

A similar plastic moulded plate is available, again in two sizes, for mounting the wafer-type multi-position switches that are extensively used in the new practice. These plates are similarly mounted on brackets across the front of the panel frame. As these switches are usually required for adjustment without removing the panel cover, the latter is pierced to carry a dial through the centre of which a knob, fixed to the switch spindle, is accessible. The knob is sunk below the face of the panel cover, and both the knob and dial are standardised plastic mouldings.

Valves are mounted either in the front space of the panel or between the cans with their bases projecting backwards into the bay. The former position is chosen when it is necessary to associate any terminals on the valve closely with particular terminals on the top of a canned apparatus unit. Mounting between the cans is used when the length of leads to the valve terminals is unimportant. In both cases, the valves are replaceable without removing the panel from the bay.

Special types of valves and sockets that permit of soldered connections have been developed for use in amplifiers and other apparatus in which a contact failure would affect transmission on a large number of circuits.

All types of valve mountings can be drilled for a variety of types of socket, although an endeavour has been made to restrict the varieties of valve bases used.

The mounting of relays has presented a problem, since access must be obtainable from the front of the panel for cleaning contacts and adjusting springs, while the length of the relays precludes their being wholly accommodated in
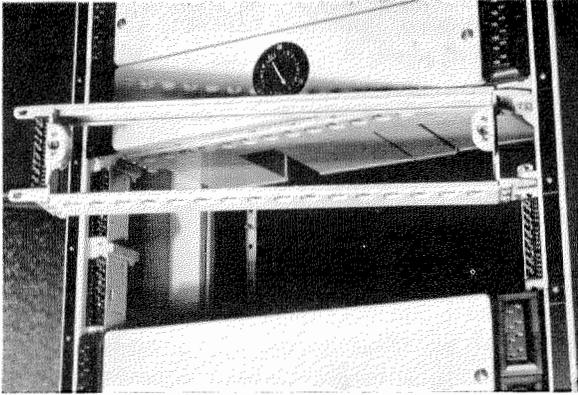
Figure 12—Hinged framework for panels requiring a large number of connecting leads.

the front space. New circuit designs have drastically reduced the number of relays used compared with earlier practices. Those remaining are fitted to mountings that are clamped to the channels of the side-plates. The contacts and springs therefore project forward into the front space, and the wiring terminals into the bay. The relays are mounted on simple bridge pieces varying with the type of relay, and spanning either $3\frac{1}{2}$- or $5\frac{1}{4}$-inch panels. The bridges are fixed at each end to a standardised bracket provided with drillings for carrying any of the bridge pieces, and which clamps to the side-plates. The space behind the bridge pieces, which provide mountings for the relays, can be employed for the mounting of resistors associated with the relay circuit. These small components can be carried on one of the moulded apparatus plates used for mounting resistors, which plate can be fixed to the drillings provided in the brackets.

2.3 SPECIAL PROBLEMS

In laying down the basic principles of the new equipment practice and in applying them to the engineering of specific systems, it was clear that there would be a number of circuits that did not fit satisfactorily into the standardised form adopted. These difficult cases were only a small minority of the whole range of circuits and could not be allowed to influence the general design principles. It was accepted that they should be dealt with on a special basis. Some of these problems and the way they were solved are given below.

Due to the greater number of circuit elements that can be accommodated on the new panels, the number of plug connections available at the ends of the panels is occasionally insufficient for the number of panel-to-bay connections required.
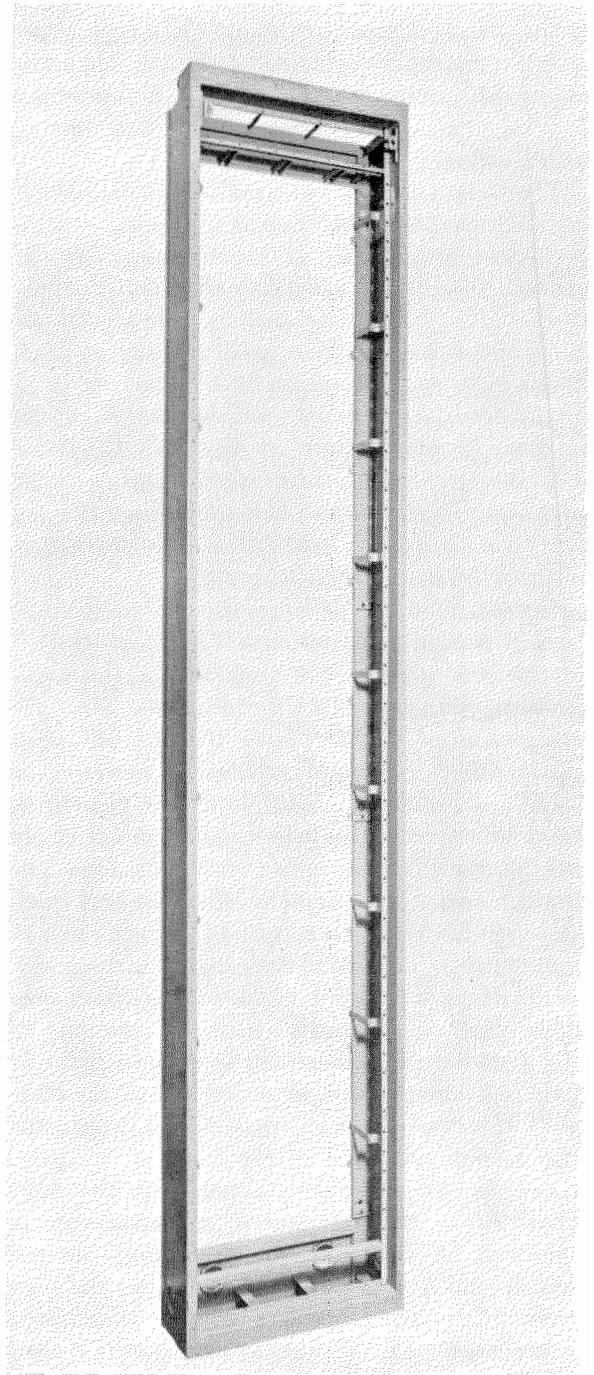
Figure 13—Empty framework for a single-sided bay.

To meet these cases, a special hinged panel is wired directly to the bay cableform. These special panels hinge out from the bay like a gate to obtain access to the components mounted behind them. They are made in $3\frac{1}{2}$- and $5\frac{1}{4}$-inch sizes and are similar to the removable plug-connected panels, except for the hinge, which replaces one die-cast panel end. A machining operation is performed on the die-casting at the opposite end from the hinge to allow for the sweep of the panel when it is swung out. Figure 12 shows one of these panels before connection to the bay cableform, which is equipped with a vertical "torsion arm" to allow for the movement. The usual standard panel-to-bay plug connections are provided at the end of the panel remote from the hinge, but the additional connections afforded by them must, of course, be broken when the panel is opened. All the normal canned apparatus units and components for front-space mounting may be used on these hinged panels, but they are particularly applicable to the mounting of groups of jacks or keys, which are sometimes required for centralised testing or switching fields. Another of their applications is when it is known that it will be necessary to add apparatus units at some future date, without taking out of service, even temporarily, the circuits already equipped on the panel.

2.4 BAY CONSTRUCTION

It has been previously indicated that the design of the bay in two separate halves of folded sheet steel was primarily to obtain additional stiffness in the side members to support the increased weight of equipment that resulted from close packing. Figure 13 shows an unequipped single-sided bay framework, and Figure 14 gives close-up views of the upper and lower portions of an equipped single-sided frame. In these two views, the rear flanging, provided for additional stiffness and for the bolting of the bay-sides back to back, can be seen. The standard height of a bay-side framework is 9 feet ($2 \cdot 74$ metres). Bay-sides shorter than this can be readily constructed, by simply varying the height of the side members, the top and bottom cross members being standard for all heights. A special bay-side 3 feet high ($0 \cdot 92$ metres) intended for wall mounting has been designed, primarily for very simple

repeater installations. This design also allows for stacking similar to the later design of military equipment. When stacked, 3 units can be bolted to the back of a standard 9-foot bay-side to form with it a double-sided bay.

The restriction imposed by the necessary cross members at the top and bottom of the framework makes the space in these two areas unsuitable for mounting panels. This space has been used advantageously for housing at the top the bay terminal blocks and at the bottom the power distribution facilities needed on the majority of bays.

The top of the framework of Figure 14 is left partially open so that wiring may be fed to the terminal strips. A step at the back, forms with a corresponding step on another bay-side bolted to it a trough that is big enough to carry the
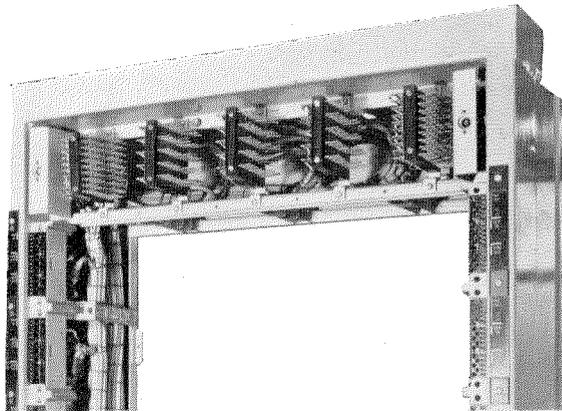
Figure 14—Upper and lower ends of a bay-side. The bay terminal blocks are mounted at the top and the power-distribution facilities are at the bottom. The flanges at the rear of the side walls act as stiffeners and permit two single-sided bays to be bolted together back to back.
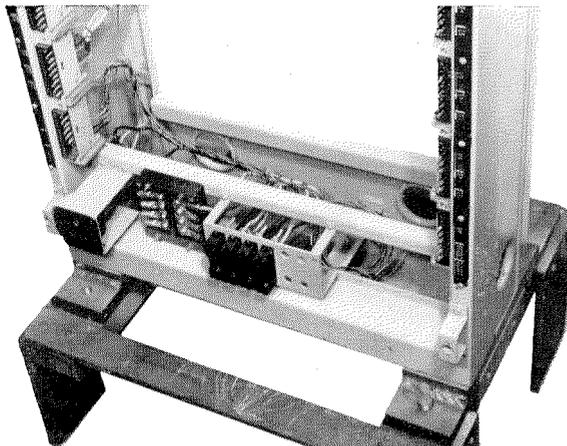
interbay cabling and small amounts of office cabling. In larger installations, the office cabling would be carried in the usual racking.

The power distribution units, mounted at the bottom of the bay-side, have also been standardised. Fully drilled frameworks can therefore be held in stock as they are suitable for widely varying equipment arrangements. The lower part of Figure 14 shows a typical assembly of units for power distribution at the foot of a bay-side. An outer "kicking plate" provided with a grille for the ventilation of the bay, covers the assembly, and may be removed by two quick-release catches. The removal of this plate gives access to the fuses only, a second perforated plate fixed by screws, prevents contact with the live power distribution terminals. A plug point for a soldering iron, inspection lamp, or for the power supplies to portable test gear is always fitted. It may be seen on the left of the picture. Suitable bushed openings in the side and back members of the bay-side framework enable the power cabling to be passed through the bays in a suite.

The bay terminal blocks, to which are connected the cableforms of the bay-side for interconnection to the office wiring or interbay cabling, are mounted directly on the top cross members of the bay-side framework and are pro-

tected by a front cover held by quick-release fasteners. They are built up of a number of standardised parts and can be assembled to provide various numbers of terminal connections. Special assemblies of screened connections are available for high-frequency coaxial leads. These assemblies of terminals, which are illustrated in Figure 15, can be mounted either separately or in conjunction with one or two rows of terminal tags for normal connections.

One or more bay cableforms run down each side member of the bay-side, the number of cableforms depending on the electrical requirements of the particular equipment. They are kept spaced as required by tying to removable steel straps as evident in Figure 16. For the great majority of bay-sides, the cableforms can be completely wired on the bench to the bay terminal blocks and to the socket blocks connecting with the panels. The fitting of the form is then restricted to the screwing of the bay-side terminal blocks to the cross members at the top of the bay and inserting the panel-connecting blocks in the panel locators as shown in Figure 16.

Adequate earthing facilities are provided by a series of lugs welded to the verticals of the framework and spaced so that at least one is available for each panel position. Interbay earthing is
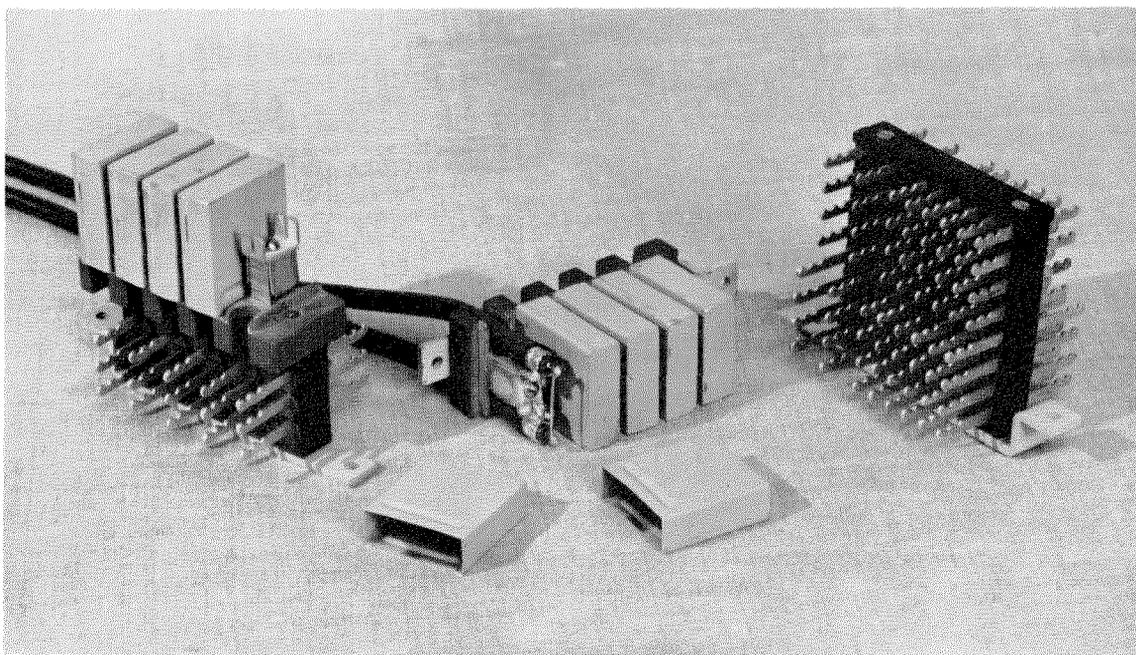
Figure 15—Bay terminal strips.

given by means of interconnecting copper earth bars fitted at the top of each bay-side immediately behind the front cross member of the framework.

The standard 9-foot bay-side is intended to be secured to the floor and stayed at the top. Holes are drilled in the stiffened bottom cross member and drilled and tapped in the top cross member for this purpose.

When the bay-side is mounted alone, or when electrical considerations make it necessary to place a screen between the equipments of two bay-sides that are mounted back to back, thin sheet-metal covers are available for closing the back of the framework.

A complete 9-foot bay-side framework, fully wired, but without panels, weighs approximately 90 pounds (41 kilograms), and is thus a conveniently handled unit.

2.5 BAY-TO-PANEL CONNECTIONS

The connections between the socket terminal blocks on the panels and those on the bay framework are made by means of U-link connectors with flat contact members. Each group of 5 such connectors is moulded in a separate plug, and each individual connector is provided with a test socket, which is accessible from the top of the plug. Routine level or voltage measurements can therefore be made when the connectors are in place. On plugs intended for carrying transmission circuits, the sockets are suitable for a flat-bladed test plug, and only two pairs of the connectors carried in a 5-way plug are equipped with test sockets. For all other circuits, the plugs used allow access to all 5 links through round holes that will admit the round test prod of a voltmeter, but prevent entry of the flat-bladed plug used for transmission measurements.

2.6 STANDARD BAY ENGINEERING

In applying the new equipment practice to various transmission systems, it has been possible to introduce a considerable degree of rationalisation in circuit engineering. For example, the terminal positions and numbering for the basic connections to most panels have been standardised. The panel earth terminal and the plate- and heater-circuit supply terminals are always in the same positions and bear the same
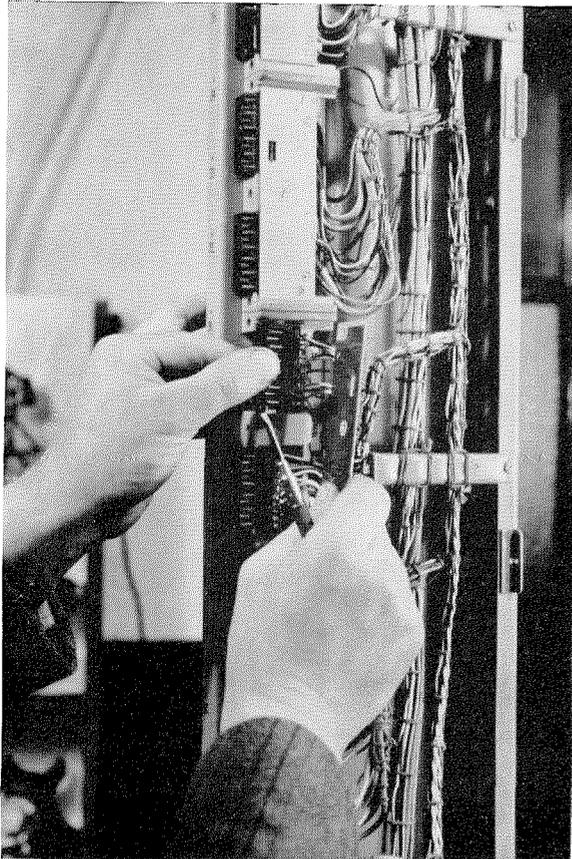
Figure 16—Assembling cableform to bay.

numbers on every panel to which they apply. Maintenance work is thereby greatly simplified.

Power supply panels, being the heaviest units, are always fitted at the bottom of the bay-side. Alternative wiring enables power panels that provide plate-circuit rectification in addition to a transformer for the heater supplies to be interchanged with other types having only heater supplies as may be desirable when growth or other factors make the supply of plate current to the valves from a central rectifier more economical. A power panel, which provides both plate and heater supplies, is shown in Figure 17. All systems engineered in the new practice have a plate-voltage supply of 220 volts. The increase in voltage enables advantage to be taken of modern high-slope valves in the voltage-amplifying stages and higher outputs needed in carrier operation to be obtained without recourse to special valve constructions. The plate supply is individually fused on each apparatus panel, one
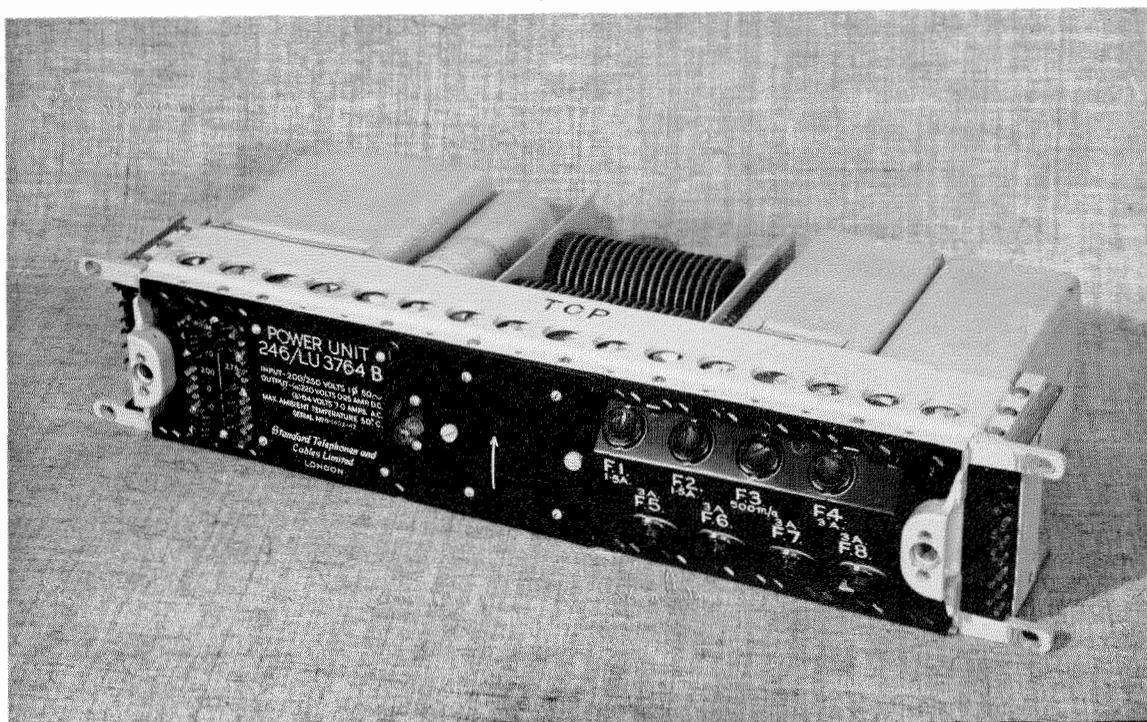
Figure 17—Typical power-supply panel.

standard rating of replaceable cartridge fuse being used throughout.

Reference has already been made to the reduction effected in the number of relays used. Previous practices generally required the use of a valve-failure alarm relay for each valve. In the new practice, a single relay suffices for all the valves equipped on a bay-side.

A valve-failure alarm panel is equipped in a standard position, approximately at eye level, on almost every bay-side on which valve equipment is installed. In the cathode circuit of each valve, irrespective of type, is a resistance of a value chosen to give a potential drop of 6 volts to earth when passing the normal cathode current of the valve. This resistance in some cases may form part of the cathode bias resistance. The 6-volt cathode potentials from all the valves on the bay-side are taken through the bay wiring to the valve-failure alarm panel. They are decoupled with capacitors and resistors, and rectifiers inserted in each lead prevent circulating currents when the leads are connected to the grid of a single valve on the alarm panel. Failure of any valve resulting in an abnormal increase or decrease of cathode current will cause an alarm.

Switches on the alarm panel enable the potentials from the cathode resistances to be individually measured to identify a faulty valve. Facilities are also provided for the testing of heater voltages and other power supplies in special equipments. An extension plug and cord enable the panel to be used as a voltmeter when checking the circuit of any panel.

The introduction of removable plug-connected panels has considerably reduced the need for patching arrangements. However, when it is inconvenient to remove a panel from the bay, another can be patched into its place with cords. Patching cords are insulated with polyvinyl-chloride or polythene, and suitable plugs for making connection either with the bay or panel terminal sockets or with the test points on the connecting plugs are moulded integral with the plastic cords.

2.7 Special Problems

As with the engineering of panels, it was to be expected that special problems would be presented in certain equipments and would influence the design of the bays. The normal terminal

blocks secured to the upper cross members at the top of each bay-side provide for a maximum of 400 connections. When the number required exceeds this, additional blocks are mounted in the space normally occupied by the topmost panel. Here they are protected by a cover similar to the normal panel cover, thus retaining the uniform appearance of the bay-side.

Another example of special equipment and wiring methods is provided by the carrier distribution bay-side used for distributing the 12-channel carrier frequencies and the two pilot frequencies required for stations in which many 12-channel carrier telephone "groups" are installed. Each panel on this bay-side allows for frequency distribution to 14 groups, requiring an ultimate number of about 200 screened paired wires to be led out directly into the interbay wiring. Here a plug-in panel would be out of the question. The distribution panel therefore is a built-up structure of steel angle, screwed to the bay framework on the normal locator fixing holes
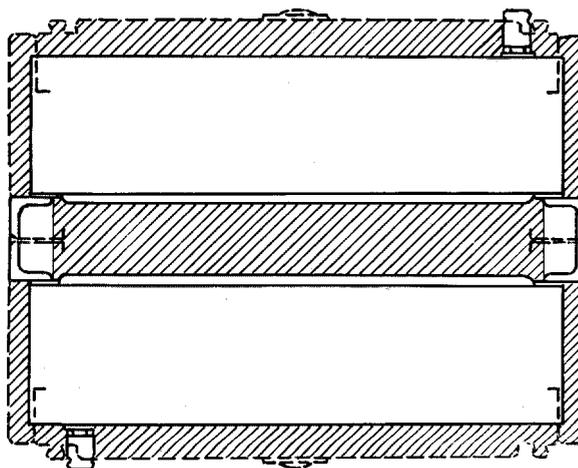
Figure 18—Sectional drawing of new and old equipment bays. The shaded area shows the increase in available mounting space in the new practice.

and mounting the distribution units on cross members.

Covers, similar to normal panel covers, are fitted over the front of the panel to ensure

TABLE 1

COMPARISON OF SPACE OCCUPIED BY STANDARD SYSTEMS

Type of System		New Practice		Former Practice		New Volume in Per Cent of Old Volume
		Bay-Sides 9 Feet High	Volume in Cubic Feet	Bay-Sides 10·5 Feet High	Volume in Cubic Feet	
12-Channel Carrier-on-Cable Terminal	1st installed	2·25	19·5	4·5	45	43
	2nd–12th installed (per terminal)	0·75	6·4	2	20	32
	13th installed	1·5	12·9	2·75	27·5	47
	14th–48th installed (per terminal)	0·75	6·4	2	20	32
24-Channel Carrier-on-Cable Terminal	1st installed	2·75	23·7	6·5	65	36
	2nd–6th installed (per terminal)	2·25	19·3	4	40	48
	7th installed	3·25	28·0	4·75	47·5	59
	8th–24th installed (per terminal)	2·25	19·3	4	40	48
Coaxial Terminal 10 Super-groups		39	336	89	884	38
12-Channel Carrier-on-Open-Wire Terminal	1st installed	6·5	56	11	110	51
	2nd–12th installed (per terminal)	3·25	28	6·5	65	43
12-Channel Carrier-on-Open-Wire Repeater	1st installed	3	25·8	7·5	75	29
	2nd installed	2·5	21·5	6	60	36
3-Channel Carrier-on-Open-Wire Terminal		1·5	13	4·5	36·4	36
3-Channel Carrier-on-Open-Wire Repeater		1	8·6	3·5	28·3	30

uniformity of appearance with the rest of the equipment. The depth into the bay taken up by the distribution panel is much less than that occupied by normal panels, so that all the space between the back of the panel and the back face of the bay-side is used for the cabling and is sufficient for the cabling of two complete distribution panels. This is the limit of the equipment for the bay. The remainder of the space in this bay-side is equipped with unwired panel locators and forms a convenient space for the storage of spare panels required for other bay-sides in the station.

3. What Has Been Achieved

The economies in station floor space that have been effected have been made, not by pure "miniaturisation," which usually degrades electrical performance (although economies in the sizes of components have been made in many instances), but rather by the more-efficient utili-

sation of available space inside the bay. Figure 18 shows a sectional drawing of a double-sided bay according to the old practice in comparison with the section of two new-type bay-sides bolted together. The areas shown cross hatched were not used in the old practice.

A number of transmission systems have been re-engineered in terms of the new practice so that the interesting comparisons set forth in Table 1 can now be made.

4. Acknowledgement

It will be realised that a development of the magnitude of the new practice described above can only result from the contribution of diverse and patient efforts from many people. The authors gratefully acknowledge help freely given by a number of their colleagues too numerous to mention by name.

Carrier Power Requirements for Long-Distance Communication by Microwaves*

By A. G. CLAVIER

Federal Telecommunication Laboratories, Incorporated, Nutley, New Jersey

MICROWAVE radio relay systems normally use a number of standardized transmitting and receiving equipments. The carrier power required for each transmitter is examined with consideration for the power losses in transmission lines between generating and receiving apparatus and their respective antennas, propagation attenuation, and the noise developed in the input circuit of the receiver. Provision must be made for fading in some or all transmission paths simultaneously. The type of modulation is significant and may reduce the required carrier power by a considerable amount.

• • •

1. General Considerations

1.1 SINGLE-HOP TRANSMISSION LINKS

The quantities involved in the case of a single-hop transmission link are shown in Figure 1.

The required carrier power P_t can, therefore, be expressed in terms of the noise power P_n at the first receiver tube as follows:

$$10 \log \frac{P_t}{nP} = \underbrace{10 \log \frac{P_t}{P_{t0}}}_{(1)} + \underbrace{10 \log \frac{P_{t0}}{P_{r0}}}_{(2)} + \underbrace{10 \log \frac{P_{r0}}{P_{r1}}}_{(3)}$$

$$+ \underbrace{10 \log \frac{P_{r1}}{P_r}}_{(4)} + \underbrace{10 \log \frac{P_r}{P_n}}_{(5)}. \quad (1)$$

The first and fourth terms represent the losses in the transmission lines; the second term is the loss due to dispersion and absorption in the propagation path; the third term is the loss due to reradiation from the receiving antenna; and the fifth term expresses the input signal-to-noise ratio available at the receiver.

1.2 INSERTION OF REPEATERS

Due to the fact that topographical conditions arising from the substantially straight-line propagation of microwaves limit the practical length of single hops, relay stations have to be provided
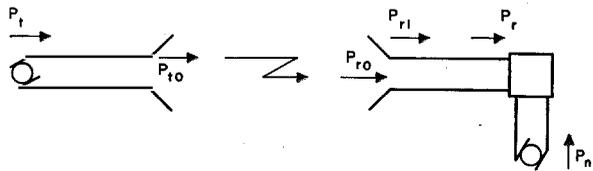
Figure 1—Power levels in single-hop transmission link.

at suitable intermediate sites between the terminal stations. Let us consider the case of n hops with $n-1$ relays.

Let $a_1, a_2, \cdots a_n$ be the numerical ratio of the radiated power at each relay to the available power at the next receiver. In (1), P_r/P_n should now be replaced by $P_{r1}/P_{n1} = P_t/a_1 P_{n1}$. In the case here considered, the outgoing power at each repeater is kept at the same level, this being generally adopted for the sake of equipment standardization and to conform to the case of cable repeaters. At the second repeater R_2, the available power is then P_t/a_2 and the available noise power is

$$P_{n1} + \frac{a_1 P_{n1}}{a_2}$$

so that

$$\frac{P_{r2}}{P_{n2}} = \frac{P_t/a_2}{P_{n1} + (a_1 P_{n1}/a_2)} = \frac{P_t}{a_1 P_{n1} + a_2 P_{n1}}.$$

The same reasoning gives immediately

$$\begin{aligned} \frac{P_{rn}}{P_{nn}} &= \frac{P_t}{P_{n1}(a_1 + a_2 + \cdots + a_n)} \\ &= \frac{P_{r1}}{P_{n1}} \frac{1}{1 + \frac{a_2}{a_1} + \frac{a_3}{a_1} + \cdots + \frac{a_n}{a_1}}. \end{aligned} \quad (2)$$

The fifth term of (1) is thus replaced by

$$10 \log \frac{P_{rn}}{P_{nn}}\left(1+\frac{a_2}{a_1}+\frac{a_3}{a_1}+\cdots+\frac{a_n}{a_1}\right).$$

In the case of equal hops, the terms in parentheses are equal to n. For all types of transmission systems for which the signal-to-noise output ratio is proportional to the signal-to-noise carrier ratio at the input of the last receiver, this means that an additional increase of $10 \log n$ in output power must be provided at each repeater. In case of unequal hops, the terms in parentheses should be computed according to the individual case.

2. Provision for Unfavorable Propagation Conditions

When unfavorable propagation conditions occur, whatever the causes may be, the factors $a_1, a_2, \cdots a_n$, valid for normal conditions, are individually multiplied by factors $\alpha_1, \alpha_2, \cdots \alpha_n$ according to the intensity of the fades in the various hops. Equation (2) thus becomes

$$\frac{P_{rn}}{P_n}=\frac{P_t}{P_{n1}(\alpha_1 a_1+\alpha_2 a_2+\cdots+\alpha_n a_n)}$$

$$=\frac{P_{r1}}{P_{n1}}\frac{1}{\left(\alpha_1+\frac{a_2}{a_1}\alpha_2+\cdots+\frac{a_n}{a_1}\alpha_n\right)}.$$

The fifth term of (1) is, consequently, replaced by

$$10 \log \frac{P_{rn}}{P_{nn}}\left(\alpha_1+\frac{a_2}{a_1}\alpha_2+\frac{a_3}{a_1}\alpha_3+\cdots+\frac{a_n}{a_1}\alpha_n\right).$$

In case of equal hops, this becomes

$$10 \log \frac{P_{rn}}{P_{nn}}(\alpha_1+\alpha_2+\cdots+\alpha_n).$$

Microwave links are generally designed to provide for a maximum fading α_M occurring on all hops simultaneously. In this case, the above expression becomes

$$10 \log \frac{P_{rn}}{P_{nn}} n\, \alpha_M.$$

The provision for fading is therefore $10 \log \alpha_M$. Should only m hops fade simultaneously, the signal-to-noise ratio would exceed by

$$10 \log \frac{n\, \alpha_M}{n-m+\sum_1 \alpha_m}$$

decibels the signal-to-noise ratio obtained in the case of maximum fading. On the other hand, the fading occurring on one hop can exceed α_M to the extent that the signal does not fall below the threshold value, under which for a given modulation system the whole link becomes inoperative.

The time distribution of fadings in a long chain of repeaters is not known with precision. For a
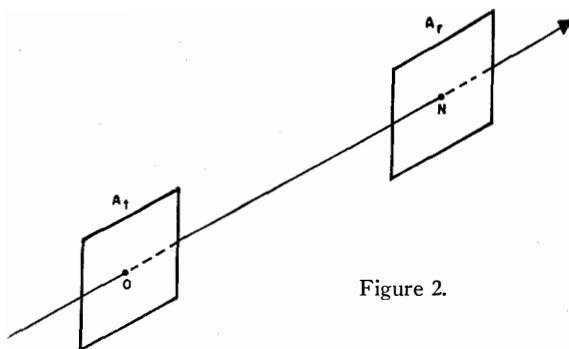
Figure 2.

hop distance of some 30 miles over land, experience indicates that fading does not exceed 20 decibels for more than 0.1 percent of the time. Fadings of that magnitude on all hops simultaneously will occur much less frequently, so that it is here considered justifiable to allow for a reduced output signal-to-noise ratio in the extreme case of 20-decibel simultaneous fading. Maximum performance would still be nearly obtained when such fades occur on only a few hops.

3. Attenuation in Propagation Path Under Favorable Conditions

What is meant here by favorable propagation conditions is the case when transmission may be considered as occurring in an unbounded, homogeneous, nondissipative medium (so called free-space propagation).

The discussion that follows is based on the fundamental assumption that any surface element δS in a wave front through which the flux of the Poynting vector is $P_0\, \delta S$ will produce at a distance L normal to δS a power flow in that direction equal to

$$P_0 \frac{\delta S^2}{\lambda^2 L^2},$$

where λ is the wavelength. This assumption originates from the diffraction theory and is found to lead to consistent results that are in good agreement with experimental facts.

Let two surfaces be considered, normal to ON of Figure 2. Let A_t be the transmitting surface and A_r the receiving surface. Let it be assumed that both surfaces are uniformly illuminated, the distance $ON = L$ being so large compared with the linear dimensions of the surfaces that all points of A_r may be considered at the same distance L from all points of A_t. The power that flows through A_r is then equal to

$$P_r = P_0 \frac{A_t^2}{\lambda^2 L^2} A_r ,$$

and the path attenuation is given by

$$\frac{P_{r0}}{P_{t0}} = \frac{A_t A_r}{\lambda^2 L^2}. \qquad (3)$$

In practice, however, the transmitting area will not be uniformly illuminated and a correction factor k_t will have to be introduced to take this into account. Conversely, the area A_r will not act uniformly on the associated antenna at the receiver, and this effect necessitates another correction factor k_r, which may be equal to k_t if identical structures are used at both ends of the transmission link. The path attenuation in power ratio can, therefore, be generally written as

$$\frac{P_{r0}}{P_{t0}} = \frac{k_t A_t \cdot k_r A_r}{\lambda^2 L^2}.$$

The second term of (1) is thus equal to

$$10 \log \frac{P_{t0}}{P_{r0}} = 10 \log \frac{\lambda^2 L^2}{k_t A_t k_r A_r}. \qquad (4)$$

Equation (4) can be put in a number of different forms, each of which will be found preferable for a particular problem.

3.1 PATH ATTENUATION EXPRESSED IN TERMS OF ANTENNA GAINS

Let the power P_{t0} be considered as emanating from a hypothetical "isotropic" antenna, that is to say, an antenna radiating equal power in all directions. The power flow per unit surface of A_r
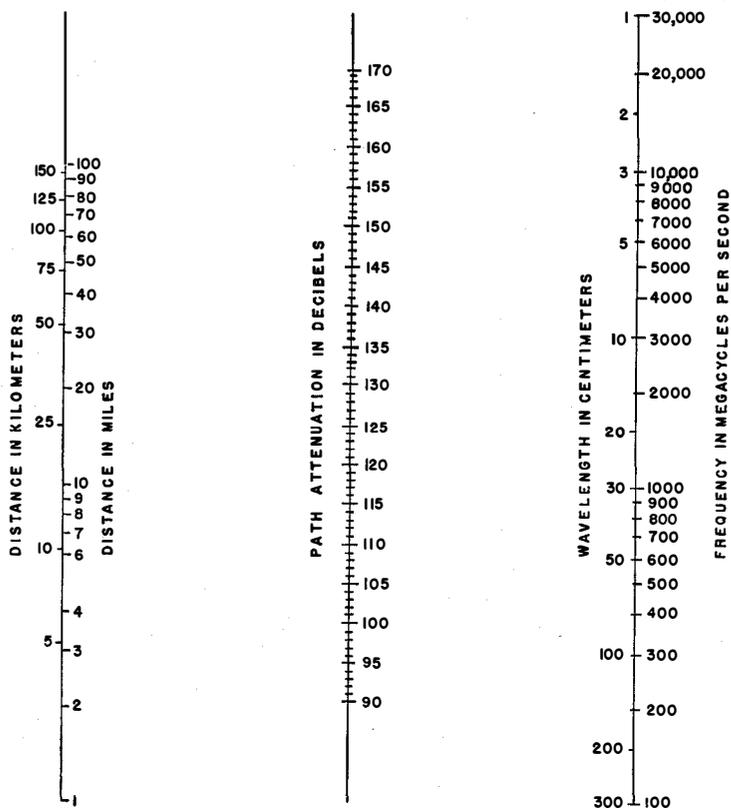
Nomograph 1—The above nomograph permits solution of the path attenuation between isotropic antennas for conditions of free-space propagation.

would be $P_{t0}/(4\pi L^2)$ and the total flow through A_r would be

$$\frac{P_{t0}}{4\pi L^2} A_r.$$

A comparison with (3) shows that the effective area of an isotropic antenna is equal to $\lambda^2/(4\pi)$. The gain of the actual antenna A_t over an isotropic antenna in the direction normal to A_t is, therefore, expressed in power by

$$G_t = \frac{k_t A_t}{\lambda^2/(4\pi)}.$$

The path attenuation in power ratio between two isotropic antennas is equal to $\lambda^2/(16\pi^2 L^2)$ and is given in Nomograph 1.

The path attenuation between actual antennas A_t and A_r is then expressed by

$$\frac{P_{r0}}{P_{t0}} = \left[\frac{P_{r0}}{P_{t0}}\right]_{\text{isot}} \times G_t G_r.$$

The antennas gains are measurable by comparison with an antenna, the gain of which is known with respect to the isotropic case. This determines the correction factors k_t and k_r. Nomograph 2 gives the gain of a parabolic antenna. An illumination factor 0.64 is assumed corresponding to average measurements.

Nomograph 2—Parabolic-antenna gain referred to an isotropic antenna. (Illumination factor = 0.64.)

3.2 PATH ATTENUATION EXPRESSED IN TERMS OF SOLID ANGLES

Mr. E. Labin has suggested that (4) may be written as follows:

$$10 \log \frac{P_{t0}}{P_{r0}} = 10 \log \frac{\lambda^2/(k_t A_t)}{(k_r A_r)/L^2}.$$

At distance L, the effective area $k_r A_r$ can be considered as viewed from the transmitter under the solid angle $(k_r A_r)/L^2 = \Omega_r$.

Let it be assumed that the total radiated power P_{t0} is concentrated uniformly in a solid angle Ω_t. The power flow per unit surface at distance L is then

$$\frac{P_{t0}}{L^2 \Omega_t}.$$

In the case of an isotropic antenna, it would be

$$\frac{P_{t0}}{4\pi L^2}.$$

The gain of the actual antenna over the isotropic source is, therefore,

$$G_t = \frac{4\pi}{\Omega_t} = \frac{4\pi k_t A_t}{\lambda^2}.$$

The equivalent transmitter solid angle is, consequently, equal to

$$\Omega_t = \frac{\lambda^2}{k_t A_t},$$

and the path attenuation can be written as

$$10 \log \frac{P_{t0}}{P_{r0}} = 10 \log \frac{\Omega_t}{\Omega_r}. \tag{5}$$

Applied to the case of a parabolic antenna with a circular aperture of diameter D, the above considerations lead to the definition of the equivalent cross-sectional angle a of the conical beam inside which the whole radiated power is assumed to be uniformly concentrated as indicated in Figure 3.

In this case, Ω_t is nearly equal to $(\pi/4)a^2$ and

$$a = \frac{4}{\pi (k_t)^{\frac{1}{2}}} \frac{\lambda}{D}.$$

Assuming $k_t = 0.64$, the value of a is nearly $1.6(\lambda/D)$.

The angle b, under which the receiver is viewed, is also easily evaluated. As $\Omega_r = (\pi/4)b^2$,

$$b = (k_r)^{\frac{1}{2}} \frac{D}{L} \simeq 0.8 \frac{D}{L}.$$

Figure 3—Antenna gain in terms of solid angles.

F = Frequency.
d_1 = Diameter of transmitting parabola.
a = Equivalent transmitting beam angle
$= (9/Fd) \cdot 10^4$.
A_0 = Attenuation
$= 10 \log (a/b)^2$.
b = Equivalent receiving angle
$= 0.15(d/l)$ as viewed from transmitter.
d_2 = Diameter of receiving parabola.
l = Distance between transmitter
and receiver.
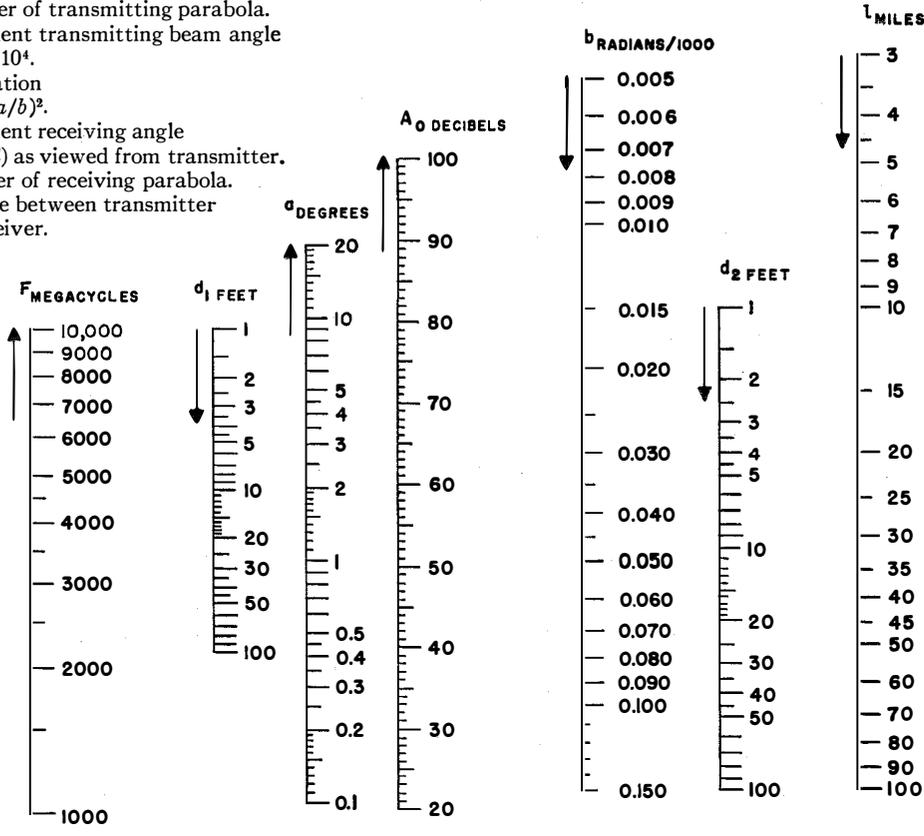
Nomograph 3—Free-space attenuation A_0 between parabolic reflectors.

In this case, (4) is very simply written as

$$10 \log \frac{P_{t0}}{P_{r0}} = 10 \log \left(\frac{a}{b}\right)^2. \qquad (6)$$

Nomograph 3 is based on this formula; the equivalent transmitting angle a and the angle b under which the receiver is seen from the transmitter can be determined separately on the nomograph in case different antennas are used on the transmitting and receiving sides.

Once a and b are found, the free-space attenuation is obtained in decibels.

The units used for distance are miles and the antenna diameters are in feet. The illumination factor is assumed to be 0.64, both for the transmitter and the receiver.

3.3 PATH ATTENUATION EXPRESSED IN TERMS OF DISTANCES

Replacing a and b by their expressions in (6) for the case of identical parabolic antennas at the transmitter and the receiver, the following relation is obtained.

$$10 \log \frac{P_{t0}}{P_{r0}} = 20 \log \frac{L}{D^2/(2\lambda)}. \qquad (7)$$

The quantity $D^2/(2\lambda)$ is nearly equal to the maximum distance at which the transmitted beam can be considered as remaining cylindrical (Fresnel region). It is the maximum distance at which a reflector of the same size as the transmitting antenna can be placed to intercept the beam without substantial dispersion losses. Equation

(7) is useful when so-called "passive" repeaters are considered in the microwave transmission chain.

4. Determination of Minimum Carrier Signal-to-Noise Ratio

The fifth term of (4), that is to say the required ratio of available carrier power to available noise power, will now be considered.

4.1 SPECIFICATION OF OUTPUT SIGNAL-TO-NOISE RATIO FOR MULTIPLEX TELEPHONY AND TELEVISION

The requirements of the Comité Consultatif International Téléphonique lead, in the case of multiplex telephony, to a signal-to-noise ratio of the order of 55 decibels, line weighted. This will be provided for by some 45 decibels of signal-to-noise ratio, unweighted. As mentioned before, however, this ratio is not considered necessary here in case of maximum fading, which occurs only a very small percentage of the time. As a provision of 20 decibels is generally adhered to for fading, the computation of carrier-to-noise ratio may safely be based on a 35-decibel output signal-to-noise ratio in case of simultaneous 20-decibel fades.

Under the same conditions, an output signal-to-noise ratio of 25 decibels will provide satisfactory transmission of television signals.

The following computations are based on these specifications.

4.2 NOISE POWER AT THE TERMINAL RECEIVER —RECEIVER NOISE FACTOR

The dominating noise source at the input terminals of the receiver will most generally be the thermal noise in the input impedance. The available power is expressed by KTB, where K is Boltzman's constant, T is the absolute temperature, and B is the root-mean-square value of the receiver bandwidth. For normal ambient temperatures, this amounts to $0.4 \cdot 10^{-14}$ watt per megacycle. For a temperature of 40 degrees centigrade, the noise power is increased by approximately $\frac{1}{2}$ decibel.

The electron tubes or mixers introduce other sources of noise, which are generally accounted for by a noise factor F, such that the apparent available noise power is expressed as $0.4F \cdot 10^{-20}$ watt per cycle. For microwave receivers up to 6000 megacycles per second, the noise factor varies between 10 and 40 with presently available tubes. A value of 25 may be taken as a basis for the predetermination of carrier power requirements. Expressed in decibels, this means that the effective noise level is some 14 decibels above thermal noise.

The additional noise due to external sources influencing the antenna (such as cosmic noise) may result in an apparent higher antenna temperature bringing the input noise power (available) to KT_aB instead of KT_0B. The tube noise sources of the receiver contribute $(F-1)KT_0B$, F having been measured at room temperature. The effective noise figure is then expressed by F' such that

$$F'KT_0B = (F-1)KT_0B + KT_aB,$$
$$F' = F - 1 + (T_a/T_0).$$

For microwave receivers, T_a/T_0 remains appreciably smaller than $F-1$, which is of the order of 24 as mentioned before, and cosmic noise remains, therefore, negligible.

The bandwidth B is determined by the nature of the modulation system utilized and the specified requirements as to over-all distortion. In certain cases, an additional bandwidth is required to take account of the cumulative selectivity of the successive repeaters, unless corrective networks are introduced along the chain.

4.3 SIGNAL-TO-NOISE RATIO IMPROVEMENT

A number of transmission systems (such as those utilizing pulse-position, pulse-code, and frequency modulations) provide for an improvement in signal-to-noise ratio between the carrier conditions and the final output signals. This is done at the cost of an increase in bandwidth. The value of the improvement has been the subject of numerous theoretical studies, and experimental verifications and figures are available in the literature. The value of the improvement factor expressed in decibels reduces by as many decibels the signal-to-noise ratio required on the carrier side and, consequently, the minimum input-signal level. To provide for this signal-to-noise improvement, however, the carrier must remain at a certain minimum level with respect to the noise power. When the bandwidth utilized allows the incoming signal to reach this threshold value, there is no further advantage to be obtained by increasing it any more.
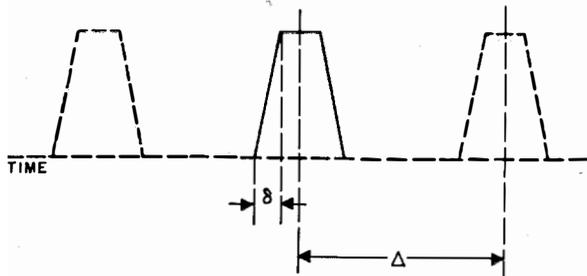
Rise time $\delta = 0.15$ microsecond.
Maximum displacement amplitude $\Delta = 1$ microsecond.
Pulse duration at base $= 0.5$ microsecond.
Guard interval between closest adjacent pulses
$= 2.7$ microseconds.
Time intervals allocated per channel $= 5.2$ microseconds.

Figure 4—Time intervals for the pulse-time-multiplex
equipment Type *10B*.

4.4 APPLICATION TO *10B* EQUIPMENT

Federal Telecommunication Laboratories equipment Type *10B* is a pulse-time multiplex radio system that can provide for 23 telephone channels. The repetition rate of the pulses is 8000 cycles. The repetition period of 125 microseconds is divided into 24 intervals of 5.2 microseconds each, the 24th interval being used for a marker signal from which a synchronized voltage is obtained at the receiver to enable separation and demodulation of the voice channels. The modulation of the pulse is by displacement proportionally to the modulating voltage of its position with respect to its unmodulated position. The various time intervals involved are shown schematically in Figure 4.

Table 1 lists the essential characteristics of the system.

TABLE 1
ESSENTIAL CHARACTERISTICS OF *10B* EQUIPMENT

Mean radiated power	2 watts
Receiver radio-frequency bandwidth	8 megacycles
Available thermal noise power at receiver input	$3.2 \cdot 10^{-14}$ watt per megacycle
Receiver noise factor	14 decibels
Total available noise power at receiver input	$0.8 \cdot 10^{-12}$ watt per megacycle
Path attenuation under favorable propagation conditions (2000 megacycles, 10-foot parabolas, 50 miles)	70 decibels
Receiver transmission-line losses	6 decibels
Reradiation loss	3 decibels
Mean power at receiver input under above conditions	$2.5 \cdot 10^{-8}$ watt
Maximum carrier peak power at receiver (10 percent duty cycle)	$25 \cdot 10^{-8}$ watt

The signal-to-noise-ratio improvement is found both theoretically and experimentally to be determined to a good approximation as follows.

$$\left(\frac{S_{\text{peak}}}{N_{\text{peak}}}\right)_{\text{out}} = \frac{\Delta}{\delta}\left(\frac{\text{Carrier}_{\text{peak}}}{N_{\text{peak}}}\right)_{\text{inp}}.$$

This leads to

$$\left(\frac{P_{\text{signal}}}{P_n}\right)_{\text{out}} = \left(\frac{\Delta}{\delta}\right)^2 \frac{P_{\text{carrier peak}}}{P_{n(\text{input})}}.$$

The receiver input conditions would, therefore, give under normal propagation conditions the following output signal-to-noise ratio.

$$10 \log \left(\frac{1}{0.15}\right)^2 \frac{25 \cdot 10^{-6}}{0.8 \cdot 10^{-12}} = 71 \text{ decibels.}$$

This will be limited in practice, however, by the signal-to-noise ratio of the terminal equipment. Adopting as previously explained a minimum figure of 35 decibels for the unweighted output signal-to-noise ratio in case of 20-decibel fades (that is to say for approximately 0.1 percent of the operating time) a provision of $71 - 55 = 16$ decibels remains available for the insertion of repeater points. The equipment is, therefore, designed to operate over distances of more than 500 miles with satisfactory performance.

4.5 APPLICATION TO FREQUENCY-MODULATION SYSTEMS

The following will apply to the case of a link so designed that it can transmit either one television channel or a certain number of simultaneous telephone channels transposed in frequency according to the frequency-division scheme.

Let it first be required to transmit a video-frequency bandwidth $b = 4.5$ megacycles over a total distance of some 4000 miles, with a maximum of 100 repeater stations. A signal-to-noise output ratio for the video-frequency signals of 25 decibels in case of simultaneous 20-decibel fades on all hops will be considered as satisfactory. This will provide for a 45-decibel ratio under favorable propagation conditions, which is more than adequate for television. The figure of 25 decibels will obtain for a small fraction of the operating time only.

The radio-frequency bandwidth B is related to b and the modulation index m by the condition that the unavoidable distortion due to sideband clipping should not exceed more than a few percent. The condition

$$2(m+1)b = B$$

may be considered as acceptable in this case.

The available thermal-noise power generated at each repeater will be assumed to be the only significant source of external noise. This is equal to

$$P_n = 0.4 \cdot 10^{-14} B$$

in watts, where B is expressed in megacycles.

The level to be assigned above P_n for the radiated output power P_{t0} at each repeater is obtained as shown in Table 2.

TABLE 2

REQUIRED REPEATER OUTPUT POWER

Factor	Power in Decibels
Average receiver noise factor	+ 14
Local loss in receiver transmission line	+ 2
Reradiation loss at receiving antenna	+ 3
Provision for 25-decibel (unweighted) signal-to-noise ratio	+ 25
Provision for simultaneous 20-decibel fades	+ 20
Provision for free-space attenuation (4000 megacycles, 40-mile hops, 10-foot antennas)	+ 60
Provision for 100 repeaters	+ 20
Signal-to-noise improvement	− I
TOTAL	$+144 - I$

The required radio-frequency power P_{t0} is, therefore, given by

$$10 \log P_{t0} = 10 \log P_n + (144 - I).$$

The required transmitter power P_t (assuming a 2-decibel loss in the transmission line) is given by

$$10 \log P_t = 10 \log P_n + 146 - I.$$

The signal-to-noise improvement I is equal to $10 \log 3m^2$ as compared with the carrier signal-to-noise ratio in the case of double-sideband amplitude modulation. Therefore

$$P_n = 0.4 \cdot 10^{-14} (2b)$$
$$10 \log P_t = 10 \log 2b + 2 - I.$$

However, P_t must remain above the threshold at the receiver, which means that it must exceed the noise power by a minimum of 9 decibels even in the case of 20-decibel fades. The minimum value P_t' required to achieve this is given by

$$10 \log P_t' = 10 \log B - 14.$$

Values of P_t and P_t' for various values of m are listed in Table 3.

TABLE 3

m	I in Decibels	B in Megacycles	P_t in Watts	P_t' in Watts
1	4.8	18	4.7	0.7
2	10.8	27	1.2	1.1
3	14.4	36	0.5	1.45
4	16.8	45	0.3	1.8

Now, let the number of possible telephone channels be determined for the same radio-frequency bandwidth and power. The minimum output signal-to-noise ratio (unweighted) must be increased in this case to conform to standard requirements. It is considered that 35 decibels for 20-decibel fades, and consequently 55 decibels under favorable propagation conditions, gives an entirely satisfactory performance. The improvement factor in this case becomes, therefore, $I' = 10 + I$ (in decibels). On the other hand, the relation between m', b', and B (m' and b' are the new values of modulation index and modulating bandwidth) must be altered to provide for the required protection against cross talk between channels. This means that the number of sidebands to be kept in the radio-frequency band must be increased and computations show that for relatively low modulation indexes, the following equation is acceptable.

$$2(m'+5)b' = B.$$

Table 4 gives the number of telephone channels for the same cases previously examined. Questions of repeater circuitry might, of course, intervene and lead to a further limitation, particularly in the case of a great number of repeaters.

The number of channels does not increase enough to warrant the increase in bandwidth. These considerations lead to the choice of an 18-megacycle band, 5 watts of radio-frequency

power being capable of transmitting one 4.5-megacycle television channel or some 280 telephone channels (provided sufficient circuit linearity is achieved).

TABLE 4

NUMBER OF TELEPHONE CHANNELS

m	I	I'	m'	B	P_t	b' in Kilocycles	Number of Channels
1	4.8	14.8	3	18	5	1125	281
2	10.8	20.8	6	27	1.2	1230	307
3	14.4	24.4	9	36	1.5	1285	321
4	16.8	26.8	12	45	1.8	1320	330

To provide for the possibility of future television transmission systems, a second type of equipment might be considered with a video-frequency bandwidth of the order of 10 megacycles. This leads to a radio-frequency band of some 40 megacycles and a radio-frequency power of at least 10 watts. This equipment could accommodate two 4.5-megacycle television channels or some 560 telephone channels.

4.6 APPLICATION TO PULSE-CODE MODULATION

To achieve a comparable performance with the 18-megacycle system described in Section 4.5, a pulse-code-modulation system should make use of a 7-digit binary code. The number of pulses per second would therefore be

$$7 \times 300 \times 4000 \times 2 = 16.8 \cdot 10^6.$$

This could be transmitted by means of double-sideband amplitude modulation or low-modulation-index frequency modulation in a bandwidth of 18 megacycles. Barring consideration of single-sideband transmission, a comparison can, therefore, be established on the basis of the same radio-frequency bandwidth and, consequently, the same thermal-noise power generated at each repeater. The levels required in both cases above this thermal-noise power (available) are given in Table 5.

TABLE 5

LEVELS IN DECIBELS REQUIRED ABOVE THERMAL-NOISE POWER

Factor	Frequency-Division-Multiplex Frequency Modulation	Time-Division-Multiplex Pulse-Code Modulation
Average receiver noise factor	+ 14	+ 14
Local loss in receiver transmission line	+ 2	+ 2
Reradiation loss at receiving antenna	+ 3	+ 3
Provision for 35-decibel (unweighted) signal-to-noise ratio	+ 35 − I	+ 18
Provision for simultaneous fades	+ 20	+ 20
Provision for free-space attenuation	+ 60	+ 60
Provision for 100 repeaters	+ 20	+ 3
TOTAL	+154 − I	+120

The difference in favor of pulse-code modulation is $34 - I$ decibels. As I is in this case equal to 17 decibels, the advantage of pulse-code-modulation is a reduction in power of approximately 17 decibels, the radio-frequency power required being 0.1 watt instead of 5 watts. The frequency-modulation link, however, would remain operative in case of fades deeper than 20 decibels up to some 27 decibels where the threshold would be reached. The pulse-code-modulation link could not stand such deep fades, the output signal-to-noise ratio deteriorating very quickly in case of fades in excess of 20 decibels.

Such a comparison is far from complete, as it deals with power and bandwidth requirements only and does not attempt to balance the circuit difficulties or expenses. It can, at least, be said that the comparison becomes more and more in favor of pulse-code modulation as the number of repeaters in the transmission chain is increased.

Reflection Cancellation in Waveguides[*]

By L. LEWIN

Standard Telecommunication Laboratories, Limited, London, England

A TAPER is a part of a waveguide system where the cross-section varies in a uniform manner. It is commonly used to provide a smooth transition from waveguides of one size of cross-section to another. It can also be used to enlarge the mouth of a radiating waveguide so as to provide a better termination, and also to control to some extent the radiation polar diagram. To be substantially reflection-free, the taper should be at least a half wavelength long, and the longer and more gradual it is, the better. At the join with the uniform waveguide, however, there will always be a small reflection, and the taper may have to be inconveniently long if this reflection is required to be very small. These reflections show up particularly when two different waveguides are joined by a tapered section, and the frequency of the source is varied. If the far waveguide is matched, the input standing-wave ratio of the near waveguide will vary rapidly with frequency, the variations being the more rapid, and their amplitude the smaller, as the length of the taper increases. Minima of total reflection occur when the taper length is an even number of quarter wavelengths, and maxima of reflection when it is an odd number. It follows that for narrow bands, the reflection can be kept low by appropriately choosing the taper length, but not so for broad bands. Hence it is important to know how long a taper must be in order to reduce the reflections at the joins below a given value, and also to know in what way these reflections can be cancelled, thus permitting the use of a shorter taper than would otherwise have been required. Both these effects are investigated.

1. Method of Analysis

Three separate cases are investigated and are shown in Figures 1, 2, and 3. In Figure 1, the narrow side of a rectangular waveguide, of cross-section $a \times b$, is flared from b to d in a taper of length L. The broad side a is constant. In Figure 2, the broad side a is tapered to a width D in a taper of length L, the narrow side being unchanged. In Figure 3, the cross-section $a \times b$ is tapered to $D \times d$ in a length L, it being supposed, for the time being, that the four tapered sides meet in a point, so that $a/b = D/d$. In each case, a dominant waveguide mode, with a reflected mode at the taper, is assumed to exist in the uniform guide, while an outgoing wave is assumed to exist in the taper. This outgoing wave is chosen to be the dominant mode for the natural co-ordinate space of the taper under consideration; i.e., cylindrical co-ordinates for tapers 1 and 2, and spherical co-ordinates for taper 3. The choice of only the dominant modes is permissible provided that the tapers are not too abrupt. In
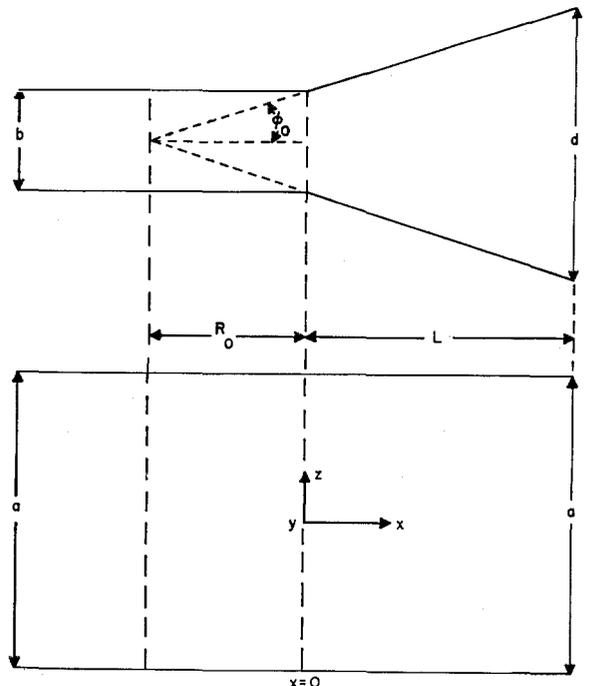
Figure 1—Taper in narrow side of waveguide.

practice this means that the angles of the tapers are assumed small, so that the distance R_0 from the virtual apex of the taper to the cross-section

Figure 2—Taper in broad side of waveguide.

at the join, is substantially constant in any one plane parallel to the plane of the taper. It follows that the equiphase surface defined by the outgoing wave in the taper coincides substantially with that defined by the waveguide dominant mode at the position of the join. It only remains to choose the various amplitudes appropriately to satisfy the boundary conditions, namely continuity of E and H at the join. These continuity conditions, which should hold, strictly, all over the cross-section, will be applied at the centre only. (The effect of applying it at other points is to bring into account just that variation of R_0 over the cross-section discussed above, and for which higher-order modes would have to be introduced. This is avoided by limiting the treatment to those cases for which R_0 is substantially constant over the cross-section; i.e., to moderate tapers only.)

1.1 TAPER IN NARROW SIDE

Referring to Figure 1, let ϕ_0 be the semi-angle of the taper, so that $R_0 = (b/2) \cot \phi_0$, R_0 being measured from the virtual apex to the join. De-

fining a reflection coefficient r and a transmission coefficient t, we can write for region 1 (waveguide) and region 2 (taper)

$$\left. \begin{aligned} {}_1E_y &= \cos \frac{\pi z}{a}(e^{-jk'x} + re^{jk'x}), \\ {}_1H_z &= \cos \frac{\pi z}{a}(e^{-jk'x} - re^{jk'x})\frac{k'}{k}, \end{aligned} \right\} \tag{1}$$

with $\qquad k = \dfrac{2\pi}{\lambda}; \qquad k' = \dfrac{2\pi}{\lambda_g} = \dfrac{2\pi}{\lambda}\left(1 - \dfrac{\lambda^2}{4a^2}\right)^{\frac{1}{2}}.$

$$\left. \begin{aligned} {}_2E_\phi &= t \cos \frac{\pi z}{a}\mathbf{H}_1^{(2)}(k'R), \\ {}_2H_z &= t \cos \frac{\pi z}{a}\mathbf{H}_0^{(2)}(k'R)\frac{jk'}{k}. \end{aligned} \right\} \tag{2}$$

Let us equate ${}_1E_y = {}_2E_\phi$ and ${}_1H_z = {}_2H_z$ at $x = 0$, $z = 0$, $R = R_0 = (b/2) \cot \phi_0$.

This gives

$$\left. \begin{aligned} 1 + r &= t\mathbf{H}_1^{(2)}\left(k'\frac{b}{2} \cot \phi_0\right), \\ 1 - r &= jt\mathbf{H}_0^{(2)}\left(k'\frac{b}{2} \cot \phi_0\right). \end{aligned} \right\} \tag{3}$$

Hence

$$\frac{1+r}{1-r} = \frac{\mathbf{H}_1^{(2)}\left(k'\dfrac{b}{2} \cot \phi_0\right)}{j\mathbf{H}_0^{(2)}\left(k'\dfrac{b}{2} \cot \phi_0\right)}.$$

Figure 3—Waveguide with double taper $(a/b = D/d)$.

Since ϕ_0 is assumed small, $k'(b/2) \cot \phi_0$ will in general be large enough to permit the use of the asymptotic expansions of the Bessel functions, giving, after some reduction

$$(1+r)/(1-r) \approx 1 - j/(k'b \cot \phi_0). \qquad (4)$$

If a reactance jX is put across a matched line, it can be shown that the reflection coefficient is $-1/(1+2jX/Z_0)$, so that

$$(1+r)/(1-r) = 1/(1+Z_0/jX).$$

This can be put equal to $1+jZ_0/X$, if X is large. Comparing with (4) we see that the effect of the taper is to introduce a negative *parallel reactance* of value $k'b \cot \phi_0$ relative to the Z_0 of the waveguide. Hence the standing-wave ratio, given by $\rho = (1 - |r|)/(1 + |r|)$ is approximately

$$\rho = 1 - 1/(k'b \cot \phi_0). \qquad (5)$$

Introducing the length of taper L, we have $\cot \phi_0 = 2L/(d-b)$.

Hence

$$\rho = 1 - \lambda(d-b)/[4\pi L b(1 - \lambda^2/4a^2)^{\frac{1}{2}}]$$
$$= 1 - \lambda_g(d-b)/4\pi L b. \qquad (6)$$

(It should be noted that this equation assumes that the far end of the taper is, in some way, matched. If this is not so, additional reflections are caused which, as explained above, will interfere with the reflection at the join, causing beating effects.)

As an example, assume a 3-inch $\times$ 1-inch waveguide, with the 1-inch side tapered to 2 inches in a distance of 4 inches. Let $\lambda = 10$ centimetres, so that $\lambda_g = 13 \cdot 3$ centimetres.

$$\rho = 1 - \frac{13 \cdot 3}{2 \cdot 54} \cdot \frac{2-1}{4 \times 1 \times 12 \cdot 56} = 1 - 0 \cdot 1 = 0 \cdot 9.$$

If a matched 3-inch $\times$ 2-inch guide is now joined at the far end of the taper, the reflection there, obtained by interchanging b and d in (6), will be, in this example, half that occurring at the 1-inch end. Since 4 inches is very nearly $3\lambda_g/4$, the reflections will add in phase, giving a total standing-wave ratio of $1 - 0 \cdot 1 - 0 \cdot 05 = 0 \cdot 85$.

2. *Reflection Cancellation*

Since the reflection is the same as that from a shunt capacitance, the provision of an inductive diaphragm at the join should provide adequate compensation. This can conveniently take the form of two thin metal strips protruding into the waveguide from the narrow side by a distance δ. The inductance (relative to Z_0) thereby introduced is given by[1]

$$X_L = (a/\lambda_g) \cot^2 (\pi\delta/a). \qquad (7)$$

Equating this to $k'b \cot \phi_0$, the negative reactance introduced at the join, we get an equation for δ,

$$\cot (\pi\delta/a) = [4\pi b L/a(d-b)]^{\frac{1}{2}}. \qquad (8)$$

For moderate tapers, $\pi\delta/a$ will not be large, and we can write

$$\delta = (a/2\pi)[a(d-b)/\pi b L]^{\frac{1}{2}}. \qquad (9)$$

This equation shows, since λ does not occur, that the compensation is, to the order we are considering, independent of frequency, and we can certainly expect the effect to be very broad-band in practice. As an example, let us find what depth of diaphragm is needed to compensate for the 1-inch to 2-inch taper in a 3-inch $\times$ 1-inch guide, with a 4-inch length of taper. Equation (9) gives

$$\delta = \frac{3}{6 \cdot 28}\left(\frac{3}{3 \cdot 14}\frac{2-1}{1 \cdot 4}\right)^{\frac{1}{2}} = 0 \cdot 234 \text{ inch.}$$

The resulting arrangement is shown in Figure 4.

At the far end of the taper, if we again go to a uniform waveguide, the sign of reflection re-
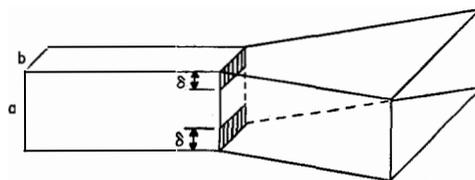
Figure 4—Expanding taper in narrow side compensated by inductive diaphragm.

verses, as may be seen by interchanging b and d in (6). Hence the effect there is *inductive*, and a shunt capacitance is needed for compensation.

---

[1] G. L. Ragan, "Microwave Transmission Circuits," McGraw-Hill Book Company, New York, New York; p. 211.
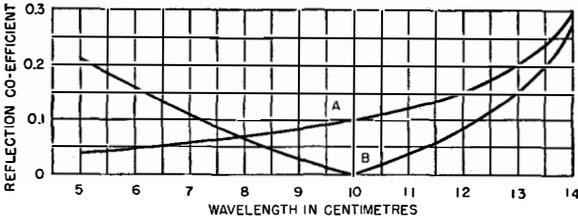
Figure 5—Theoretical frequency response of expanding-taper to waveguide combination ($d=3$ inches); taper in broad side. A uncompensated, B compensated.

This can take the form of a diaphragm of two strips protruding a distance δ into the guide from the broad side.

For such a diaphragm we have[1]

$$X_c = -\frac{\lambda_g/4b}{\log_e (\sec \pi\delta/b)}, \qquad (10)$$

so that the equation for δ becomes, since d now replaces b as the narrow side,

$$\frac{\lambda_g/4b}{\log_e (\sec \pi\delta/d)} = (2\pi/\lambda_g)d \cot \phi_0. \qquad (11)$$

Here $\cot \phi_0 = 2L/(d-b)$ as before.

For moderate tapers, δ will be small, so that we can write

$$\log_e (\sec \pi\delta/d) \approx \log_e \left[1+\tfrac{1}{2}(\pi\delta/d)^2\right] \approx \tfrac{1}{2}(\pi\delta/d)^2$$

giving

$$\delta \approx (\lambda_g/2\pi)[(d-b)/2\pi L]^{\frac{1}{2}}. \qquad (12)$$

This differs from the previous case (9) in that δ now depends on frequency, since λ_g occurs in (12). For example, if the uncorrected taper to a 3-inch broad guide gives a reflection coefficient of 0·1 at $\lambda = 10$ centimetres, and this is corrected by a capacitive iris at this wavelength, then the resultant response will be as curve B in Figure 5. Curve A shows the response of the uncorrected taper. It will be seen that compensation is possible over a reasonable band. Figure 6 shows the arrangement of the diaphragm.

2.1 Taper in Broad Side

Referring to Figure 2, let θ_0 be the semi-angle of the taper, so that $R_0 = (a/2) \cot \theta_0$. Proceeding

as before, we have:

$$\left.\begin{aligned} {}_1E_y &= \cos \frac{\pi z}{a}(e^{-ik'x}+re^{ik'x}), \\ {}_1H_z &= \cos \frac{\pi z}{a}(e^{-ik'x}-re^{ik'x})\frac{k'}{k}, \end{aligned}\right\} \qquad (13)$$

$$\left.\begin{aligned} {}_2E_y &= t \cos (\theta\psi)\mathbf{H}_\psi^{(2)}(kR), \\ {}_2H_\theta &= jt \cos (\theta\psi)\mathbf{H}_\psi^{(2)\prime}(kR), \end{aligned}\right\} \qquad (14)$$

where $\psi = \pi/2\theta_0$. The field forms in region 2 are chosen so as to give zero tangential electric field at $\theta = \pm\theta_0$; i.e., on the metal surface of the taper.
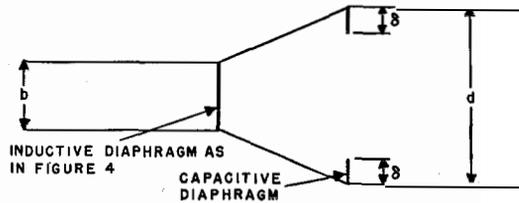
Figure 6—Compensation for narrow-side taper (expanding-taper to waveguide).

If we match the fields at $x=z=0$, $\theta=0$, $R=R_0=(a/2) \cot \theta_0$, we get

$$\left.\begin{aligned} 1+r &= t\mathbf{H}_\psi^{(2)}(\tfrac{1}{2}ka \cot \theta_0), \\ 1-r &= jt\frac{k}{k'}\mathbf{H}_\psi^{(2)\prime}(\tfrac{1}{2}ka \cot \theta_0). \end{aligned}\right\} \qquad (15)$$

Hence

$$\frac{1+r}{1-r} = \frac{(k'/k)\mathbf{H}_\psi^{(2)}(\tfrac{1}{2}ka \cot \theta_0)}{j\mathbf{H}_\psi^{(2)\prime}(\tfrac{1}{2}ka \cot \theta_0)}. \qquad (16)$$

Now for θ_0 small, $\frac{\tfrac{1}{2}ka \cot \theta_0}{\pi/2\theta_0} \approx 2\frac{a}{\lambda}$ which is greater than, but of order, unity. Also, since $\pi/2\theta_0$ is large, this means that we are interested in the expansion of Bessel functions of large order, whose argument is greater than the order. An expression for $\mathbf{H}_\nu(\nu \sec \beta)$ exists[2] when ν is large and β acute, from which can be derived the relation

$$\frac{\mathbf{H}_\nu^{(2)}(\nu \sec \beta)}{\mathbf{H}_\nu^{(2)\prime}(\nu \sec \beta)} \approx \frac{1+j/(2\nu \sec \beta \sin^3 \beta)}{-j \sin \beta}.$$

[2] G. N. Watson, "A Treatise on the Theory of Bessel Functions," Cambridge University Press, Cambridge, England; p. 228.

Putting $\nu \sec \beta = x$, $\sin \beta = (1 - \nu^2/x^2)^{\frac{1}{2}}$, we get

$$\frac{\mathbf{H}_\nu^{(2)}(x)}{\mathbf{H}_\nu^{(2)'}(x)} \approx j\frac{1 + j/[2x(1 - \nu^2/x^2)^{\frac{1}{2}}]}{(1 - \nu^2/x^2)^{\frac{1}{2}}}. \quad (17)$$

In our case $\nu = \pi/2\theta_0$, $x = \frac{1}{2}ka \cot \theta_0$, $\nu/x \approx \lambda/2a$; substituting into (16) gives

$$\frac{1+r}{1-r} = 1 + \frac{j}{ka \cot \theta_0 (1 - \lambda^2/4a^2)^{\frac{1}{2}}}. \quad (18)$$

This means that the discontinuity is equivalent to an inductive reactance whose value, relative to Z_0, is

$$X_L = ka \cot \theta_0 (1 - \lambda^2/4a^2)^{\frac{1}{2}}. \quad (19)$$

2.2 CANCELLATION OF THE REFLECTION

As in (10) the reflection can be cancelled by a capacitive diaphragm, whose insertion δ in the broad side is given by

$$\frac{\lambda_g}{4b \log (\sec \pi\delta/b)} = \frac{2\pi a}{\lambda}\left(1 - \frac{\lambda^2}{4a^2}\right)^{\frac{3}{2}} \cot \theta_0. \quad (20)$$

Writing $\log (\sec \pi\delta/b) = \frac{1}{2}(\pi\delta/b)^2$ as before, and using the relation $\cot \theta_0 = 2L/(D-a)$ we get an approximate equation for δ.

$$\delta \approx \frac{\lambda}{(1 - \lambda^2/4a^2)} \cdot \frac{1}{2\pi} \cdot \left[\frac{(D-a)b}{2\pi aL}\right]^{\frac{1}{2}}. \quad (21)$$

The dependence of the response on frequency is shown in Figure 7, for the example of a 3-inch waveguide where the uncorrected taper gives a reflection of 0·1 at $\lambda = 10$ centimetres. In Figure 7, A is the uncompensated response, and B corrected with a capacitive diaphragm designed according to (21). Although the response is poorer
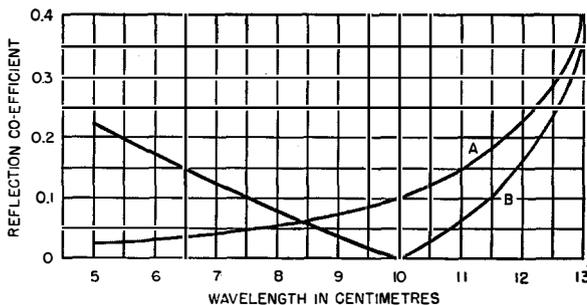
Figure 7—Theoretical frequency response of waveguide to expanding-taper combination ($a = 3$ inches); taper in broad side. A uncompensated, B compensated.

than in Figure 6, a reasonable bandwidth suitable for most purposes can now be covered. The diaphragm arrangement is shown in Figure 8.

In the second case, when we go from taper to waveguide of dimensions $D \times b$, the reflection is as from a capacitance,

$$X_c = kD \cot \theta_0 (1 - \lambda^2/4D^2)^{\frac{1}{2}},$$

where $\cot \theta_0 = 2L/(D-a)$. The compensating inductive diaphragm has an insertion in the narrow side of amount δ given by

$$\frac{D}{\lambda_g} \cot^2 \frac{\pi\delta}{D} = \frac{2\pi D}{\lambda}\left(1 - \frac{\lambda^2}{4D^2}\right)^{\frac{3}{2}} \cdot \frac{2L}{D-a}, \quad (22)$$

or, approximately

$$\delta = (D/2\pi)\{(D-a)/[2L(1 - \lambda^2/4D^2)]\}^{\frac{1}{2}}. \quad (23)$$

This arrangement is very frequency insensitive, since in practice D is considerably greater than $\lambda/2$.

3. Double Taper

The difficulty in applying the method of the previous two cases to the double taper is that two contiguous sides of the double taper do not constitute a pair of orthogonal surfaces, so that the normal method of resolution of the wave equation into orthogonal co-ordinate systems is not applicable here. It does not seem worthwhile to go to generalized curvilinear co-ordinates to solve this problem, but it appears possible to get a reliable result by using spherical polar co-ordinates. This method suggests itself in the particular case in which the four sides of the taper meet at a point, the virtual apex of the taper. Actually, the surfaces appropriate to spherical co-ordinates, $\phi = $ constant and $\theta = $ constant are respectively planes and cones, but if the angle ϕ_0 is small, the small part of the conical surface considered will not differ sensibly from a flat surface. In fact, the replacement causes a dip at the centre of the horn aperture of $(D/2)(1 - \cos \phi_0)$, which is a second-order correction. Referring to Figure 3, the four sides of the taper will be taken as $\theta = \pm\theta_0$ and $\theta = \pm\phi_0$ for the broad and narrow sides respectively.

In the waveguide we have as before

$$_1E_y = \cos \frac{\pi z}{a}[e^{-jk'x} + re^{jk'x}],$$
$$_1H_z = \cos \frac{\pi z}{a}[e^{-jk'x} - re^{jk'x}]\frac{k'}{k}, \qquad (24)$$

and in the double taper

$$_2E_\phi = \frac{t}{R}[R^{\frac{1}{2}}\mathbf{H}_{n+\frac{1}{2}}^{(2)}(kR)]\cos\phi$$
$$\times [A\mathbf{P}_n'(\sin\theta) + B\mathbf{Q}_n'(\sin\theta)],$$
$$_2H_\theta = \frac{jt}{kR}\cdot\frac{d}{dR}[R^{\frac{1}{2}}\mathbf{H}_{n+\frac{1}{2}}^{(2)}(kR)]\cos\phi \qquad (25)$$
$$\times [A\mathbf{P}_n'(\sin\theta) + B\mathbf{Q}_n'(\sin\theta)].$$

Here A and B have to be chosen so that $A\mathbf{P}_n'(\sin\theta) + B\mathbf{Q}_n'(\sin\theta)$ is symmetrical about $\theta = 0$ and n is such that, when A and B have been
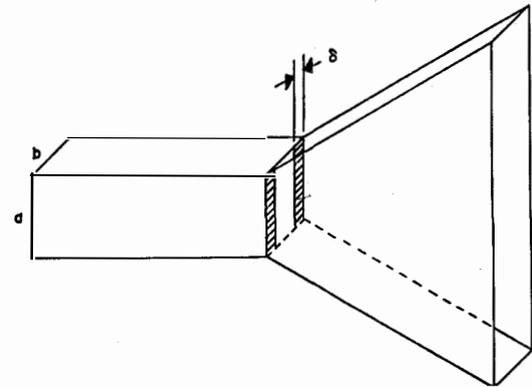
Figure 8—Expanding taper in broad side compensated by capacitive diaphragm.

so chosen, $A\mathbf{P}_n'(\sin\theta_0) + B\mathbf{Q}_n'(\sin\theta_0) = 0$. This latter is the condition for zero tangential electric field at the sides of the taper $\theta = \pm\theta_0$. A glance at curves of $\mathbf{P}_n'$ and $\mathbf{Q}_n'$ shows that, for small θ_0, n is large, so that it is permissible to use asymptotic expansions of $\mathbf{P}_n'$ and $\mathbf{Q}_n'$. These expansions[3] permit us to write, for large n

$$A\mathbf{P}_n + B\mathbf{Q}_n \approx [2/(\pi n \cos\theta)]^{\frac{1}{2}}\sin\overline{(n+\tfrac{1}{2}\theta)},$$

which, when differentiated, has the required symmetry. Since n is large and θ_0 small, the effect of the variation of $\cos\theta$ relative to that of $\sin\overline{(n+\tfrac{1}{2}\theta)}$ can be ignored, so that the equation for n becomes

$$\cos\overline{(n+\tfrac{1}{2}\theta_0)} = 0 \quad \text{or} \quad n \approx \pi/2\theta_0. \qquad (26)$$

[3] Jahnke and Emde, "Tables of Functions," p. 117.

Equating the fields at $x = y = z = 0$, $\theta = \phi = 0$,

$$R = R_0 = \tfrac{1}{2}a \cot\theta_0 = \tfrac{1}{2}b \cot\phi_0,$$

we get, after division

$$\frac{1+r}{1-r} = \frac{-j(k'/k)(kR_0)^{\frac{1}{2}}\mathbf{H}_{n+\frac{1}{2}}^{(2)}(kR_0)}{\dfrac{d}{d(kR_0)}[(kR_0)^{\frac{1}{2}}\mathbf{H}_{n+\frac{1}{2}}^{(2)}(kR_0)]}, \qquad (27)$$

n being given by (26).

Using now the expansion of (17), we find, after some reduction

$$\frac{1+r}{1-r} = 1 + \frac{j}{ka \cot\theta_0(1-\lambda^2/4a^2)^{\frac{1}{2}}}$$
$$\frac{j\theta_0}{ka(1-\lambda^2/4a^2)^{\frac{1}{2}}}. \qquad (28)$$

Since, to our order of approximation, $\cot\theta_0 = 1/\theta_0$, this means the effect is that of an inductive reactance of value, relative to Z_0, of

$$X_L = (\lambda^2/4a^2)(\lambda\theta_0/2\pi a)/(1-\lambda^2/4a^2)^{\frac{1}{2}}. \qquad (29)$$

Corresponding to (21) we have, for the insertion, δ, of the compensating capacitive iris

$$\delta \approx \frac{\lambda}{2a}\cdot\frac{\lambda}{1-\lambda^2/4a^2}\cdot\frac{1}{2\pi}\left[\frac{(D-a)b}{2\pi aL}\right]^{\frac{1}{2}}. \qquad (30)$$

3.1 General Double Taper

Since the main use of a double taper will probably be to enlarge the mouth of a waveguide into a radiating horn, it is undesirable to be tied down to the spherical co-ordinate requirement, namely $a/b = D/d$. Moreover, (29) shows that there is nothing particularly virtuous about this combination as the taper is not self-compensating, as we would like.

Now (28) can be put in the form

$$\frac{1+r}{1-r} = 1 + \frac{j}{ka \cot\theta_0(1-\lambda^2/4a^2)^{\frac{1}{2}}} - \frac{j}{k'b \cot\phi_0}, \qquad (31)$$

by virtue of the relation $R_0 = \tfrac{1}{2}a \cot\theta_0 = \tfrac{1}{2}b \cot\phi_0$ which has so far been assumed. Comparing (31) with (18) and (4) it is apparent that the total reflection is simply the sum of the reflections to be expected if the two tapers were combined independently. It seems reasonable, therefore, to assume this to be so in general (provided only that the taper angles are small), and not limited to the special case $a/b = D/d$. Assuming this to

be the case, (31) gives directly the reflection to be expected for the general taper. In particular, the taper should be self-compensating if

$$ka \cot \theta_0 (1 - \lambda^2/4a^2)^{\frac{3}{2}} = k'b \cot \phi_0, \qquad (32)$$

i.e.,

$$\phi_0/\theta_0 = b/[a(1 - \lambda^2/4a^2)].$$

This relation is substantially frequency independent, except near cut-off.

As $\cot \theta_0 = 2L/(D-a)$ and $\cot \phi_0 = 2L/(d-b)$, this equation can be put in the form

$$(d-b)/(D-a) = b/[a(1 - \lambda^2/4a^2)], \qquad (33)$$

which is independent of the length of the taper. (The taper length must not, of course, be so short that the flare angles become too large for the preceding analysis to remain valid.)

4. Experimental Results

Some measurements have been made on a horn flared in the narrow side from 0·67 inch to 2·75 inches in a taper length of 2·625 inches. The broad side, 2 inches, was unflared. This arrangement gives a flare semi-angle of $\theta_0 = 22$ degrees, which is rather large. The standing-wave ratio, taken between $\lambda = 5·5$ and 9 centimetres is shown in Figure 9A. It has to be noted that the reflection at the mouth may change considerably over this band, and some allowance has to be made for this. Nevertheless, the curve is seen to possess maxima and minima separated by the required $\lambda_g/4$ period. According to (9) the reflections should be compensated by an inductive diaphragm of depth

$$\delta = \frac{2}{2\pi}\left(\frac{2}{2\pi}\frac{2·75 - 0·67}{0·67 \times 2·625}\right)^{\frac{1}{2}} = 0·195 \text{ inch.}$$

The curve when this diaphragm is inserted is shown in Figure 9B. Apart from the very slight ripple that remains, the curve correctly shows the variation in standing-wave ratio to be expected from the horn mouth. In particular, the violent

peaks at the half-wavelength and wavelength positions have gone, and the minima centred at the quarter and three-quarter wavelength positions have been filled in. The drop near the quarter-wave position is a property of the horn itself, since the cut-off wavelength is very close. The dip at $\lambda = 5·7$ centimetres is common to both curves, and does not seem to be directly due to the taper.

Considering the rather abrupt change occurring at the taper in this horn, it is considered that the difference in the curves of Figure 9 due to the insertion of the diaphragm, is adequate evidence that satisfactory compensation is achieved by the use of the formulae developed here for the insertion.

5. Conclusions

The formulae here obtained for the effects of small-angle tapers would appear to be valid up to taper half-angles of about 20 degrees. This prob-
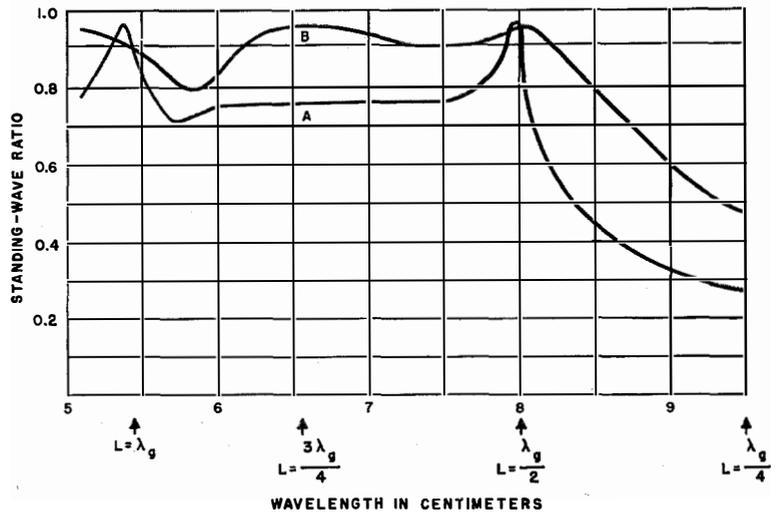
Figure 9—Experimental response curves from tapered horn, A without, and B with the theoretically designed compensating diaphragm.

ably covers the range of tapers most likely to be of use in practice. The diaphragm method of reflection compensation is seen to be sound, and the diaphragm sizes, as obtained from the formulae, seem near enough to the optimum to warrant their use directly, in most cases.

The field-fitting method, possible in the simple cases first treated, yields results that are capable of generalization, particularly to the

general double taper. Although an independent derivation would be desirable, it is believed that the results thus obtained, and in particular, those for the self-compensating double taper, are substantially correct.

6. Summary of Formulae

6.1 TAPER IN NARROW SIDE

Waveguide of dimensions $a \times b$ tapered to $a \times d$ in a taper length L. The half-angle ϕ_0 of the taper is given by $\cot \phi_0 = 2L/(d-b)$. The reflection at the taper is equivalent to that produced by a capacitance of value relative to Z_0, given by

$$X_c = (2\pi b/\lambda_g) \cot \phi_0.$$

If the rest of the system is matched, the resulting standing-wave ratio ρ, is

$$\rho = 1 - \lambda_g/2\pi b \cot \phi_0.$$

The reflection can be matched out by an inductive diaphragm at the taper whose insertion from each of the narrow sides of the waveguide is given by

$$\delta = \frac{a}{2\pi}\left(\frac{a}{\pi} \cdot \frac{d-b}{bL}\right)^{\frac{1}{2}}.$$

When going from an expanding taper back to a waveguide of dimensions $a \times d$, interchange b and d and change the sign of ϕ_0 in the previous formulae. Since this reverses the phase of the reflection, a capacitive diaphragm is needed to provide compensation. The required insertion from each of the broad sides of the guide is given by

$$\delta = (\lambda_g/2\pi)[(d-b)/2\pi L]^{\frac{1}{2}}.$$

6.2 TAPER IN BROAD SIDE

Waveguide dimensions $a \times b$ tapered to $D \times b$ in a taper length L. The half-angle of the taper is θ_0, so that

$$\cot \theta_0 = 2L/(D-a).$$

The reflection at the taper is equivalent to an inductive reactance, of value relative to Z_0, given by

$$X_L = \frac{2\pi a}{\lambda} \cot \theta_0 \cdot (1 - \lambda^2/4a^2)^{\frac{3}{2}}.$$

If the rest of the system is matched, the resulting standing-wave ratio is

$$\rho = 1 - \lambda/[2\pi a \cot \theta_0 (1 - \lambda^2/4a^2)^{\frac{3}{2}}].$$

The reflection can be matched out by a capacitive diaphragm at the taper, whose insertion from each of the broad sides is given by

$$\delta = \frac{\lambda}{2\pi(1 - \lambda^2/4a^2)} \cdot \left[\frac{b(D-a)}{2\pi aL}\right]^{\frac{1}{2}}.$$

When going from an expanding taper back to a waveguide of dimensions $D \times b$, interchange D and a, and change the sign of θ_0 in the previous formulae. Since this reverses the phase of the reflection, an inductive diaphragm is needed to provide compensation. The insertion from each of the narrow sides is given by

$$\delta = (D/2\pi)\{(D-a)/[\pi L(1 - \lambda^2/4D^2)]\}^{\frac{1}{2}}.$$

6.3 DOUBLE TAPER

Waveguide dimensions $a \times b$ tapered to $D \times d$ in a taper length L. The half-angles in the narrow and broad side are

$$\cot \phi_0 = 2L/(d-b); \quad \cot \theta_0 = 2L/(D-a).$$

The effect of the taper is that of a susceptance given by

$$Y = \lambda/[2\pi a \cot \theta_0 (1 - \lambda^2/4a^2)^{\frac{3}{2}}] - \lambda_g/2\pi b \cot \phi_0.$$

According to the sign of this quantity it can be matched out by a suitable diaphragm of an inductive or capacitive nature.

The taper is self-compensating when

$$\phi_0/\theta_0 = b/[a(1 - \lambda^2/4a^2)]$$

or

$$(d-b)/(D-a) = b/[a(1 - \lambda^2/4a^2)].$$

Design of Dissipative Band-Pass Filters Producing Desired Exact Amplitude–Frequency Characteristics*

By MILTON DISHAL

Federal Telecommunication Laboratories, Incorporated, Nutley, New Jersey

THE PURPOSE of this paper is to present a basic method of obtaining the *exact* required values for all circuit constants in a band-pass network using n finite-Q resonant circuits to obtain either of two types of exact amplitude responses; the so-called critical-shape-coupled, Butterworth, or transitional type of response, and the so-called over-coupled or Chebishev† type of response.

The equation giving the gain obtained with the desired response shape is derived. Equations for the exact phase characteristics associated with the above exact amplitude characteristics are also given.

Some comments are made concerning a somewhat similar method of design, which makes use of the so-called "poles" of the network.

Design sheets are presented giving the necessary equations for single-, double-, triple-, and stagger-tuned networks to produce either of the above two amplitude-response shapes.

• • •

1. Symbols

n = total number of resonant circuits in networks of Figures 3 and 4.

N = total number of cascaded networks between which there is no coupling, e.g., separated by vacuum tubes.

$\vec{V}$ = complex voltage output at any frequency.

V = magnitude of the voltage output at any frequency. (See Figure 7.)

V_p = magnitude of the voltage output at the frequency of peak response. (See Figure 7.)

V_β = magnitude of the voltage output at that point on the response curve that the designer defines as the edge of the pass band. For response-shape C, this voltage output is identical with the response at the valleys of the response inside the pass band. (See Figure 7.)

Δf = frequency bandwidth between response points whose voltage output is V. (See Figure 7.)

Δf_p = frequency bandwidth between the peaks of response-shape C at the voltage output of V_p. (See Figure 7.)

Δf_β = frequency bandwidth between the response points whose voltage output is V_β, i.e., the frequency bandwidth between the edges of the defined pass bandwidth. (See Figure 7.)

f_0 = resonant frequency of each resonant circuit. See Section 3.2. f_0 is also the geometric mean frequency $(f_1 f_2)^{1/2}$ between two frequencies f_1 and f_2 having the same voltage response.

ω_0 = resonant radian frequency = $2\pi f_0$.

F = total percentage bandwidth between two frequencies
$$= (f/f_0 - f_0/f) = (f_2 - f_1)/f_0,$$
$$\text{where } f_0 = (f_1 f_2)^{1/2}.$$

F_p = percentage bandwidth between peaks of response-shape C $(= \Delta f_p/f_0)$.

F_β = percentage bandwidth between edges of the defined pass bandwidth $[= (f_{\beta 2} - f_{\beta 1})/(f_{\beta 2} f_{\beta 1})^{1/2}]$.

d = total decrement of a resonant circuit. See Figures 3 and 4.

G_n = *total* conductance across nth resonant circuit of node network
$$\left(= \frac{1}{R_n} + \frac{1}{Q_L X_{0Ln}} + \frac{1}{Q_c X_{0Cn}} \right).$$
See Figure 4A.

$R_n = total$ resistance in series with nth resonant circuit of mesh network $\left(= R_n + \dfrac{X_{0Ln}}{Q_L} + \dfrac{X_{0C_n}}{Q_C}\right)$. See Figure 4B.

$Q =$ inverse of the total resonant-circuit decrement.

$K =$ resultant coefficient of coupling between resonant circuits. (See Figures 3 and 4, and Sections 3.1.2 and 3.2.2.

$I =$ magnitude of the equivalent constant-current generator that drives the network of Figure 3. For a pentode generator, $I = g_m V_g$. For a "transformed" low-resistance generator, see Figure 6.

$C_n = total$ resonated capacitance in the nth resonant circuit.

$L_n = total$ resonated inductance in the nth resonant circuit.

$U_p =$ general symbol for a coefficient of some power of (jF) in the complex polynomial form of the circuit-response equations. The subscript of the U is identical with the power of (jF) for which U is the coefficient. (See Section 6.2 and (2).)

$U_p{}^b, U_p{}^c =$ general symbol for a coefficient in that complex polynomial that produces the desired response-shape B and C, respectively. The subscript is identical with the power of (jF) for which U is the coefficient.

$A_p, B_p, C_p,$ etc. $=$ specific coefficient of that (jF) whose power is p, in that specific complex polynomial for a network that has as many resonant circuits as the numerical position of the letter in the alphabet, e.g., C_2 would be the coefficient of $(jF)^2$ in the polynomial for a triple-tuned network. (See Design Equations—Group 1.)

$A_p{}^b, B_p{}^b; A_p{}^c, B_p{}^c;$ etc. $=$ same as above, except applied to that specific polynomial that produces response-shapes B and C, respectively. (See Design Equations—Groups 2 and 4.)

$|\Delta_n|_{\min} =$ minimum value of the magnitude of the complex polynomial for an n-resonant-circuit network. (See (3).)

$|\Delta_n{}^b|_{\min}, |\Delta_n{}^c|_{\min} =$ same as above, except for the complex polynomial for shapes B and C, respectively.

$r_m{}^b, i_m{}^b =$ magnitudes of the real and imaginary parts, respectively, of the general expression for the complex roots of the equation giving response-shape B. These roots always occur in conjugate pairs and m is the pair number. (See Section 7.1 and (6).)

$r_m{}^c, i_m{}^c =$ same as above for response-shape C. (See (26).)

$\theta_n{}^b, \theta_n{}^c =$ phase angle, at the percentage bandwidth F, of the response shape $(V_p/\vec{V})$, i.e., the θ in $(V_p/V)\underline{/\theta}$, for amplitude-response-shapes B and C, respectively, for an n-resonant-circuit network. (See (10).)

$T_n(F/F_\beta) =$ general Chebishev polynomial in terms of the variable $(\Delta f/\Delta f_\beta)$ of highest power n. (See (17), (18), and (19).)

$s_n, c_n =$ defined by (19).

2. Introduction

As the need increases for more and more channels in a given frequency band and as the voltage ratios between desired and undesired signals continue to increase, there will also be an increasing need for design information for band-pass filter networks that is more exact than that supplied by classical filter theory.

It is well known that when a continuously increasing attenuation is required outside of a given pass band, a straightforward method of producing a very high rate of increase in attenuation is to use a large number of correctly coupled and correctly damped resonant circuits.

For many designers, a further very important practical requirement arises at this point. For the exact design to be of practical value, *no lossless elements (no infinite Q's) should be required.* For multiple-resonant-circuit filters, this last requirement has apparently not received much attention. In general, it has been stated that any dissipation in the reactive elements of a filter degrades its performance at the edges of the pass band. With correctly designed networks, this last statement is not true. With correct circuit-element
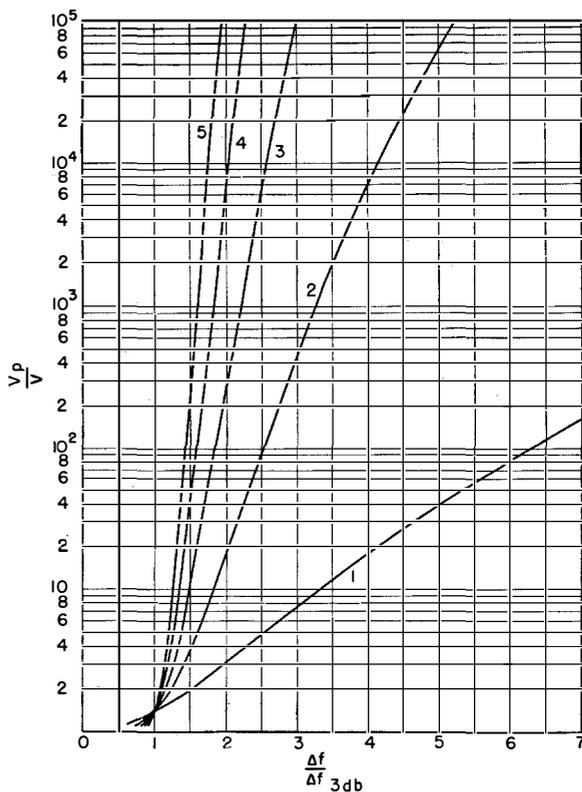
Figure 1—Selectivity characteristic of 5 cascaded stages, each stage containing a correctly resonated n-resonant-circuit network having a proper Q distribution and being critical-shape-coupled. When f_0 and Δf are given, the two frequencies between which Δf occurs are $f_{12} = [f_0^2 + (\Delta f/2)^2]^{1/2} \pm (\Delta f/2)$. When f_1 and f_2 are given, then $f_0 = (f_1 f_2)^{1/2}$. The number of tuned circuits per stage n is indicated on each curve. See (4) and (4A).

Figure 2—Selectivity characteristic of 5 cascaded stages, each stage containing a correctly resonated n-resonant-circuit network having a proper Q distribution and over-coupled for a resultant 1-decibel peak-to-valley ratio. When f_0 and Δf are given, the two frequencies between which Δf occurs are $f_{12} = [f_0^2 + (\Delta f/2)^2]^{1/2} \pm (\Delta f/2)$. When f_1 and f_2 are given, then $f_0 = (f_1 f_2)^{1/2}$. The number of tuned circuits per stage n is indicated on each curve. See (14) and (15).

values using finite Q's, the amplitude response can be made identical to that obtained with infinite-Q elements.

To show the increase in sharpness of cutoff as the number of resonant circuits is increased, the graphs of Figures 1 and 2 should be examined. For 5 cascaded stages and a required adjacent-channel rejection of 100 decibels, the use of three resonant circuits per stage having an allowable peak-to-valley ratio in the pass band of 1 decibel more than doubles the available number of channels over the use of two resonant circuits per stage with critical-shape-coupled characteristics.

The major purpose of this paper is to present a method and some of the resulting equations for obtaining the necessary n simultaneous equations that must be solved to determine the exact

circuit constants required for band-pass circuits that use n finite-Q resonant circuits ($n = 1, 2, 3, 4, 5$, etc.) to produce either one of two types of exact response shapes; the so-called critical-shape-coupled (maximally flat or transitional-shape-coupled) response, and the so-called over-coupled response.

Briefly, the method proposed is as follows:

A. Express the determinant of the exact *circuit-response* equation in the form of a polynomial in $j(\Delta f/f_0)$ of highest power n, with descending consecutive powers.

B. Solve for the complex roots of the exact amplitude equation that describes the *desired-response* shape.

C. Use these roots to place the desired-response equation in the complex polynomial form described in A.

D. Equate the corresponding n coefficients.

3. Circuits and Circuit Constants

3.1 CIRCUIT PRODUCING AN AMPLITUDE-FREQUENCY CHARACTERISTIC HAVING EXACT GEOMETRIC SYMMETRY

Figure 3 shows the basic unbalanced band-pass "ladder network." As in the well-known constant-K filter, the reactance structure of the series and shunt arms are inverse arms. However, it should be noted that in this paper each resonant circuit is considered to be dissipative, each circuit having its own specific Q. When correctly designed, this circuit can produce *for any percentage bandwidth* an amplitude response exactly described by the Butterworth and Chebishev equations given in Sections 7 and 8. *This result can be accomplished using finite Q's in all resonant circuits.* It is worth repeating that, when this circuit can be used, no small-percentage pass-band approximation is required.

The chain may start and/or end with either a series or a shunt arm. It should be realized that if the network starts with a series arm and a constant-current generator (e.g., pentode tube) drives the network, then the constant-current generator should be connected across the resistor that produces the required resonant-circuit decrement. Similarly, if the network ends in a series arm and output voltage is to be used, it must be obtained across the resistor that produces the correct resonant-circuit decrement.

The circuit constants that exactly and conveniently describe the circuit of Figure 3 are the resonant frequency f_0 of the series and shunt arms, the coefficient of coupling K between adjacent resonant circuits, and the decrement d of each resonant circuit. The definitions of these circuit constants are obtained from examination of the exact circuit response equations for a specific network in the form of Figure 3 (using, for example, 5 resonant circuits).

3.1.1 Resonant Frequency f_0

In the circuit of Figure 3, all series and shunt arms are tuned to exactly the same resonant frequency, $f_0 = 1/2\pi \, (LC)^{1/2}$. This frequency will also be the geometric mean frequency $(f_1 f_2)^{1/2}$ between any two frequencies f_1 and f_2 having the same amplitude response.

3.1.2 Coefficients of Coupling

It is found that the determinant of the network of Figure 3 can be expanded into the form of a polynomial in descending consecutive powers of $j[(f/f_0) - (f_0/f)]$; the coefficients of these various powers are completely independent of frequency and involve only the decrements of the resonant circuits and certain capacitance ratios. The capacitance appearing in the numerator of these ratios is always that of a series-resonant circuit, and the denominator capacitance is
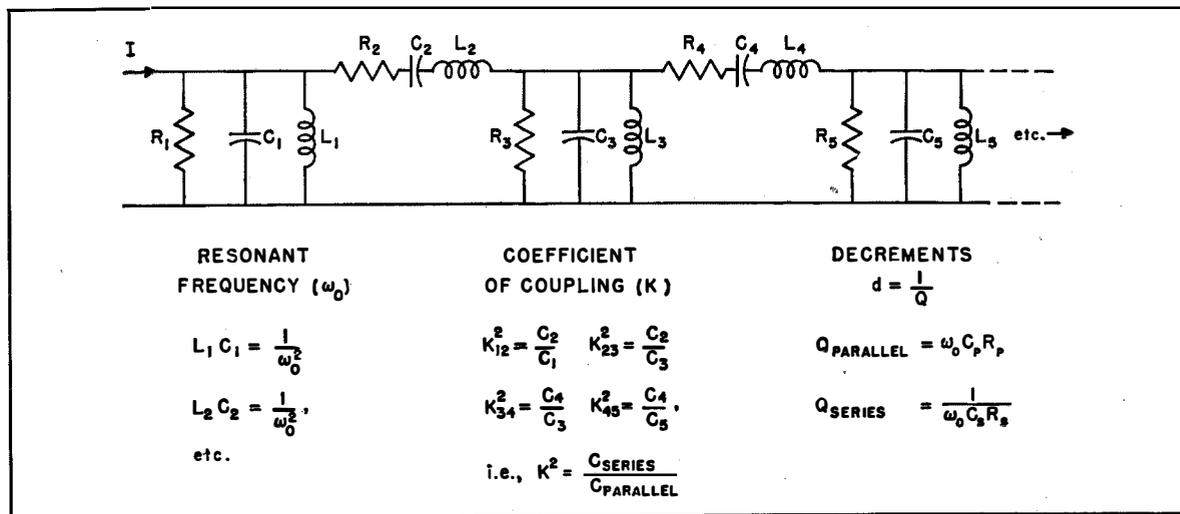
Figure 3—The basic band-pass circuit that is analyzed and the circuit constants. The network may begin and/or end with either a series or a parallel arm. This network produces a response–frequency characteristic having perfect geometric symmetry for any percentage bandwidth $(f_2 - f_1)/(f_2 f_1)^{1/2}$.
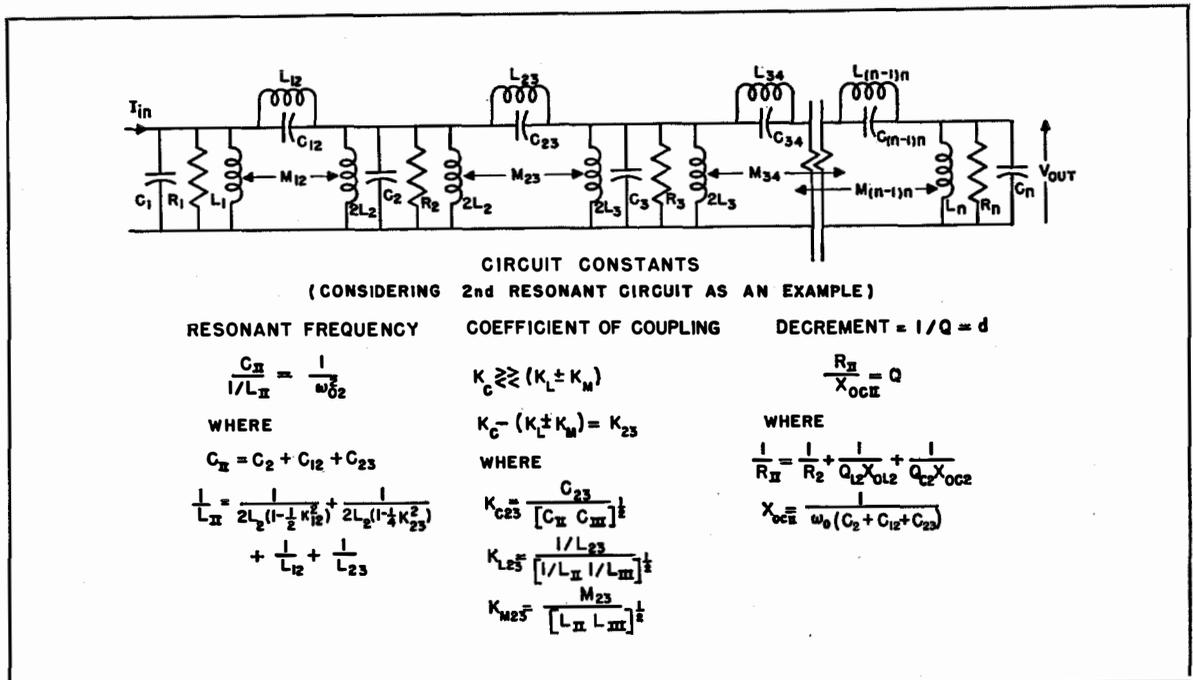
Figure 4A—Basic node network to be analyzed and the resonant-circuit constants that are used. For small-percentage pass bands, this network is exactly equivalent to that of Figure 3, when equal numbers of resonant circuits are used.
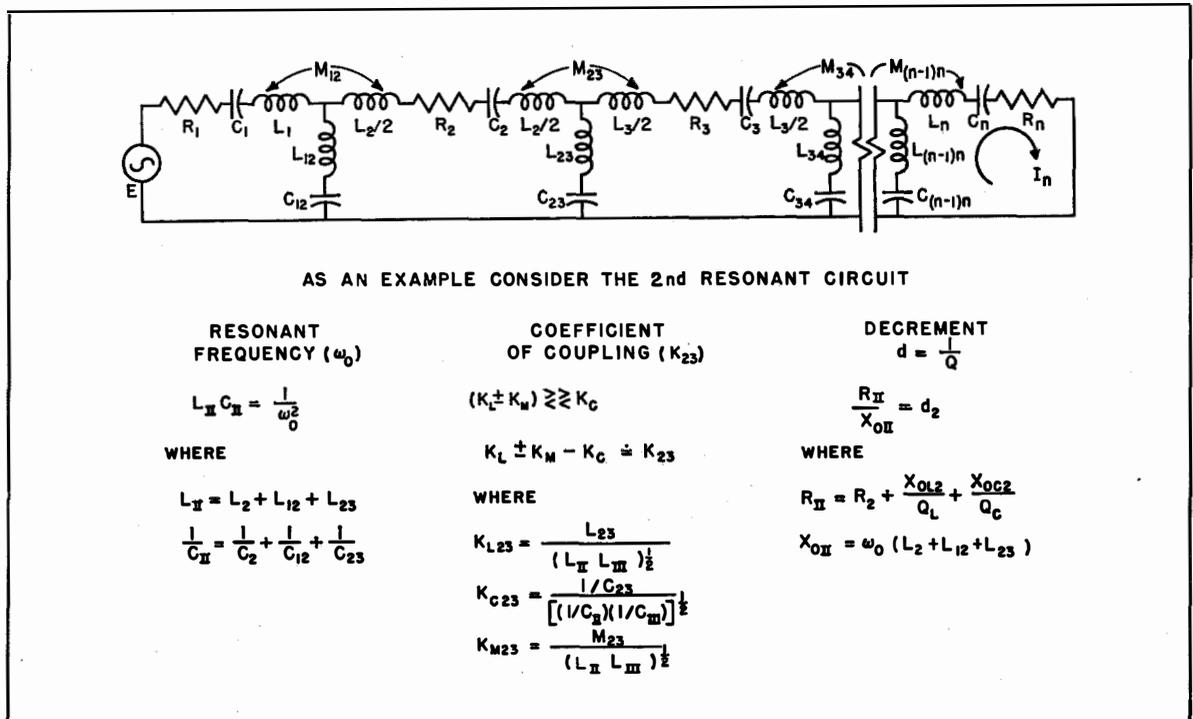
Figure 4B—Basic mesh network to be analyzed and the resonant-circuit constants that describe it. For small-percentage pass bands, this network is exactly equivalent to that of Figure 3, when equal numbers of resonant circuits are used.

always that of an adjacent shunt-resonant circuit. In this paper, these capacitance ratios will be called coefficients of coupling (squared) because they define a required relation between adjacent resonant circuits, and also because they are exactly equivalent to the well-known coefficients of coupling in the small-percentage pass-band circuits of Figures 4A and 4B. Thus, between any two adjacent resonant circuits, $K = C_{series}/C_{parallel}$.

3.1.3 Resonant-Circuit Decrement

As they appear in the determinantal equation, the resonant-circuit decrements d are the inverse of the well-known resonant-circuit Q's. For any series arm, $d = R_s \omega_0 C_s$, where R_s is the resistance in series with that arm and C_s is the resonated capacitance of the arm. For any shunt arm, $d = 1/R_p \omega_0 C_p$, where R_p is the resistance in parallel with that arm and C_p is the resonated capacitance of the arm.

For high- and very-high-frequency band-pass circuits (where shunt capacitance of the usual generators cannot be neglected), it should be noted that if the circuit of Figure 3 is used, only odd numbers of resonant circuits can be employed, i.e., the first and last resonant circuits must be parallel arms.

3.2 CIRCUITS PRODUCING AN AMPLITUDE-FREQUENCY CHARACTERISTIC HAVING GEOMETRIC SYMMETRY FOR ONLY A SMALL-PERCENTAGE BANDWIDTH

When the required pass band is small, the circuits of Figures 4A and 4B are exactly equivalent to that of Figure 3, and are usually more practical to build physically. When a small-percentage band pass is needed, the circuit of Figure 3 is often not the most desirable. For instance, the required values for the coefficients of coupling between adjacent resonant circuits [($C_{series}/C_{parallel}$) for Figure 3] are approximately equal to the percentage bandwidth; thus we see that, for a 5-percent bandwidth, the resonating capacitance of a series arm would have to be approximately 5 percent of that used in the adjacent parallel branch; to satisfy the resonance requirement, the inductance in the series branch must be 20 times that in the adjacent shunt branch; a satisfactory inductance of this size is often undesirable or impractical.

Figures 4A and 4B are not exactly equivalent to Figure 3 because the effective coefficients of coupling between adjacent resonant circuits, which appear in the determinantal equations for the circuits of Figures 4A and 4B, are functions of frequency; i.e., we find that for Figure 4A, e.g., $K = K_C(f/f_0) - (K_L \pm K_M)(f_0/f)$. If we make the approximation that $K_C \lessgtr (K_L + K_M)$ and $f/f_0 \doteq 1$, then the above K varies negligibly with frequency, and for the same number of resonant circuits the determinantal equations for Figures 4A and 4B are identical.

The above assumption automatically means that the response null, which can be obtained with the circuits of Figures 4A and 4B, is placed far from the pass band. In the circuits of Figure 4A, this response null occurs exactly at $f_{null}/f_0 = [(K_L \pm K_M)/K_C]^{1/2}$. In the circuits of Figure 4B, this response null occurs exactly at $f_{null}/f_0 = [K_C/(K_L \pm K_M)]^{1/2}$.

Since the circuit of Figure 4A has n nodes (where n is the number of resonant circuits used) and is most simply analyzed by the use of node equations, it will be called the node network, and the n-mesh circuit of Figure 4B will be called the mesh network. It should be realized that these networks are physically different (thus supplying the designer with a variety of physical configurations) but are electrically related, in that wherever G, C, L, I, and V appear in the determinantal equation for Figure 4A, then R, L, C, E, and I appear in the corresponding determinantal equation for Figure 4B (principle of duality).

It may be noted that when we use only the first two nodes of Figure 4A with mutual-inductive coupling between these nodes, the familiar intermediate-frequency transformer of the common broadcast receiver is obtained.

For a small-percentage band pass, the constants that best describe the above circuits are the coefficients of coupling K between resonant circuits, the resonant frequency f_0 of the resonant circuits, and the decrement d of the resonant circuits (inverse of the resonant-circuit Q).

It may be helpful for the reader to realize that the definitions of the above circuit constants are obtained from the exact node equations for a node network and from the exact mesh equations for a mesh network. Thus, if the reader will write the exact node equations for a triple-tuned

circuit, then by correct manipulation, the above constants will be recognized. These constants, as they appear in the exact node and mesh equations, will now be described briefly.

3.2.1 Exact Resonant Frequency f_0

The resonant frequency f_0 of each node is that frequency at which the susceptance of the total capacitance (including mutual) attached to the node equals the susceptance of the *total* inductance (including mutual) attached to the node. Figures 4A and 4B give this exact general resonant frequency.

In line with this definition, it should be noted that a fundamental and practical method of experimentally "tuning up" the resonant circuit attached to any node is effectively to short-circuit the two nodes on either side of the node in question, and then tune this resonant circuit for maximum output. In practice, the effective short-circuiting can be done by completely detuning the two adjacent nodes, thus allowing some signal transfer through the filter so that an output indicator at the end of the filter chain can be used for all the nodes. Mesh networks can be tuned up by effectively open-circuiting the two meshes on either side of the mesh in question, and then tuning the desired mesh for maximum response.

3.2.2 Coefficient of Coupling

The coefficient of any one type of coupling, C, L, or M, between any two nodes is the ratio of the susceptance of that type common to the two nodes in question to the geometric mean of the *total* susceptance of that type connected to each node. For the correct coefficient of coupling between any two meshes of Figure 4B, substitute in the above statement the word reactance for susceptance and mesh for node. Figures 4A and 4B give these coefficients.*

Either inductive, capacitive, or mutual-inductive coupling, or a combination of them, may be used between the adjacent resonant circuits. The

---

* It should be noted that when more than two resonant circuits are in the network, this definition of coefficient of coupling is different from that given in Section IX of reference 16 of the Bibliography. The required triple-tuned-circuit K given in references 16 and 17 must be divided by 1.414 to correspond to the K of this paper. The definition of coefficient of coupling given in this present paper leads to simpler numerical constants in the equations for the circuit response.

resultant coefficient of coupling is

$$K = [K_C(f/f_0)] - (K_L \pm K_M)(f_0/f)$$

and in the analysis to be considered, the frequency at which this quantity equals zero must not occur within or near the pass band.

It should be realized that it is not necessary to use the same type of coupling between all the nodes of the network.

The designer will find that there is less chance of making an error in designing the coefficient of coupling if the following procedure is used: first, decide whether to use a node or a mesh network; second, decide what type of coupling to use; third, if a *node* network is to be used design the network *using the exact circuit configuration of Figure 3* or if a *mesh* network is to be used use *the exact configuration of Figure 4;* fourth, after the above design is completed then the T, π, or transformer equivalents of Figure 5 can be used to obtain different circuit configurations that, depending on the specific problem, may be desirable.

3.2.3 Resonant-Circuit Decrement $d = 1/Q$

For node networks, the decrement d of the resonant circuit is the ratio of the resultant equivalent conductance across the resonant circuit to the susceptance of the resonant frequency of either the total capacitance or total inductance. The term "equivalent" is used to indicate that any series resistance in the inductance or capacitance of the resonant circuit should be transformed into its equivalent shunt conductance and added to any actual shunt conductance present to obtain the total resonant-circuit conductance. Figures 3 and 4 give the resonant-circuit decrement. Naturally any shunt conductance due to the generator and the load must be considered when calculating the decrement of the input and output resonant circuits.

3.2.4 Equivalent Generator

With reference to the equivalent constant-current generator that drives the first node, there are in practice two situations to be considered. If a vacuum tube is attached directly to the input circuit, the equivalent generator is, of course,
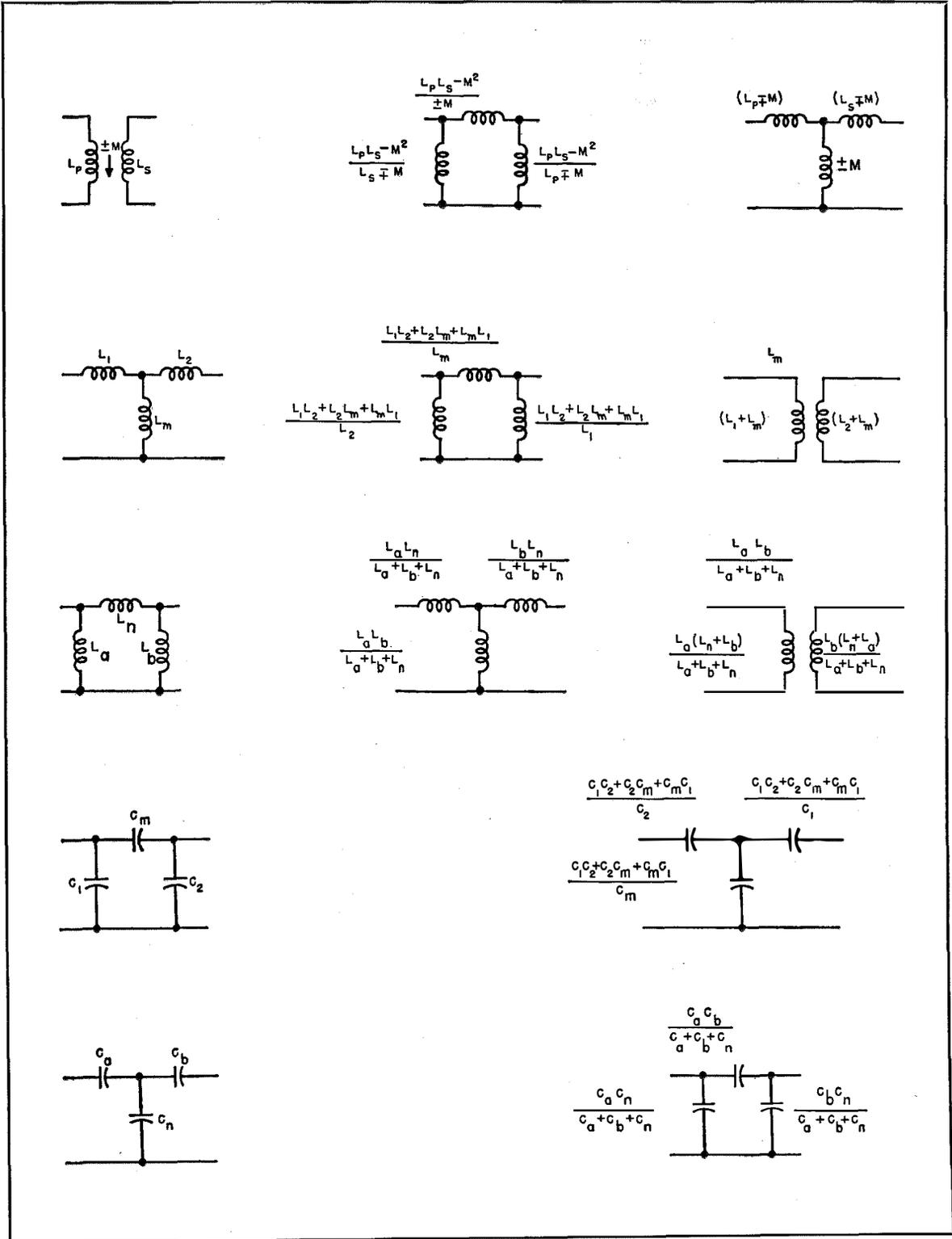
Figure 5—Five different coupling methods and the transformer, T, and π equivalents. The use of these equivalents in the circuit of Figure 4 enables the designer to obtain the same electrical performance with a large number of physically different circuits.

TRANSFORMING CIRCUIT	IN ALL BELOW EQUIVALENTS, $I = \left(\dfrac{R_1}{Q_{out}X_2}\right)^{\frac{1}{2}}\dfrac{E_1}{R_1}$	IN ALL BELOW EQUIVALENTS, $E = \left(\dfrac{X_2}{Q_{out}R_1}\right)^{\frac{1}{2}}E_1$	REQUIRED RELATIONSHIP TO OBTAIN A DESIRED Q_{out}
$K = \dfrac{M}{(L_1 L_2)^{\frac{1}{2}}}$ R_1, L_1, E_1, L_2	$\doteq L_2\left[1 - \dfrac{K^2}{1+(R_1/X_{L1})^2}\right]$ I $\leftarrow Q_{out}$	$\doteq L_2\left[1 - \dfrac{K^2}{1+(R_1/X_{L1})^2}\right]$ $\leftarrow Q_{out}$ E	$K^2 = \dfrac{R_1/X_{L1}+X_{L1}/R_1}{Q_{out}} \times \dfrac{1}{1+\dfrac{X_{L1}/R_1}{Q_{out}}}$ EXACT
L_2, R_1, L_1, E_1	I $L_2 + L_1 \leftarrow Q_{out}$	$\doteq L_2 + L_1$ $\leftarrow Q_{out}$ E	$\dfrac{L_1}{L_2} \doteq \left(\dfrac{R_1}{Q_{out}X_2}\right)^{\frac{1}{2}}$ $\dfrac{L_1}{L_2} \ll 1 \qquad \dfrac{R_1}{X_{L1}} \gg 1$
C_1, R_1, C_2, E_1	I $C_2 + C_1 \leftarrow Q_{out}$	$\doteq C_2 + C_1$ $\leftarrow Q_{out}$ E	$\dfrac{C_1}{C_2} \doteq \left(\dfrac{X_2}{Q_{out}R_1}\right)^{\frac{1}{2}}$ $\dfrac{C_1}{C_2} \ll 1 \qquad \dfrac{R_1}{X_{C1}} \ll 1$
C_2, R_1, C_1, E_1	I $\dfrac{C_2 C_1}{C_2 + C_1} \leftarrow Q_{out}$	$\doteq \dfrac{C_2 C_1}{C_2 + C_1}$ $\leftarrow Q_{out}$ E	$\dfrac{C_1}{C_2} \doteq \left(\dfrac{Q_{out}X_2}{R_1}\right)^{\frac{1}{2}}$ $\dfrac{C_1}{C_2} \gg 1 \qquad \dfrac{R_1}{X_{C1}} \gg 1$
L_1, R_1, L_2, E_1	I $\dfrac{L_2 L_1}{L_2 + L_1} \leftarrow Q_{out}$	$\doteq \dfrac{L_2 L_1}{L_2 + L_1}$ $\leftarrow Q_{out}$ E	$\dfrac{L_1}{L_2} \doteq \left(\dfrac{Q_{out}R_1}{X_2}\right)^{\frac{1}{2}}$ $\dfrac{L_1}{L_2} \gg 1 \qquad \dfrac{R_1}{X_{L1}} \ll 1$
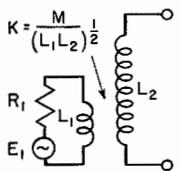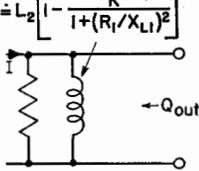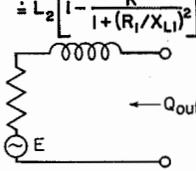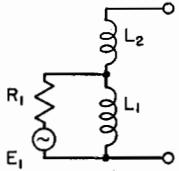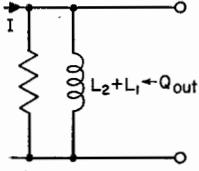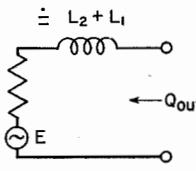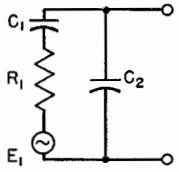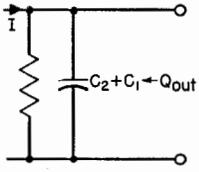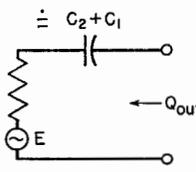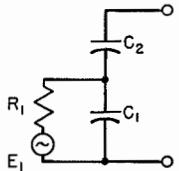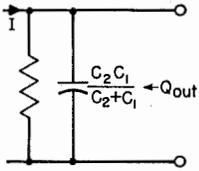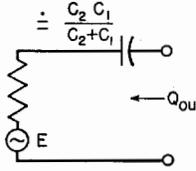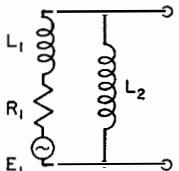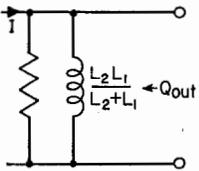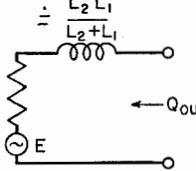
Figure 6—Five methods of "transforming" a nonresonant generator and/or load into the first and/or last resonant circuit of the network, the equivalent constant-current (and constant-voltage) generator, and "reflected decrement." (See Section 3.)

$g_m V_{kg}$. If a transforming circuit is used to couple the generator to the resonant circuit, then Figure 6 gives the equivalent "reflected constant-current generator" for use with the node circuits (equivalent constant-voltage generator for use with the mesh circuits) and the "reflected decrement" portion of the total resonant-circuit decrement that results when a resistive generator and/or load are "transformed" into the first and last resonant circuits of the network. The equivalents of Figure 6 thus allow application of the following analysis to the important practical cases where the actual generator is not a pentode but is, for example, the much-used equivalent 50-ohm gen-

erator and the load is, for example, a low-input-resistance crystal mixer. For this example, one could use a transforming circuit as given in Figure 6 to couple the untuned generator and untuned load to the first and last resonant circuits of the chain.

When a certain response *shape* is to be produced, the function of the transforming circuit that couples a nonresonant generator and/or load to the first and/or last resonant circuit should be thought of in the following manner: The transforming circuit is used in conjunction with the generator and/or load resistance to couple a certain amount of decrement to the resonant circuit to make the total resulting resonant-circuit decrement equal to that value required to produce the desired-response shape. Note that one does not design the transforming circuit to produce a certain desired equivalent constant-current (or constant-voltage) generator.

The total resonant-circuit decrement is the sum of the above-considered "reflected decrement" and the "unloaded decrement" of the resonant circuit (which is the inverse of the unloaded Q of the resonant circuit). The inverse of the sum of these two decrements is then, of course, the resultant resonant-circuit Q.

4. Basic Response Shapes

When the resonant circuits are correctly tuned, there are three basic types of symmetrical band-pass shapes that can be used to give the same pass bandwidth.

Shape A: *This shape corresponds to that obtained with the well-known "undercoupled" condition for the familiar double-tuned circuit.* It may be described as a shape having a single maximum in the center of the pass band. It is not the squarest possible single maximum and the attenuation outside the pass band does not increase as rapidly as possible.

Shape B: *This shape corresponds to that obtained with the well-known "critical-shape coupled" condition for the familiar double-tuned circuit, and has also been called the "maximally flat" and the "transitional" shape.* It may be described as the type having the squarest possible single maximum in the center of the pass band and its attenuation outside the pass band increases as

rapidly as possible while still maintaining a single peaked response.

Shape C: *This shape corresponds to that obtained with the well-known "overcoupled" condition for the familiar double-tuned band-pass circuit.* This type of shape has n maxima of equal height and $(n-1)$ minima of equal height inside the pass band, where n is the number of resonant circuits used. For a given allowable number of decibels down for the edges of the pass band, this shape gives the maximum possible rate of increase of attenuation outside the pass band.

An additional characteristic of response-shape C should be mentioned here: It will be found that no matter what the peak-to-valley ratio, there is a fixed ratio, dependent only on n, between the bandwidth across the outside peaks and the bandwidth of the skirts at that number of decibels down equal to the valley response. With response-shape C, the symbol Δf_β denotes this particular skirt bandwidth at the response value V_β that is equal to the valley response V_v.

Shape C_1: In many practical cases, the designer can allow, for example, 1-decibel dips inside the pass band, but would like to define the edges of the pass band as the 3-decibel down points. This type of response shape is a simple modification of the basic shape-C response. For example, suppose four coupled resonant circuits are to be used with an allowable peak-to-valley ratio of 1 decibel; the ratio between Δf_{1db} and Δf_{3db} is fixed by the above data and, if we know this ratio, we thus know that Δf_{1db} required to give the desired Δf_{3db} bandwidth. One then designs for the basic shape-C response (i.e., 1-decibel dips and the "pass-band edges" at 1 decibel down equal to the above-found Δf_{1db}).

In this paper, only response-shapes B and C will be considered. Figure 7 gives the above described three response shapes, and the shape constants that describe the responses, for the voltage produced across the last node when the node network of Figure 4A is driven by a constant-current generator, and for the current produced in the last mesh when the mesh network of Figure 4B is driven by a constant-voltage generator.

5. Mathematical Procedure

The analytical procedure to be used in this paper consists of the following steps.

A. Express the general circuit response in its simplest possible form. For the networks of Figures 3, 4A, and 4B, this form is that in which the determinantal equation is expressed as a polynomial in descending powers of $j[(f/f_0) - (f_0/f)]$.

B. Express the desired-response equation in the same form as the general circuit-response equation.

C. Equate the corresponding coefficients in the two equations.

This will produce the necessary number of simultaneous equations.

6. Circuit Response Equations

6.1 POLYNOMIAL COEFFICIENTS OF COMPLEX-CIRCUIT-RESPONSE EQUATION

Consider the design of the shape of the transfer impedance of the networks of Figures 3 and 4A, i.e., the resulting output voltage when the networks are correctly driven by a constant-current generator; and for the shape of the transfer admittance of the networks of Figures 3 and 4B, i.e., the resulting output current when the networks are correctly driven by a constant-voltage generator.

By the straightforward application of Kirchhoff's laws to any specific network in the form of Figures 3 and 4, we find that the above-described transfer admittance and transfer impedance can be exactly written as

For all the node networks of Figure 4A and for all the networks of Figure 3 that begin and end with shunt arms, the numerator for (V_{out}/I_{gen}) of (1) is

$$(\text{Numerator})_n = \frac{1}{\omega_0(C_1C_n)^{1/2}} K_{12}K_{23}K_{34}\cdots K_{(n-1)n},$$

$$(1A)$$

where the K's are defined in Figures 3 and 4A.

For all the mesh networks of Figure 4B and for all the networks of Figure 3 that begin and end with series arms, the numerator for (I_{out}/E_{gen}) of (1) is

$$(\text{Numerator})_n = \frac{1}{\omega_0(L_1L_n)^{1/2}} K_{12}K_{23}K_{34}\cdots K_{(n-1)n},$$

$$(1B)$$

where the K's are defined in Figures 3 and 4B.

The denominator of (1) is a polynomial in consecutive powers of $j[(f/f_0) - (f_0/f)]$, the highest power being n the number of resonant circuits used and, within the limitations of the discussion of Section 3, the coefficients U of the polynomial are independent of frequency and are functions of only the coefficients of coupling K and decrements d as they are described in Section 3.

Since the numerator of (1) is independent of frequency within the limitations of the discussion of Section 3, *the response shape is fixed entirely by the denominator* of (1). For the same number of

$$\left(\frac{V_{out}}{I_{gen}}\right) \quad \text{or} \quad \left(\frac{I_{out}}{E_{gen}}\right) = \frac{(\text{Numerator})_n}{(jF)^n + U_{n-1}(jF)^{n-1} + U_{n-2}(jF)^{n-2}\cdots U_2(jF)^2 + U_1(jF) + U_0}. \quad (1)$$
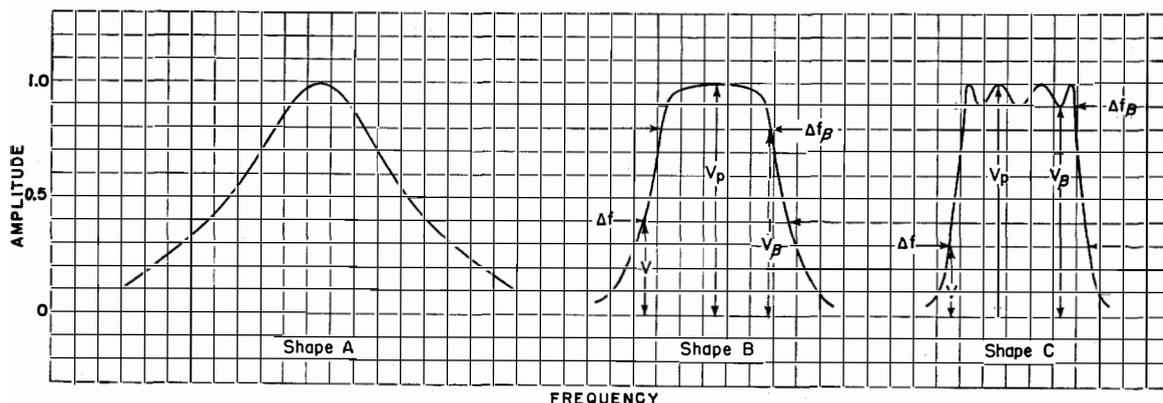
Figure 7—The three geometrically symmetrical amplitude-response shapes considered and the shape constants to be used. These shapes are physically symmetrical when plotted on a logarithmic frequency scale.

resonant circuits, the denominators Δ_n are identical for all the networks of Figures 3 and 4.

In the general notation of (1), U is used to denote an arbitrary number of resonant circuits. For any specific network, the letter used in the coefficients will be that one whose numerical position in the alphabet corresponds to the number of resonant circuits in the network. Thus, for a 5-resonant-circuit network, we would use E to represent the coefficients. The subscript on any coefficient is exactly the same as the power of the (jF) for which it is the coefficient. Thus, for example, for a 4-resonant-circuit network, the coefficient of $(jF)^3$ would be represented by D_3.

Since the numerator of (1) is independent of frequency, the peak value of the transfer admittance or transfer impedance is given by

$$\left(\frac{V_{\text{out}}}{I_{\text{gen}}}\right)_{\text{peak}} \quad \text{or} \quad \left(\frac{I_{\text{out}}}{E_{\text{gen}}}\right)_{\text{peak}} = \frac{(\text{Numerator})_n}{|\Delta_n|_{\text{min}}}, \quad (2)$$

where $|\Delta_n|_{\text{min}}$ is the minimum magnitude of the polynomial of (1).

Equation (2) will be used in a later section of this paper to find the gain obtained at the amplitude-response peaks.

Dividing (2) by (1), we obtain the ratio of the peak response to the response at any frequency; this is the basic response-*shape* equation:

$$\frac{V_p}{V} \quad \text{or} \quad \frac{I_p}{I} = \frac{1}{|\Delta_n|_{\text{min}}}[(jF)^n + U_{n-1}(jF)^{n-1}$$
$$+ U_{n-2}(jF)^{n-2} + \cdots + U_2(jF)^2$$
$$+ U_1(jF) + U_0]. \quad (3)$$

In Design Equations—Group 1, the specific circuit-response-shape equations are listed for $n = 1, 2, 3,$ and 4.

Careful study of the series of response equations given in Design Equations—Group 1 will show the law of formation of the coefficients, and it should now be possible to write the general exact complex-response equation for a chain containing any number of resonant circuits.

$$\frac{V_p}{V} = \left\{ 1 + \left[\left(\frac{V_p}{V_\beta}\right)^2 - 1\right] \left(\frac{F}{F_\beta}\right)^{2n} \right\}^{\frac{1}{2}}$$
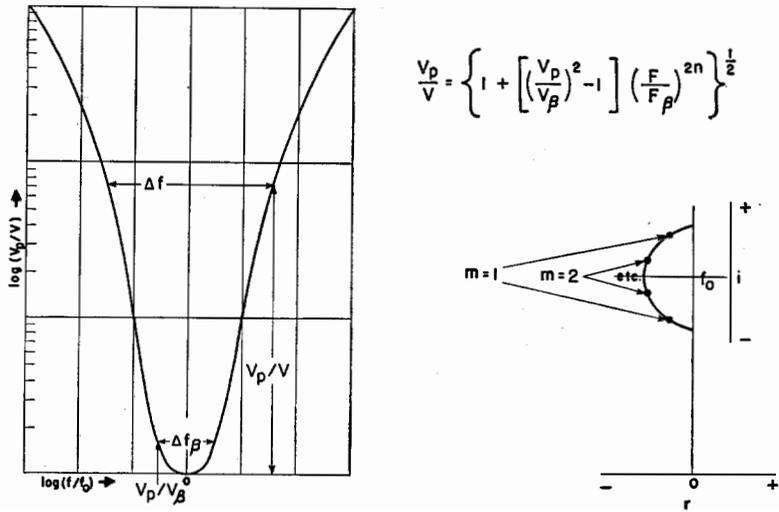
Figure 8—The exact equation describing response-shape B and the location of the roots of this equation on a semi-circle on the complex plane. Equation (6) gives the exact root values. n is the number of resonant circuits used and the response equation for an n-resonant-circuit network will have n roots.

Insofar as plotting of a response curve is concerned, the above equations enable us to obtain methodically the equations required to plot the amplitude- and phase-response shapes for any number of tuned circuits, once the various circuit coefficient of couplings and Q's are specified. The complex equations of Design Equations—Group 1 are, of course, expanded into their magnitude and phase-angle form when we plot the amplitude- and phase-response shapes. (All the even powers of (jF) are algebraically added together to give the real part of the determinant; all the odd powers of (jF) are added together algebraically to give the imaginary part of the determinant.)

7. Response-Shape B

7.1 DESIRED-SHAPE EQUATION

Our next step is to express the desired-shape equation given below in the form of Design Equations—Group 1, so that we can equate the above coefficients (U_1, U_2, U_3, etc.) to the corresponding coefficients of the desired-response equation.

By straightforward application of Kirchhoff's laws to the simple cases of $n = 1, 2, 3$, i.e., single-, double-, and triple-tuned filters, we find that the magnitude equations that result are exactly given by the general equation (4). This equation and

the corresponding response shape are also shown in Figure 8.

$$\left(\frac{V_p}{V}\right)^2 = \{1 + [(V_p/V_\beta)^2 - 1](F/F_\beta)^{2n}\}. \quad (4)$$

We will here assume that this type of response shape given by (4) can be obtained for any number of coupled resonant circuits.

Remember that $F = [(f/f_0) - (f_0/f)]$ has the same numerical value for two different frequencies related to each other by $f_1 = f_0^2/f_2$, i.e., the actual response-frequency curve of Figure 4 will have geometric symmetry. To make the two sides of the response–frequency curve physically symmetrical, we should use a logarithmic frequency scale. Also, realize that

$$F_\beta = \left(\frac{f_{\beta 2}}{f_0} - \frac{f_0}{f_{\beta 2}}\right) = -\left(\frac{f_{\beta 1}}{f_0} - \frac{f_0}{f_{\beta 1}}\right) = \frac{f_{\beta 2} - f_{\beta 1}}{(f_{\beta 2}f_{\beta 1})^{1/2}} = \frac{\Delta f_\beta}{f_0}.$$

Solving for $\Delta f/\Delta f_\beta$, we have the useful equation

$$\frac{F}{F_\beta} = \left[\frac{(V_p/V)^2 - 1}{(V_p/V_\beta)^2 - 1}\right]^{1/2n}, \quad (4A)$$

where n is the total number of resonant circuits used in the filter chain. Equation (4A) was used to plot the response curves of Figure 1.

Figures 1 and 2 (see (14) and (15)) have been plotted in terms of the *numerical* bandwidth Δf to make them independent of a particular percentage bandwidth. The two frequencies producing a given Δf are then related to the resonant frequency f_0 by $f_{12} = [f_0^2 + (\Delta f/2)^2]^{1/2} \pm \Delta f/2$. We note from this equation that for small-percentage bandwidths, i.e., $f_0 \gg \Delta f/2$ the frequency plot of the resonance curve will have arithmetic symmetry.

Insofar as cascades of networks are concerned, it should be realized, of course, that the voltage ratios of (4) and (4A) apply to one network, and when N identical networks are cascaded (i.e., separated by tubes) the voltage ratios to be used in (4) and (4A) must be the Nth root of the desired resultant voltage ratio.

Solving for the roots of (4), we find this equation can be expressed in complex form

where the real r_m^b and imaginary i_m^b parts of the roots are given by (6A) and (6B).

$$r_m^b = F_\beta\{1/[(V_p/V_\beta)^2 - 1]^{1/2n}\} \sin\left(\frac{2m-1}{n}\frac{\pi}{2}\right), \quad (6A)$$

$$i_m^b = F_\beta\{1/[(V_p/V_\beta)^2 - 1]^{1/2n}\} \cos\left(\frac{2m-1}{n}\frac{\pi}{2}\right), \quad (6B)$$

$m = 1, 2, 3, \cdots n/2$ for n even or $(n+1)/2$ for n odd, where n is the total number of tuned circuits used.

The meaning of the letter m should be made clear by the following discussion. The complex roots of the response equation always occur in conjugate pairs, i.e., $(r+ji)$ and $(r-ji)$, and m is the *pair number* of the various pairs of roots. As plotted in the complex plane, these roots fall on a *half circle* whose center is f_0 as shown in Figure 8 for 4 resonant circuits. It will be seen that $m = 1$ *gives the pair of roots whose real frequency components are farthest from the midfrequency*, $m = 2$ gives the pair of roots whose real frequency components are next farthest from the midfrequency, etc. The maximum value that m can reach is that which makes the cosine factor equal zero and simultaneously, of course, the sine factor equals unity. Thus $m_{\max}$ is $n/2$ for an even number of resonant circuits and $(n+1)/2$ for an odd number of resonant circuits.

By multiplying out the correct number of terms of the above general equation (5), we can prepare a list of general-shape equations for $n = 1, 2, 3$, etc., which are in exactly the form taken by the general-response equations of Design Equations—Group 1. *We use exactly as many factors of (5) as there are tuned circuits n.* These resulting equations are given in Design Equations—Group 2. We can now compare Design Equations—Groups 1 and 2 and equate the corresponding coefficients. Carrying out this procedure, we obtain the sets of simultaneous equations given in Design Equations—Group 3 that have to be solved to find the required circuit

$$\frac{V_p}{V} = \frac{1}{\dfrac{F_\beta^n}{[(V_p/V_\beta)^2 - 1]^{1/2}}} \{[jF - (-r_1^b + ji_1^b)][jF - (-r_1^b - ji_1^b)]$$

$$\times [jF - (-r_2^b + ji_2^b)][jF - (-r_2^b - ji_2^b)] \cdots \}, \quad (5)$$

constants that will produce the B type of response shape. The simultaneous equations up to $n=4$ are listed, and the procedure for obtaining the simultaneous equations for any number of tuned circuits should now be quite clear.

7.2 Gain Obtained with Response-Shape B

By comparing the equations of Design Equations—Groups 2 and 1, we see that the quantity $|\Delta_n{}^b|_{min}$, which is the minimum value of the determinantal polynomial for response-shape B is given in (7).

$$|\Delta_n{}^b|_{min} = F_\beta{}^n/[(V_p/V_\beta)^2-1]^{1/2}. \qquad (7)$$

Therefore, the gain at the peak of the response obtained with response-shape B is as given in (8).

$$V_p{}^b = \frac{I}{2\pi\Delta f_\beta(C_1C_n)^{1/2}}[(V_p/V_\beta)^2-1]^{1/2}$$
$$\times \left(\frac{K_{12}}{F_\beta}\right)\left(\frac{K_{23}}{F_\beta}\right)\left(\frac{K_{34}}{F_\beta}\right)\cdots\left(\frac{K_{(n-1)n}}{F_\beta}\right). \qquad (8)$$

Equation (8) alone is not of much use insofar as numerical gain calculations are concerned because the values of the K's in (8) must first be determined from the solution of the simultaneous equations given in Design Equations—Group 3. The required values for coefficients of coupling as obtained from Design Equations—Group 3 will be found to be in terms of $(\Delta f_\beta/f_0)$ and $[(V_p/V_\beta)^2-1]$ and, when the expressions for the required coefficients are substituted in (8), a useful gain equation will result, which is in terms of C_1, C_n, Δf_β, (V_p/V_β), and the constant-current generator I.

7.3 Resulting Phase Response of Amplitude-Response Shape B

The exact phase-response shape associated with amplitude-response shape B can, of course, be obtained from (5). We are neglecting the actual magnitude of the phase shift at the mid-frequency, which from (2) is always plus or minus some multiple of 90 degrees, depending on the number of inductive and capacitive couplings used. From (5), we see that θ_n, the phase shift of $(V_p/\vec{V})$ at any percentage bandwidth F is

given by

$$\theta_n{}^b = \tan^{-1}\left(\frac{F-i_1{}^b}{r_1{}^b}\right)+\tan^{-1}\left(\frac{F+i_1{}^b}{r_1{}^b}\right)$$
$$+\tan^{-1}\left(\frac{F-i_2{}^b}{r_2{}^b}\right)+\tan^{-1}\left(\frac{F+i_2{}^b}{r_2{}^b}\right)+\cdots, \qquad (9)$$

where $r_m{}^b$ and $i_m{}^b$ are given by (6A) and (6B). *There will be exactly as many terms in (9) as there are resonant circuits in the network.*

As an example of the use of (9), (6A), and (6B), we see that when a triple-tuned circuit is used to produce amplitude-response shape B, the resulting phase shift of $(V_p/\vec{V})$ at any $(\Delta f/\Delta f_\beta)$ is given by

$$\theta_3{}^b = \tan^{-1}\left\{2[(V_p/V_\beta)^2-1]^{1/6}\left(\frac{\Delta f}{\Delta f_\beta}\right)-1.73\right\}$$
$$+\tan^{-1}\left\{2[(V_p/V_\beta)^2-1]^{1/6}\left(\frac{\Delta f}{\Delta f_\beta}\right)+1.73\right\}$$
$$+\tan^{-1}\left\{[(V_p/V_\beta)^2-1]^{1/6}\left(\frac{\Delta f}{\Delta f_\beta}\right)\right\}. \qquad (10)$$

In a similar way, the exact phase-shift equation may be written for any number of coupled circuits that are correctly used to obtain response-shape B.

7.4 Exact Design Equations for Response-Shape B ($n=1, 2, 3$)

The design sheets given next in this paper for single-, double-, and triple-tuned circuits used to produce shape B were obtained by solving the first three sets of simultaneous equations given in Design Equations—Group 3 for the required circuit constants; substitution in (8) then gives the gain equations and substitution in (9) gives the phase-shift equation. In each case, the Q distribution chosen is the one that allows the designer to use the lowest possible Q value in the high-Q circuits of the network.[17] Thus for the double-tuned network, the case of $Q_1=Q_2$ is considered. For the triple-tuned network, the Q distribution $Q_1=Q_2$ (or $Q_3=Q_2$) is considered. The reader should realize that the equations of Design Equations—Group 3 are perfectly general and any Q distribution can be investigated.

The problem of successfully solving the simultaneous equations of Design Equations—Group 3

---

[17] Numbered references will be found in the Bibliography, Section 10, page 77.

in the cases where there are more than three resonant circuits per network, will be considered in another paper. It should be clearly realized that the coefficients of Design Equations—Group 2 give exact *numerical* values to which the general coefficients of Design Equations—Group 1 are equated; thus, even though it may be impossible to obtain closed-form design equations for the required circuit-element values, it may still be possible to obtain the numerical solutions of these simultaneous equations by some form of "try-and-try-again" method. Graphs or alignment charts can then be prepared from these numerical values and thus complete and exact design information can be satisfactorily presented to the engineer.

7.4.1 Exact Design Equations for N Cascaded Triple-Tuned Circuits for Response-Shape B. (See Figures 3, 4, and 7)

$$Q_1 = Q_2 = \left(\frac{f_0}{\Delta f_\beta}\right) 3.12 [(V_p/V_\beta)^{2/N} - 1]^{1/6}.$$

$$Q_3 = \left(\frac{f_0}{\Delta f_\beta}\right) 0.734 [(V_p/V_\beta)^{2/N} - 1]^{1/6}.$$

$$K_{12} = K_{23} = \left(\frac{\Delta f_\beta}{f_0}\right) 0.716 \frac{1}{[(V_p/V_\beta)^{2/N} - 1]^{1/6}}.$$

$$\text{Gain}_{\text{per stage}}$$
$$= \frac{G_m}{2\pi \Delta f_\beta (C_I C_{III})^{1/2}} 0.511 [(V_p/V_\beta)^{2/N} - 1]^{1/6}.$$

$$V_p/V = \{1 + [(V_p/V_\beta)^{2/N} - 1](\Delta f/\Delta f_\beta)^6\}^{N/2}$$

or $$\frac{\Delta f}{\Delta f_\beta} = \frac{[(V_p/V)^{2/N} - 1]^{1/6}}{[(V_p/V_\beta)^{2/N} - 1]^{1/6}}.$$

$$\theta_{\text{per stage}} = \tan^{-1}\left\{2[(V_p/V_\beta)^{2/N} - 1]^{1/6}\left(\frac{\Delta f}{\Delta f_\beta}\right) - 1.73\right\}$$
$$+ \tan^{-1}\left\{2[(V_p/V_\beta)^{2/N} - 1]^{1/6}\left(\frac{\Delta f}{\Delta f_\beta}\right) + 1.73\right\}$$
$$+ \tan^{-1}\left\{[(V_p/V_\beta)^{2/N} - 1]\left(\frac{\Delta f}{\Delta f_\beta}\right)\right\}.$$

7.4.2 Exact Design Equations for N Cascaded Double-Tuned Circuits for Response-Shape B. (See Figures 3, 4, and 7)

$$Q_1 = Q_2 = \left(\frac{f_0}{\Delta f_\beta}\right) 1.414 [(V_\beta/V_p)^{2/N} - 1]^{1/4}.$$

$$K_{12} = \left(\frac{\Delta f_\beta}{f_0}\right) 0.707 \frac{1}{[(V_p/V_\beta)^{2/N} - 1]^{1/4}}.$$

$$\text{Gain}_{\text{per stage}}$$
$$= \frac{G_m}{2\pi \Delta f (C_I C_{II})^{1/2}} 0.707 [(V_p/V_\beta)^{2/N} - 1]^{1/4}.$$

$$\frac{V_p}{V} = \left\{1 + \left[\left(\frac{V_p}{V_\beta}\right)^{2/N} - 1\right]\left(\frac{\Delta f}{\Delta f_\beta}\right)^4\right\}^{N/2} \text{ or}$$

$$\frac{\Delta f}{\Delta f_\beta} = \frac{\left[\left(\frac{V_p}{V}\right)^{2/N} - 1\right]^{1/4}}{\left[\left(\frac{V_p}{V_\beta}\right)^{2/N} - 1\right]^{1/4}}.$$

$$\theta_{\text{per stage}}$$
$$= \tan^{-1}\left\{1.414 [(V_p/V_\beta)^{2/N} - 1]^{1/4}\left(\frac{\Delta f}{\Delta f_\beta}\right) - 1\right\}$$
$$+ \tan^{-1}\left\{1.414 [(V_p/V_\beta)^{2/N} - 1]^{1/4}\left(\frac{\Delta f}{\Delta f_\beta}\right) + 1\right\}.$$

7.4.3 Exact Design Equations for N Cascaded Single-Tuned Circuits for Response-Shape B

$$Q = \left(\frac{f_0}{\Delta f_\beta}\right) [(V_p/V_\beta)^{2/N} - 1]^{1/2}.$$

$$\text{Gain}_{\text{per stage}} = \frac{G_m}{2\pi \Delta f_\beta C} [(V_p/V_\beta)^{2/N} - 1]^{1/2}.$$

$$V_p/V = \left\{1 + [(V_p/V_\beta)^{2/N} - 1]\left(\frac{\Delta f}{\Delta f_\beta}\right)^2\right\}^{N/2}$$

or $$\frac{\Delta f}{\Delta f_\beta} = \frac{[(V_p/V)^{2/N} - 1]^{1/2}}{[(V_p/V_\beta)^{2/N} - 1]^{1/2}}.$$

$$\theta = \tan^{-1}\left\{[(V_p/V_\beta)^{2/N} - 1]\left(\frac{\Delta f}{\Delta f_\beta}\right)\right\}.$$

8. Response-Shape C

8.1 Desired-Shape Equation

By straightforward application of Kirchhoff's laws to the simple cases of single-, double-, and triple-tuned networks, the three resulting shape equations can be generalized for *n* resonant circuits into the following general form

$$V_{p/m} = \{1 + [(V_p/V_\beta)^2 - 1][T_n(F/F_\beta)]^2\}^{1/2}, \quad (11)$$

where T_n is the Chebishev polynomial of highest power *n* as given by

$$T_n\left(\frac{F}{F_\beta}\right) = 2^{n-1}\left[\left(\frac{F}{F_\beta}\right)^n - \frac{n}{1!2^2}\left(\frac{F}{F_\beta}\right)^{n-2}\right.$$
$$+ \frac{n(n-3)}{2!2^4}\left(\frac{F}{F_\beta}\right)^{n-4}$$
$$\left. - \frac{n(n-4)(n-5)}{3!2^6}\left(\frac{F}{F_\beta}\right)^{n-6} + \cdots\right]. \quad (12)$$

It is known that the above Chebishev polynomial is also given by (13).

$$T_n\left(\frac{F}{F_\beta}\right) = \begin{cases} \cos\left[n\cos^{-1}\left(\frac{F}{F_\beta}\right)\right], \\ \qquad\qquad \text{for}\quad \left(\frac{F}{F_\beta}\right) < 1 \quad (13A) \\ \cosh\left[n\cosh^{-1}\left(\frac{F}{F_\beta}\right)\right], \\ \qquad\qquad \text{for}\quad \left(\frac{F}{F_\beta}\right) > 1. \quad (13B) \end{cases}$$

Thus we can write the shape equation for type C as

$$V_p/V = \left\{1 + \left[(V_p/V_\beta)^2 - 1\right]\left[\cos\left(n\cos^{-1}\left(\frac{F}{F_\beta}\right)\right)\right]^2\right\}^{1/2}, \quad \text{inside pass band,} \qquad (14A)$$

$$V_p/V = \left\{1 + \left[(V_p/V_\beta)^2 - 1\right]\left[\cosh\left(n\cosh^{-1}\left(\frac{F}{F_\beta}\right)\right)\right]^2\right\}^{1/2}, \quad \text{outside pass band,} \qquad (14B)$$

and, solving (14) for $(\Delta f/\Delta f_\beta)$, we obtain the useful equations

$$\left(\frac{F}{F_\beta}\right) = \cos\left[\frac{1}{n}\cos^{-1}\left(\frac{(V_p/V)^2 - 1}{(V_p/V_\beta)^2 - 1}\right)^{1/2}\right], \quad \text{inside pass band,} \qquad (15A)$$

$$\left(\frac{F}{F_\beta}\right) = \cosh\left[\frac{1}{n}\cosh^{-1}\left(\frac{(V_p/V)^2 - 1}{(V_p/V_\beta)^2 - 1}\right)^{1/2}\right], \quad \text{outside pass band,} \qquad (15B)$$

where n is the total number of resonant circuits used in the filter chain.

Equation (15B) was used to obtain selectivity curves given in Figure 2. The discussion following (4) and (4A) concerning the quantities F and Δf should now be reread. The voltage ratios in (14) and (15) are the ratios for one network so that for N cascaded identical networks the voltage ratios to be used in (15) are the Nth root of the desired resultant voltage ratios.

8.2 LOCATION OF PEAKS AND VALLEYS INSIDE PASS BAND

A little thought will show that we will obtain the location of the peaks of the response if, in (15A) we set V equal to V_p; and we will obtain the locations of the valleys of the response if in (15A) we set $V = V_\beta$.

Making the above substitutions, we obtain (16), which gives the location of the maxima of the response, and (17), which gives the location of the minima of the response.

$$\frac{\Delta f_{\text{peaks}}}{\Delta f_\beta} = \cos\left(\frac{2m-1}{n}\frac{\pi}{2}\right). \qquad (16)$$

$$\frac{\Delta f_{\text{valleys}}}{\Delta f_\beta} = \cos\left(\frac{2m}{n}\frac{\pi}{2}\right). \qquad (17)$$

As before, $m = 1, 2, 3, \cdots n/2$ for n even, or $(n+1)/2$ for n odd. $m = 1$ gives the location of the pair of peaks and pair of valleys that are most distant from the midfrequency; $m = 2$ gives the location of the pair of peaks and pair of valleys that are second most distant from the midfrequency, etc.

From (16), we note the interesting point that the ratio of the bandwidth between outside peaks Δf_{p1} to the bandwidth Δf_β (where the skirt response equals the valley response) is 0.707 for double-tuned circuits; 0.866 for triple-tuned circuits; 0.922 for quadruple-tuned circuits, etc.

8.3 MATHEMATICAL MANIPULATION

Solving for the roots of (14), we find it can be expressed in the complex form (18).

$$\begin{aligned} \frac{V_p}{V} = \frac{1}{F_\beta{}^n/2^{n-1}\left[(V_p/V_\beta)^2 - 1\right]^{1/2}} \\ \times\{[jF - (-r_1{}^c + ji_1{}^c)] \\ \times[jF - (-r_1{}^c - ji_1{}^c)] \\ \times[jF - (-r_2{}^c + ji_2{}^c)] \\ \times[jF - (-r_2{}^c - ji_2{}^c)]\cdots\}, \quad (18) \end{aligned}$$

where the real $r_m{}^c$ and imaginary $i_m{}^c$ parts of the roots are given by (19A) and (19B).

$$\left.\begin{aligned} r_m{}^c &= F_\beta(s_n)\sin\left(\frac{2m-1}{n}\frac{\pi}{2}\right), \\ i_m{}^c &= F_\beta(c_n)\cos\left(\frac{2m-1}{n}\frac{\pi}{2}\right), \end{aligned}\right\} \quad (19A)$$

where

$$\left.\begin{aligned} s_n &= \sinh\left\{\frac{1}{n}\sinh^{-1}1/[(V_p/V_\beta)^2 - 1]^{1/2}\right\} \\ c_n &= \cosh\left\{\frac{1}{n}\sinh^{-1}1/[(V_p/V_\beta)^2 - 1]^{1/2}\right\} \end{aligned}\right\} \quad (19B)$$

and $m = 1, 2, 3, 4 \cdots n/2$ for n even, or $(n+1)/2$ for n odd.

Consideration of (19) shows that if plotted in the complex plane, the roots of the Chebishev or shape-C type of response fall on a half ellipse as shown in Figure 9.

The meaning and use of m in (19) should be clear from Figure 8 and from the paragraph in Section 7 that gives the meaning of m in connection with (6).

By "multiplying out" the correct number of terms of the above general equation (18), we can prepare a list of general-shape equations for $n = 1$, 2, 3, etc., which are in exactly the form taken by general response equations of Design Equations—Group 1. These resulting equations are given in Design Equations—Group 4. (*We use exactly as many factors of (18) as the number of resonant circuits in the networks.*)

We can now compare Design Equations—Groups 4 and 1 and equate the corresponding coefficients. Carrying out this procedure, we obtain the sets of simultaneous equations given in Design Equations—Group 5, which have to be solved to obtain the exact required circuit constants (Q and K) that will produce the C type of response shape. The simultaneous equations up to $n = 4$ are listed, and the procedure for obtaining the simultaneous equations for any n should now be quite clear.

8.4 Gain Obtained with Response-Shape C

Comparison of the equation given in Design Equations—Group 1 and those given in Design Equations—Group 4 shows that for response-shape C the value of $|\Delta_n{}^c|_{min}$ is

$$|\Delta_n{}^c|_{min} = \frac{F_\beta{}^n}{2^{n-1}[(V_p/V_\beta)^2 - 1]^{1/2}}, \quad (20)$$

and using (2) and (1A), we see that the gain obtained at the voltage response peaks with

response-shape C can be written as

$$V_p{}^c = \frac{I}{2\pi\Delta f_\beta(C_1 C_n)^{1/2}} 2^{n-1}[(V_p/V_\beta)^2 - 1]^{1/2}$$
$$\times \left(\frac{K_{12}}{F_\beta}\right)\left(\frac{K_{23}}{F_\beta}\right)\left(\frac{K_{34}}{F_\beta}\right)\cdots\left(\frac{K_{(n-1)n}}{F_\beta}\right). \quad (21)$$

Equation (21) alone does not enable us to make any numerical gain calculations, because the re-
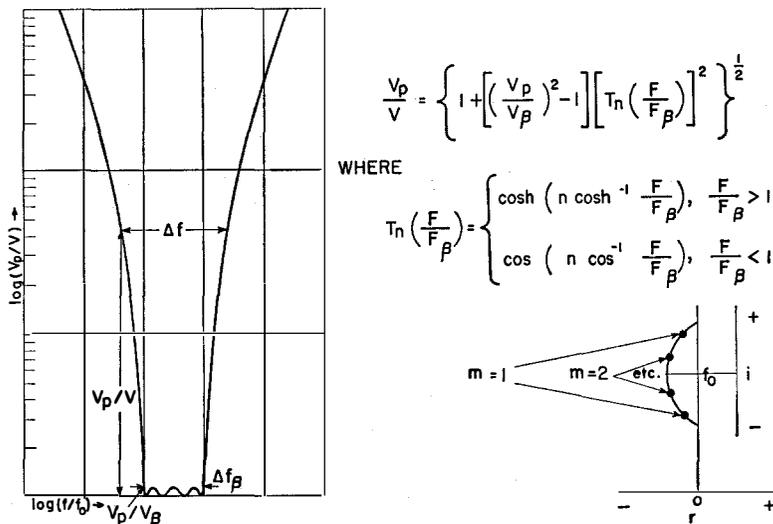
Figure 9—The exact equation describing response-shape C and the location of the roots of the equation on a semi-ellipse on the complex plane. Equation (19) gives the exact root values. n is the number of resonant circuits used and the response equation for an n-resonant-circuit network will have n roots.

quired values for the coefficients of coupling K must first be found from the solution of the simultaneous equations given in Design Equations—Group 5. It will be found that the required coefficients of coupling will be a function of the desired percentage bandwidth F_β and the ratio (V_p/V_β), and when the expression for the required coefficient of coupling is substituted in (21) a useful gain equation results.

8.5 Resulting Phase Response of Amplitude-Response Shape C

From (18), we can obtain the exact phase response shape that is obtained when response-shape C is used. This will neglect the actual magnitude of the phase shift at the midfrequency, which from (2) is always plus or minus some multiple of 90 degrees, depending on the number of inductive and capacitive couplings used. From

(18), we see that the phase shift θ_n of $(V_p/\vec{V})$ at any percentage bandwidth F is given by

$$\theta_n{}^c = \tan^{-1}\left(\frac{F-i_1{}^c}{r_1{}^c}\right) + \tan^{-1}\left(\frac{F+i_1{}^c}{r_1{}^c}\right)$$
$$+ \tan^{-1}\left(\frac{F-i_2{}^c}{r_2{}^c}\right) + \tan^{-1}\left(\frac{F+i_2{}^c}{r_2{}^c}\right) + \cdots, \quad (22)$$

where $r_m{}^c$ and $i_m{}^c$ are given by (19). There will be exactly as many terms in (22) as there are resonant circuits in the network.

As an example of the use of (22) and (19), we see that when a triple-tuned circuit is used to produce amplitude-response shape C, the resulting phase shift of $(V_p/\vec{V})$ is given by

$$\theta_3{}^c = \tan^{-1}\left[\frac{2}{s_3}\left(\frac{\Delta f}{\Delta f_\beta}\right) - 1.73\frac{c_3}{s_3}\right]$$
$$+ \tan^{-1}\left[\frac{2}{s_3}\left(\frac{\Delta f}{\Delta f_\beta}\right) + 1.73\frac{c_3}{s_3}\right]$$
$$+ \tan^{-1}\left[\frac{1}{s_3}\left(\frac{\Delta f}{\Delta f_\beta}\right)\right],$$

where s_3 and c_3 are given by (19).

In an exactly similar way, the exact phase-shift equation may be written for any number of resonant circuits when they are used to obtain response-shape C.

8.6 EXACT DESIGN EQUATIONS FOR RESPONSE-SHAPE C ($n = 1, 2, 3$)

The design sheets given next in this paper for single-, double-, and triple-tuned circuits used to produce response-shape C were obtained by solving the first three sets of simultaneous equations in Design Equations—Group 5 for the required circuit constants (with the Q distribution given below). Single-tuned design is, of course, identical for both response-shapes B and C. Substitution in (21) gives the gain equation, and substitution in (22) gives the phase-shift equation.

In the case of the double-tuned circuit, the Q distribution considered is the one that allows the designer to use the lowest possible Q, i.e., the distribution $Q_1 = Q_2$.

In the case of the triple-tuned circuit, the Q distribution considered here is the one that pro-

duced the simplest mathematical solution, i.e., $Q_1 = Q_3 = Q$ and $Q_2 = \infty$. This is not the most practical useful Q distribution because of the infinite Q required in the middle resonant circuit.[17] The solution of the three simultaneous equations given in Design Equations—Group 5 for the triple-tuned circuit has been accomplished for the much more practical Q distribution of $Q_1 = Q_2 = Q$ (or $Q_3 = Q_2 = Q$), and this solution will be presented in a later paper.

The problem of successfully solving the simultaneous equations of Design Equations—Group 5 for the cases where there are more than three resonant circuits per network will be considered in another paper. It should be clearly realized that the coefficients of Design Equations—Group 4 give us exact numerical values to which we are equating the general coefficients of Design Equations—Group 1. Thus, even though it may be impossible to obtain closed-form design equations for the required circuit-element values, it may still be possible to obtain the numerical solution of these simultaneous equations by some form of "try-and-try-again" method. Graphs or alignment charts can then be prepared from these numerical values, and complete exact design information can thus be satisfactorily presented to the engineer.

8.6.1 Exact Design Equations for N Cascaded Triple-Tuned Circuits for Response-Shape C (See Figures 3, 4, and 7)

Let $s_3 = \sinh\{\frac{1}{3}\sinh^{-1} 1/[(V_p/V_\beta)^{2/N} - 1]^{1/2}\}$

$$Q_1 = Q_3 = \frac{f_0}{\Delta f_\beta}\frac{1}{s_3}.$$

$$Q_2 = \infty$$

$$K_{12} = K_{23} = \frac{\Delta f_\beta}{f_0}(0.375 + 0.5s_3{}^2)^{1/2}.$$

$$\text{Gain}_{\text{per stage}} = \frac{G_m}{2\pi\Delta f_\beta(C_I C_{III})^{1/2}}$$
$$\times (1.5 + 2s_3{}^2)[(V_p/V_\beta)^{2/N} - 1]^{1/2}.$$

$$\frac{\Delta f}{\Delta f_\beta} = \cosh\left\{\frac{1}{3}\cosh^{-1}\left[\frac{(V_p/V)^{2/N} - 1}{(V_p/V_\beta)^{2/N} - 1}\right]^{1/2}\right\}$$

outside pass band,

$$\frac{\Delta f}{\Delta f_\beta} = \cos\left\{\tfrac{1}{3}\cos^{-1}\left[\frac{(V_p/V)^{2/N}-1}{(V_p/V_\beta)^{2/N}-1}\right]^{1/2}\right\},$$

inside pass band.

$$\theta_{\text{per stage}} = \tan^{-1}\frac{2}{s_3}\left[\frac{\Delta f}{\Delta f_\beta}-0.87(1+s_3{}^2)^{1/2}\right]$$

$$+\tan^{-1}\frac{2}{s_3}\left[\frac{\Delta f}{\Delta f_\beta}+0.87(1+s_3{}^2)^{1/2}\right]$$

$$+\tan^{-1}\frac{1}{s_3}\left[\frac{\Delta f}{\Delta f_\beta}\right].$$

8.6.2 *Exact Design Equations for N Cascaded Double-Tuned Stages for Response-Shape C (See Figures 3, 4, and 7)*

Let $s_2 = \sinh\{\tfrac{1}{2}\sinh^{-1}1/[(V_p/V_\beta)^{2/N}-1]^{1/2}\}$.

$$Q_1 = Q_2 = \frac{f_0}{\Delta f_\beta}\frac{1.414}{s_2}.$$

$$K_{12} = \frac{\Delta f_\beta}{f_0}0.707(1+s_2{}^2)^{1/2}.$$

$$\text{Gain}_{\text{per stage}} = \frac{G_m}{2\pi\Delta f_\beta(C_\mathrm{I}C_\mathrm{II})^{1/2}}1.414(1+s_2{}^2)^{1/2}$$

$$\times[(V_p/V_\beta)^{2/N}-1]^{1/2}.$$

$$\frac{\Delta f}{\Delta f_\beta} = \cosh\left\{\tfrac{1}{2}\cosh^{-1}\left[\frac{(V_p/V)^{2/N}-1}{(V_p/V_\beta)^{2/N}-1}\right]^{1/2}\right\},$$

outside pass band,

$$\frac{\Delta f}{\Delta f_\beta} = \cos\left\{\tfrac{1}{2}\cos^{-1}\left[\frac{(V_p/V)^{2/N}-1}{(V_p/V_\beta)^{2/N}-1}\right]^{1/2}\right\},$$

inside pass band.

$$\theta_{\text{per stage}} = \tan^{-1}\frac{1.414}{s_2}\left[\frac{\Delta f}{\Delta f_\beta}-0.707(1+s_2{}^2)^{1/2}\right]$$

$$+\tan^{-1}\frac{1.414}{s_2}\left[\frac{\Delta f}{\Delta f_\beta}+0.707(1+s_2{}^2)^{1/2}\right].$$

9. Comments on Method of Design that Uses Complex Roots (or "Poles") of Network-Response Equation

9.1 MATHEMATICAL PROCEDURE

Although perhaps not stated from quite the viewpoint given below, there has recently been presented a method of design that also finds the complex roots of the desired amplitude-response-shape equation, and then finds the complex roots

or poles of the circuit-response equations given in Design Equations—Group 1. The complex roots of the desired amplitude-response equation are then equated to the corresponding complex roots of the circuit-response equation to obtain the necessary n simultaneous equations required for the solution for the n unknown circuit constants.

Now, unfortunately, as we increase the number of resonant circuits in our n resonant-circuit band-pass network, the expressions for the complex roots or poles of the network in terms of the circuit constants K and Q become more and more complicated. To generalize, we can see from (2) that it will be necessary to solve an nth order equation to find the roots or poles of an n resonant-circuit band-pass network. It is thus theoretically impossible to obtain general expressions for the poles of band-pass circuits employing more than 5 resonant circuits and, in practice, the general expression for the poles of even a triple-tuned circuit having three finite and different Q's seems almost hopelessly complicated.

To demonstrate the above fact, the pole location $(r\pm ji)$ for single-, double-, and triple-tuned networks are given below in (23), (24), (25), i.e., these are the roots of the corresponding equations of Design Equations—Group 1.

$$F_1 = -d\pm j0, \text{ single tuned,} \tag{23}$$

$$F_{1,2} = -\left(\frac{d_1+d_2}{2}\right)$$

$$\pm j\left[K_{12}{}^2-\left(\frac{d_1-d_2}{2}\right)^2\right]^{1/2}, \text{ double tuned.} \tag{24}$$

The roots of a triple-tuned circuit are

$$F_{1,2} = -[\tfrac{1}{3}C_2+\tfrac{1}{2}(\alpha+\beta)]\pm j\tfrac{3}{2}^{1/2}(\alpha-\beta),$$
$$F_3 = -[\tfrac{1}{3}C_2-(\alpha+\beta)]\pm j0,$$

where

$$\alpha = \left\{-\left(\frac{q}{2}\right)+\left[\left(\frac{q}{2}\right)^2+\left(\frac{p}{3}\right)^3\right]^{1/2}\right\}^{1/3},$$

$$\beta = \left\{-\left(\frac{q}{2}\right)-\left[\left(\frac{q}{2}\right)^2+\left(\frac{p}{3}\right)^3\right]^{1/2}\right\}^{1/3},$$

where

$$q = C_0-\tfrac{1}{3}C_2C_1+\tfrac{2}{27}C_2{}^3,$$
$$p = C_1-\tfrac{1}{3}C_2{}^2,$$

where

C_0, C_1, C_2 are given in Design Equations —Group 1.

$$\tag{25}$$

When the above three roots of the triple-tuned-circuit-response equation are simultaneously equated to the corresponding three roots of the desired triple-tuned-response equation, as obtained from (6) or (19), it is readily apparent that the solution of the resulting simultaneous equations for the required values of the circuit constants (K's and Q's) will indeed be a formidable task.

9.2 STAGGER TUNING OF SIMPLE INTERSTAGE CIRCUITS

The great practical importance of the pole type of design method must not be overlooked, however. When we consider the case of an overall network consisting of many simple band-pass networks (i.e., single and double tuned) *that are separated from each other by vacuum tubes, i.e., there is no coupling between the different simple circuits*, then this design method is extremely useful. For this case, the expressions for each of the many poles retain the simplicity of (23) and (24), and it is a relatively simple matter to solve the resulting simultaneous equations for the required circuit constants. (It will be noted that the expression for the poles of a double-tuned circuit (24) becomes quite simple for the case of $Q_1 = Q_2$.)

9.2.1 Single-Tuned Interstage Circuits as Used to Obtain Response-Shape B (Small-Percentage Pass Band)

For example, let us briefly consider the case of stagger tuning of a single-tuned interstage circuit. When obtaining the expressions for the poles of the networks, it is always important to consider the question of whether the *resonant frequency* of the networks used is identical with the *midfrequency* of the desired response shape. For the case of stagger tuning of *single-tuned* interstage circuits, it is of course obvious that this cannot be the case, and therefore it is necessary to express the equation for the pole of the network in terms of both the desired midfrequency of the response and the resonant frequency of the circuits.

A little thought will show that for the small-percentage pass-band case, the desired general expression for the pole of a single-tuned network,

which allows us mathematically to place the pole anywhere on the frequency axis, is given by (26).

$$P_m = d_m \pm j(\Delta f_{rm}/f_0), \tag{26}$$

where the subscript m has the same significance as in Sections 7 and 8, d is the decrement (i.e., reciprocal of Q) of the single-tuned circuit being considered, and $(\Delta f_{rm}/f_0)$ is the percentage bandwidth (from the midfrequency of the desired response) between the required pair of resonant frequencies of the mth pair of single-tuned interstages. (Equation (26) can be obtained from the usual simple expression for the transfer impedance of a single-tuned circuit by effectively changing the coordinate-system reference by simply expressing the resonant frequency of the resonant circuit as $f_r = f_0(1 \pm K/2)$, where K is twice the percentage frequency difference between the desired midfrequency f_0 and the circuit resonant frequency f_r.)

By equating the above circuit pole expression of (26) to the amplitude-response-shape-B pole expression of (6), we obtain the first two design equations of the design sheet for stagger tuning to produce response-shape B.

The following equations give the desired-response-shape equation in three different forms. The final equations are the gain equations in two different forms. These gain equations are obtained by realizing that the total output voltage of the stagger-tuned chain at any frequency is given by simply multiplying together the responses of all the networks in the chain, thus obtaining (27).

$$\vec{V} =$$

$$\frac{I_1/\omega_0 C_1 \quad I_2/\omega_0 C_2 \quad I_3/\omega_0 C_3 \quad I_4/\omega_0 C_4 \cdots}{\left[jF - \left(-d_1 \pm j\frac{\Delta f_{r1}}{f_0} \right) \right] \left[jF - \left(-d_2 \pm j\frac{\Delta f_{r2}}{f_0} \right) \right] \left[\cdots \right]}$$

$$\tag{27}$$

The gain at the peak of the response is obtained when the magnitude of the denominator of (27) has its minimum value. We have already seen that for response-shape B this minimum value is given by (8). Thus, making use of (8), we obtain the total-gain equation; the nth root of this total-gain equation gives the equation for gain per stage as included in the design sheet.

9.2.2 Single-Tuned Interstage Circuits Used to Obtain Response-Shape C (Small-Percentage Pass Band)

By going through exactly the same line of reasoning used in Section 9.2.1, using the pole expressions of (19) for amplitude-response shape C, and the value of $|\Delta_n{}^c|_{\min}$ for response-shape C given by (20), we obtain the equations given on the design sheet for stagger tuning of single-tuned interstage networks used to produce response-shape C.

It should be realized that the voltage ratios given on the stagger-tuning design sheets are the ratios for a one-staggered n-tuple design, if N of these n-tuples are to be cascaded, then the voltage ratios to be used on the design sheets should be the Nth root of the over-all resulting desired voltage ratio.

In the interests of simplicity, a general many-termed phase-shift equation has not been included on the stagger-tuned design sheets. By referring to Sections 7.3 and 8.5, the reader should be able to write the correct phase-shift equation for any specific stagger-tuned design.

9.3 STAGGER TUNING OF SINGLE-TUNED INTER-STAGE CIRCUITS FOR RESPONSE-SHAPE B (SEE FIGURE 10)

$$\frac{1}{Q_m} = \frac{\Delta f_\beta / f_0}{[(V_p/V_\beta)^2 - 1]^{1/2n}} \sin\left(\frac{2m-1}{n} 90°\right).$$

$$(f_a - f_b)_m = \frac{\Delta f_\beta}{[(V_p/V_\beta)^2 - 1]^{1/2n}} \cos\left(\frac{2m-1}{n} 90°\right).$$

$$V_p/V = \{1 + [(V_p/V_\beta)^2 - 1](\Delta f/\Delta f_\beta)^{2n}\}^{1/2}$$

or $$\frac{\Delta f}{\Delta f_\beta} = \left[\frac{(V_p/V)^2 - 1}{(V_p/V_\beta)^2 - 1}\right]^{1/2n}$$

or $$n = \frac{\log\left[\frac{(V_p/V)^2 - 1}{(V_p/V_\beta)^2 - 1}\right]^{1/2}}{\log(\Delta f/\Delta f_\beta)}.$$

$$\text{Gain}_{\text{per stage}} = \frac{G_m}{2\pi\Delta f_\beta C}[(V_p/V_\beta)^2 - 1]^{1/2n}$$

or $$n = \frac{\log\left(\frac{\text{Gain}_{\text{total}}}{[(V_p/V_\beta)^2 - 1]^{1/2}}\right)}{\log\left(\frac{G_m}{2\pi\Delta f_\beta C}\right)},$$

where

G_m = geometric mean of all G_m's,

C = geometric-mean capacitance.

9.4 STAGGER TUNING OF SINGLE-TUNED INTER-STAGE CIRCUITS FOR RESPONSE-SHAPE C (SEE FIGURE 10)

$$\frac{1}{Q_m} = \frac{\Delta f_\beta}{f_0} s_n \sin\left(\frac{2m-1}{n} 90 \text{ degrees}\right).$$

$$s_n = \sinh\left\{\frac{1}{n} \sinh^{-1} \frac{1}{[(V_p/V_\beta)^2 - 1]^{1/2}}\right\}$$

$$(f_a - f_b)_m = \Delta f_\beta c_n \cos\left(\frac{2m-1}{n} 90 \text{ degrees}\right).$$

$$c_n = \cosh\left\{\frac{1}{n} \sinh^{-1} \frac{1}{[(V_p/V_\beta)^2 - 1]^{1/2}}\right\}.$$

For shape outside the pass band,

$$\frac{V_p}{V} = \{1 + [(V_p/V_\beta)^2 - 1]$$

$$\times \{\cosh^2[n \cosh^{-1}(\Delta f/\Delta f_\beta)]\}\}^{1/2}$$

or $$\frac{\Delta f}{\Delta f_\beta} = \cosh\left\{\frac{1}{n} \cosh^{-1}\left[\frac{(V_p/V)^2 - 1}{(V_p/V_\beta)^2 - 1}\right]^{1/2}\right\}$$

$m = \frac{n+1}{2}$ (n, odd)

$m = \frac{n}{2}$ (n, even)
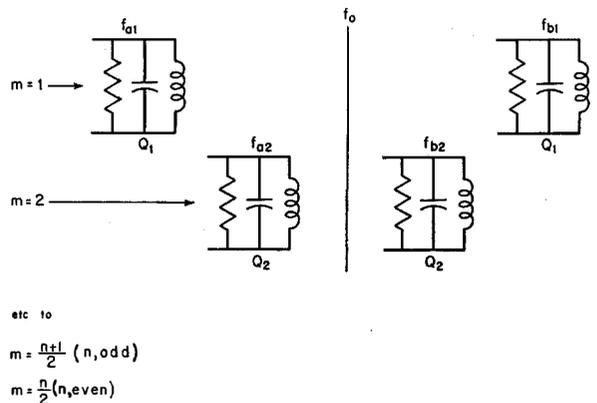
Figure 10—Definition of symbols in the stagger-tuning design equations. Thus $m = 1$ gives the resonant-frequency difference and the required Q for that pair of circuits that are staggered the greatest distance from the midfrequency, $m = 2$ is for the next greatest distance, to the limiting cases $m_{\max} = (n+1)/2$ for n odd and $m_{\max} = n/2$ for n even.

or
$$n = \frac{\cosh^{-1}\left[\dfrac{(V_p/V)^2 - 1}{(V_p/V_\beta)^2 - 1}\right]^{1/2}}{\cosh^{-1}(\Delta f/\Delta f_\beta)}.$$

For shape inside the pass band,

$$V_p/V = \{1 + [(V_p/V_\beta)^2 - 1]$$
$$\times \{\cos^2[n\cos^{-1}(\Delta f/\Delta f_\beta)]\}\}^{1/2},$$

$$\frac{\Delta f_{\max}}{\Delta f_\beta} = \cos\left(\frac{2m-1}{n}\,90\text{ degrees}\right),$$

$$\frac{\Delta f_{\min}}{\Delta f_\beta} = \cos\left(\frac{2m}{n}\,90\text{ degrees}\right).$$

$$\text{Gain}_{\text{per stage}} = \frac{G_m}{2^{1/n}\pi\Delta f_\beta C}[(V_p/V_\beta)^2 - 1]^{1/2n}$$

or
$$n = \frac{\log\left\{\dfrac{2\,\text{Gain}_{\text{total}}}{[(V_p/V_\beta)^2 - 1]^{1/2}}\right\}}{\log\left(\dfrac{G_m}{\pi\Delta f_\beta C}\right)},$$

where

$$G_m = \text{geometric mean of all } G_m\text{'s},$$
$$C = \text{geometric mean of all } C\text{'s}.$$

10. Bibliography

1. S. Butterworth, "On the Theory of Filter-Amplifiers," *Experimental Wireless* and *Wireless Engineer*, v. 7, pp. 536–541; October, 1930.

2. W. Cauer, "Siebschaltungen," VDI Verlag; 1931.

3. W. R. Bennett, United States Patent 1,849,656; March, 1932.

4. H. W. Bode, "General Theory of Electric Wave-Filters," *Journal of Mathematics and Physics*, v. 13, pp. 275–362; November, 1934.

5. H. W. Bode and R. L. Dietzold, "Ideal Wave Filters," *Bell System Technical Journal*, v. 14, pp. 215–252; April, 1935.

6. W. Cauer, "New Theory and Design of Wave Filters," *Physics;* April, 1939.

7. S. Darlington, "Synthesis of Reactance Four Poles Which Produce a Prescribed Insertion Loss Characteristic," *Journal of Mathematics and Physics*, v. 18, pp. 257–353; September, 1939.

8. V. D. Landon, "Cascade Amplifiers with Maximal Flatness," *RCA Review*, Part I, v. 5, pp. 347–363; January, 1941: Part II, v. 5, pp. 481–498; April, 1941.

9. H. Wallman, "Stagger-Tuned Intermediate-Frequency Amplifiers," *M.I.T. Radiation Laboratory, Report 524;* February, 1944. (Presented, 1946 Institute of Radio Engineers National Convention, New York, New York.)

10. W. W. Hansen and O. C. Lundstrom, "Experimental Determination of Impedance Functions by Use of an Electrolytic Tank," *Proceedings of the I.R.E.,* v. 33, pp. 528–534; August, 1945.

11. W. W. Hansen, "On Maximum Gain-Bandwidth Product in Amplifiers," *Journal of Applied Physics*, v. 16, pp. 528–534; September, 1945.

12. R. H. Baum, "Design of Broad-Band Intermediate-Frequency Amplifiers," *Journal of Applied Physics*, Part I, v. 17, pp. 519–529; June, 1946. Part II, v. 17, pp. 721–729; September, 1946.

13. P. I. Richards, "Universal Optimum-Response Curves for Arbitrarily Coupled Resonators," *Proceedings of the I.R.E.*, v. 34, pp. 624–629; September, 1946.

14. K. R. Spangenberg, "The Universal Characteristics of Triple-Resonant-Circuit Band-Pass Filters," *Proceedings of the I.R.E.*, v. 34, pp. 629–635; September, 1946. [This reference makes an approximation in the triple-tuned analysis so that the expression for the poles of the network are not as exact as those considered in the present paper.]

15. W. E. Bradley, "A Theory of Wide-Band Amplifier Design," presented, 1947 Institute of Radio Engineers National Convention, New York, New York.

16. Milton Dishal, "Exact Design and Analysis of Double- and Triple-Tuned Band-Pass Amplifiers," *Proceedings of the I.R.E.*, v. 35, pp. 606–626; June, 1947. Also, *Electrical Communication*, v. 24, pp. 349–373; September, 1947.

17. V. D. Landon and Milton Dishal, Discussion of "Exact Design and Analysis of Double- and Triple-Tuned Band-Pass Amplifier," by Milton Dishal, *Proceedings of the I.R.E.*, v. 35, pp. 1507–1510; December, 1947. Also, *Electrical Communication*, v. 25, pp. 100–102; March, 1948.

18. W. H. Huggins, "A Note on Frequency Transformations for Use with the Electrolytic Tank," *Proceedings of the I.R.E.*, v. 36, pp. 421–424; March, 1948.

19. W. H. Huggins, "The Natural Behavior of Broad-Band Circuits," Electronics Research Laboratories (AMC). Report E5013; May, 1948.

Design Equations—Group 1

Exact Circuit-Response-Shape Equations in the Complex Polynomial Form for an n-Resonant-Circuit Network

Single-Tuned Circuit

$$\frac{V_p}{\vec{V}_1}=\frac{1}{|\Delta_1|_{\min}}[jF+A_0].$$
$$A_0=d_1.$$

Double-Tuned Circuit

$$\frac{V_p}{\vec{V}_2}=\frac{1}{|\Delta_2|_{\min}}[(jF)^2+B_1(jF)+B_0].$$
$$B_1=d_1+d_2.$$
$$B_0=K_{12}^2+d_1d_2.$$

Triple-Tuned Circuit

$$\frac{V_p}{\vec{V}_3}=\frac{1}{|\Delta_3|_{\min}}[(jF)^3+C_2(jF)^2+C_1(jF)+C_0].$$
$$C_2=d_1+d_2+d_3.$$
$$C_1=K_{12}^2+K_{23}^2+d_1d_2+d_1d_3+d_2d_3.$$
$$C_0=K_{12}^2d_3+K_{23}^2d_1+d_1d_2d_3.$$

Quadruple-Tuned Circuit

$$\frac{V_p}{\vec{V}_4}=\frac{1}{|\Delta_4|_{\min}}[(jF)^4+D_3(jF)^3+D_2(jF)^2+D_1(jF)+D_0].$$
$$D_3=d_1+d_2+d_3+d_4.$$
$$D_2=K_{12}^2+K_{23}^2+K_{34}^2+d_1d_2+d_1d_3+d_1d_4+d_2d_3+d_2d_4+d_3d_4.$$
$$D_1=K_{12}^2d_3+K_{12}^2d_4+K_{23}^2d_1+K_{23}^2d_4+K_{34}^2d_1+K_{34}^2d_2+d_1d_2d_3+d_1d_2d_4+d_1d_3d_4+d_2d_3d_4.$$
$$D_0=K_{12}^2K_{34}^2+K_{12}^2d_3d_4+K_{23}^2d_1d_4+K_{34}^2d_1d_2+d_1d_2d_3d_4.$$

Design Equations—Group 2

Exact Complex Polynomials for Response-Shape B

Single-Tuned Circuit

$$\frac{V_p}{\vec{V}_1}=\frac{1}{F_\beta/[(V_p/V_\beta)^2-1]^{1/2}}[jF+A_0^b].$$
$$A_0^b=1\left\{\frac{1}{[(V_p/V_\beta)^2-1]^{1/2}}\right\}F_\beta.$$

Double-Tuned Circuit

$$\frac{V_p}{\vec{V}_2}=\frac{1}{F_\beta^2/[(V_p/V_\beta)^2-1]^{1/2}}[(jF)^2+B_1^b(jF)+B_0^b].$$
$$B_1^b=1.414\left\{\frac{1}{[(V_p/V_\beta)^2-1]^{1/4}}\right\}F_\beta.$$
$$B_0^b=1\left\{\frac{1}{[(V_p/V_\beta)^2-1]^{1/4}}\right\}^2F_\beta^2.$$

Triple-Tuned Circuit

$$\frac{V_p}{V_3} = \frac{1}{F_\beta{}^3/[(V_p/V_\beta)^2-1]^{1/2}}\big[(jF)^3 + C_2{}^b(jF)^2 + C_1{}^b(jF) + C_0{}^b\big].$$

$$C_2{}^b = 2\left\{\frac{1}{[(V_p/V_\beta)^2-1]^{1/6}}\right\}F_\beta.$$

$$C_1{}^b = 2\left\{\frac{1}{[(V_p/V_\beta)^2-1]^{1/6}}\right\}^2 F_\beta{}^2.$$

$$C_0{}^b = 1\left\{\frac{1}{[(V_p/V_\beta)^2-1]^{1/6}}\right\}^3 F_\beta{}^3.$$

Quadruple-Tuned Circuit

$$\frac{V_p}{V_4} = \frac{1}{F_\beta{}^4/[(V_p/V_\beta)^2-1]^{1/2}}\big[(jF)^4 + D_3{}^b(jF)^3 + D_2{}^b(jF)^2 + D_1{}^b(jF) + D_0{}^b\big].$$

$$D_3{}^b = 2.61\left\{\frac{1}{[(V_p/V_\beta)^2-1]^{1/8}}\right\}F_\beta.$$

$$D_2{}^b = 3.41\left\{\frac{1}{[(V_p/V_\beta)^2-1]^{1/8}}\right\}^2 F_\beta{}^2.$$

$$D_1{}^b = 2.61\left\{\frac{1}{[(V_p/V_\beta)^2-1]^{1/8}}\right\}^3 F_\beta{}^3.$$

$$D_0{}^b = 1\left\{\frac{1}{[(V_p/V_\beta)^2-1]^{1/8}}\right\}^4 F_\beta{}^4.$$

Design Equations—Group 3

EXACT SIMULTANEOUS EQUATIONS TO BE SOLVED FOR CIRCUIT CONSTANTS (K'S AND Q'S)
OF AN n-RESONANT-CIRCUIT NETWORK TO PRODUCE RESPONSE-SHAPE B
WHEN THE CIRCUITS ARE CORRECTLY RESONATED

Single-Tuned Circuit

$$d_1 = \frac{F_\beta}{[(V_p/V_\beta)^2-1]^{1/2}}.$$

Double-Tuned Circuit

$$d_1 + d_2 = 1.414\frac{F_\beta}{[(V_p/V_\beta)^2-1]^{1/4}}.$$

$$K_{12}{}^2 + d_1 d_2 = \frac{F_\beta{}^2}{[(V_p/V_\beta)^2-1]^{2/4}}.$$

Triple-Tuned Circuit

$$d_1 + d_2 + d_3 = 2\frac{F_\beta}{[(V_p/V_\beta)^2-1]^{1/6}}.$$

$$K_{12}{}^2 + K_{23}{}^2 + d_1 d_2 + d_1 d_3 + d_2 d_3 = 2\frac{F_\beta{}^2}{[(V_p/V_\beta)^2-1]^{2/6}}.$$

$$K_{12}{}^2 d_3 + K_{23}{}^2 d_1 + d_1 d_2 d_3 = \frac{F_\beta{}^3}{[(V_p/V_\beta)^2-1]^{3/6}}.$$

Quadruple-Tuned Circuit

$$d_1+d_2+d_3+d_4=2.61\frac{F_\beta}{[(V_p/V_\beta)^2-1]^{1/8}}.$$

$$K_{12}^2+K_{23}^2+K_{34}^2+d_1d_2+d_1d_3+d_1d_4+d_2d_3+d_2d_4+d_3d_4=3.41\frac{F_\beta^2}{[(V_p/V_\beta)^2-1]^{2/8}}.$$

$$K_{12}^2d_3+K_{12}^2d_4+K_{23}^2d_1+K_{23}^2d_4+K_{34}^2d_1+K_{34}^2d_2$$
$$+d_1d_2d_3+d_1d_2d_4+d_1d_3d_4+d_2d_3d_4=2.61\frac{F_\beta^3}{[(V_p/V_\beta)^2-1]^{3/8}}.$$

$$K_{12}^2K_{34}^2+K_{12}^2d_3d_4+K_{23}^2d_1d_4+K_{34}^2d_1d_2+d_1d_2d_3d_4=\frac{F_\beta^4}{[(V_p/V_\beta)^2-1]^{4/8}}.$$

Design Equations—Group 4

Exact Complex Polynomials for Response-Shape C

Single-Tuned Circuit

$$\frac{V_p}{\vec{V}}=\frac{1}{F_\beta/[(V_p/V_\beta)^2-1]^{1/2}}[jF+A_0^c].$$

$$A_0^c=\frac{1}{[(V_p/V_\beta)^2-1]^{1/2}}F_\beta.$$

Double-Tuned Circuit

$$\frac{V_p}{\vec{V}}=\frac{1}{F^2/2[(V_p/V_\beta)^2-1]^{1/2}}[(jF)^2+B_1^c(jF)+B_0^c].$$

$$B_1^c=1.414s_2F_\beta.$$

$$B_0^c=0.5(s_2^2+c_2^2)F_\beta^2.$$

$$s_2=\sinh\left\{\frac{1}{2}\sinh^{-1}\frac{1}{[(V_p/V_\beta)^2-1]^{1/2}}\right\}.$$

$$c_2=\cosh\left\{\frac{1}{2}\sinh^{-1}\frac{1}{[(V_p/V_\beta)^2-1]^{1/2}}\right\}.$$

Triple-Tuned Circuit

$$\frac{V_p}{\vec{V}}=\frac{1}{F_\beta^3/4[(V_p/V_\beta)^2-1]^{1/2}}[(jF)^3+C_2^c(jF)^2+C_1^c(jF)+C_0^c].$$

$$C_2^c=2s_3F_\beta.$$

$$C_1^c=(1.25s_3^2+0.75c_3^2)F_\beta^2.$$

$$C_0^c=s_3(0.25s_3^2+0.75c_3^2)F_\beta^3.$$

$$s_3=\sinh\left\{\frac{1}{3}\sinh^{-1}\frac{1}{[(V_p/V_\beta)^2-1]^{1/2}}\right\}.$$

$$c_3=\cosh\left\{\frac{1}{3}\sinh^{-1}\frac{1}{[(V_p/V_\beta)^2-1]^{1/2}}\right\}.$$

Quadruple-Tuned Circuit

$$\frac{V_p}{\overline{V}} = \frac{1}{F_\beta{}^4/8[(V_p/V_\beta)^2-1]^{1/2}}[(jF)^4 + D_3{}^c(jF)^3 + D_2{}^c(jF)^2 + D_1{}^c(jF) + D_0{}^c].$$

$$D_3{}^c = 2.61s_4 F_\beta.$$

$$D_2{}^c = (2.41s_4{}^2 + c_4{}^2)F_\beta{}^2.$$

$$D_1{}^c = s_4(0.923s_4{}^2 + 1.69c_4{}^2)F_\beta{}^3.$$

$$D_0{}^c = 0.125(s_4{}^4 + 6s_4{}^2c_4{}^2 + c_4{}^4)F_\beta{}^4.$$

$$s_4 = \sinh\left\{\frac{1}{4}\sinh^{-1}\frac{1}{[(V_p/V_\beta)^2-1]^{1/2}}\right\}.$$

$$c_4 = \cosh\left\{\frac{1}{4}\sinh^{-1}\frac{1}{[(V_p/V_\beta)^2-1]^{1/2}}\right\}.$$

Design Equations—Group 5

EXACT SIMULTANEOUS EQUATIONS TO BE SOLVED FOR CIRCUIT CONSTANTS (K'S AND Q'S)
OF AN n-RESONANT-CIRCUIT NETWORK TO PRODUCE RESPONSE-SHAPE C
WHEN THE CIRCUITS ARE CORRECTLY RESONATED

Single-Tuned Circuit

$$d_1 = \frac{F_\beta}{[(V_p/V_\beta)^2-1]^{1/2}}.$$

Double-Tuned Circuit

$$d_1 + d_2 = 1.414s_2 F_\beta.$$

$$K_{12}{}^2 + d_1 d_2 = (0.5 + s_2{}^2)F_\beta{}^2.$$

Triple-Tuned Circuit

$$d_1 + d_2 + d_3 = 2s_3 F.$$

$$K_{12}{}^2 + K_{23}{}^2 + d_1 d_2 + d_1 d_3 + d_2 d_3 = (0.75 + 2s_3{}^2)F_\beta{}^2.$$

$$K_{12}{}^2 d_3 + K_{23}{}^2 d_1 + d_1 d_2 d_3 = s_3(0.75 + s_3{}^2)F_\beta{}^3.$$

Quadruple-Tuned Circuit

$$d_1 + d_2 + d_3 + d_4 = 2.61s_4 F_\beta.$$

$$K_{12}{}^2 + K_{23}{}^2 + K_{34}{}^2 + d_1 d_2 + d_1 d_3 + d_1 d_4 + d_2 d_3 + d_2 d_4 + d_3 d_4 = (1 + 3.41s_4{}^2)F_\beta{}^2.$$

$$K_{12}{}^2 d_3 + K_{12}{}^2 d_4 + K_{23}{}^2 d_1 + K_{23}{}^2 d_4 + K_{34}{}^2 d_1 + K_{34}{}^2 d_2$$
$$+ d_1 d_2 d_3 + d_1 d_2 d_4 + d_1 d_3 d_4 + d_2 d_3 d_4 = s_4(1.69 + 2.61s_4{}^2)F_\beta{}^3.$$

$$K_{12}{}^2 K_{34}{}^2 + K_{12}{}^2 d_3 d_4 + K_{23}{}^2 d_1 d_4 + K_{34}{}^2 d_1 d_2 + d_1 d_2 d_3 d_4 = (0.125 + s_4{}^2 + s_4{}^4)F_\beta{}^4.$$

In all the above equations,

$$s_n = \sinh\left\{\frac{1}{n}\sinh^{-1}[(V_p/V_\beta)^2-1]\right\}.$$

In Memoriam

JOHN LENORD MERRILL

JOHN LENORD MERRILL was born on September 17, 1866, in Orange, New Jersey, and died in New York City on December 18, 1949, in his 84th year.

In 1884, he was employed by the Mexican Telegraph Company and the Central and South American Telegraph Company, which were jointly operated. In 1918, he became president of these companies and soon merged them under the name of All America Cables, Incorporated. In 1927, All America became part of the International Telephone and Telegraph Corporation system, and Mr. Merrill continued as president until he became chairman of the board in 1939. He also served the American Cable and Radio Corporation as chairman of its board from 1940 to 1947.

Mr. Merrill was a member of the board of directors of the International Telephone and Telegraph Corporation from 1924 to 1947 and was a vice president from 1927 to 1944.

He was active in the affairs of most of the Latin American associations in the United States. He was president of the Pan American Society from 1927 to 1940 and served as honorary president of the American Brazilian Association, Chamber of Commerce of Argentina, Chamber of Commerce of Mexico, Colombian-American Chamber of Commerce, Ecuadorian-American Association, Pan American Society, and the Venezuelan Chamber of Commerce of the United States.

In recognition of his contributions to inter-American goodwill, Mr. Merrill received decorations of the highest order from Bolivia, Brazil, Chile, Colombia, Dominican Republic, Ecuador, Haiti, Peru, and Venezuela. Among these, he received in 1936 the Silver Key to the city of Lima, Peru, and in 1944 the Silver Medal of the Bolivarian Society of the United States for his endeavors in perpetuating the memory of the South American liberator, Simon Bolivar.

Contributors to This Issue

R. J. M. ANDREWS

R. J. M. ANDREWS was born in Plymouth, Devonshire, England, in 1903. He received an honours degree in mechanical sciences from Cambridge University in 1925.

He joined the Western Electric Company in London as an engineering student in 1925 and was engaged on the engineering of the first carrier telephone system manufactured by the company. After a few years with the International Telephone and Telegraph Laboratories, he rejoined Standard Telephones and Cables, Limited, in 1934, where he has been active in the transmission laboratory on mechanical problems. In 1946, he was assigned to standardization of equipment practices for transmission systems.

• • •

A. G. CLAVIER was born in Cambrai, France, in 1894. He received a degree in electrical engineering from Ecole Supérieure d'Electricité in 1919 and then joined the staff of engineers organized by General Ferrié at the Etablissement Central de la Radiotélégraphie Militaire. He was in charge of research on high frequencies from 1920 to 1925.

In 1929, Mr. Clavier joined Les Laboratoires Standards in Paris which later became Laboratoire Central de Télécommunications, and has been continuously engaged in research on centimeter and millimeter waves. He was in charge of the experiments which, in 1930, resulted in 17-centimeter-wave transmission across the English Channel and of the developments for the Lympne-St. Inglevert microwave radiotelephone link, which was inaugurated commercially in 1934. He was assistant director of research in 1945, when he was transferred to Federal Telecommunication Laboratories in New York, where he now holds the same position.

He has published extensively on high-frequency oscillators, wave guides, and general electromagnetic theory, and has taught field theory and applications of ultra-high frequencies at the Ecole Supérieure d'Electricité.

Mr. Clavier is president of the section of the Société des Radioélectriciens dealing with hyperfrequencies. He is a Fellow of the Institute of Radio Engineers, and a Member of the Institution of Electrical Engineers.

• • •

A. G. DELAMARE was born in London in 1912. He served an apprenticeship on electro-mechanical railway signaling. In 1934, he was awarded the Higher National Certificate with distinction and an endorsement to this in 1936.

He entered the transmission laboratory of Standard Telephones and Cables, Limited, in 1936, and was engaged on mechanical design problems. During the war, he designed transmission equipment for the armed services and since 1946 has been in charge of the mechanical development group in the laboratory.

A. G. DELAMARE

Mr. Delamare is an Associate Member of the Institution of Electrical Engineers.

• • •

MILTON DISHAL was born on March 20, 1918, in Philadelphia, Pennsylvania. Temple University conferred on him two degrees, the B.S. in 1939 and M.A. in 1941. He was a Teaching Fellow in physics in that University from 1939 to 1941.

Mr. Dishal entered Federal Telecommunication Laboratories in 1941 and is now a senior engineer in the development of radio receivers having special characteristics.

Mr. Dishal is a Senior Member of the Institute of Radio Engineers.

• • •

A. G. CLAVIER
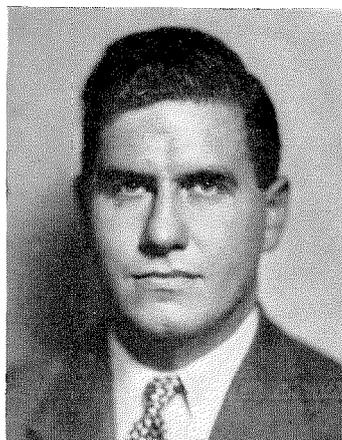
MILTON DISHAL

FRANK FAIRLEY

SIDNEY FRANKEL

H. P. MILLER, JR.

FRANK FAIRLEY was born in Preston, Lancashire, England in 1904. He received an honours degree in physics from Cambridge University in 1926.

Joining the European engineering department of International Standard Electric Corporation in 1927, he was transferred later to Standard Telephones and Cables, Limited.

From 1926 to 1936, he was engaged in planning and installing carrier systems, mostly in Malaya and India. Since then, he has developed transmission systems in London where he is now in charge of the planning and engineering of such systems.

• • •

SIDNEY FRANKEL was born on October 6, 1910 in New York City. Rensselaer Polytechnic Institute conferred three degrees on him: the B.A. degree in electrical engineering in 1931, and in mathematics the M.A. degree in 1934 and the Ph.D. degree in 1936. He was an instructor in mathematics from 1931 to 1933.

For a year after leaving college, Dr. Frankel served as a sound-recording engineer with the Brooklyn Vita-

phone Corporation. In 1937–1938, he was an assistant engineer in the design and development of electronic flight instruments for the Eclipse Aviation Corporation.

He joined the Federal Telegraph Company staff at Newark, New Jersey, in 1938 as an engineer on the design and development of radio transmitters. In 1943, he was transferred to Federal Telephone and Radio Laboratories, now Federal Telecommunication Laboratories. At present he is engaged in the development of components for microwave systems.

He is a member of Sigma Xi and a Senior Member of the Institute of Radio Engineers.

• • •
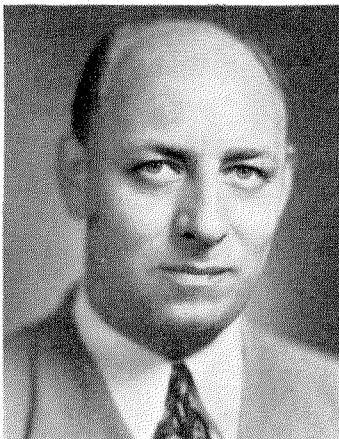
LEONARD LEWIN was born in 1919 at Southend-on-Sea, England. He studied mathematics with particular reference to transcendental functions and the electromagnetic theory of radiation.

During the war, he did research work on antennas and mirrors at the British Admiralty and in 1945 served as chairman of the Inter-Service Committee on Radar Camouflage.

He joined the engineering staff of Standard Telecommunication Laboratories in London in 1946.

• • •

H. P. MILLER, JR., was born on August 10, 1895, in Harrisburg, Pennsylvania. Stanford University granted him an A.B. degree in mechanical engineering in 1917 and the degree of Electrical Engineer in 1925.

In 1917, he joined the Federal Telegraph Company at Palo Alto, California. With the exception of the period from 1937 to 1941 when he was engaged in highway traffic studies in Pennsylvania, he has continued in the International Telephone and Telegraph System.

Mr. Miller has spent most of his time on high-power low-frequency transmitters and antennas, with special attention to the design of radio-frequency chokes. He was project engineer for the construction of a pair of 200-kilowatt high-frequency broadcast transmitters installed during the war.

He is a Senior Member of the Institute of Radio Engineers, a member of the American Institute of Electrical Engineers, and a licensed professional engineer in the state of Pennsylvania.

INTERNATIONAL TELEPHONE AND TELEGRAPH CORPORATION

Associate Manufacturing and Sales Companies

United States of America

International Standard Electric Corporation, New York, New York

Federal Telephone and Radio Corporation, Clifton, New Jersey

International Standard Trading Corporation, New York, New York

Capehart-Farnsworth Corporation, Fort Wayne, Indiana

Great Britain and Dominions

Standard Telephones and Cables, Limited, London, England

Branch Offices: Birmingham, Bristol, Leeds, Manchester, England; Glasgow, Scotland; Dublin, Ireland; Cairo, Egypt; Calcutta, India; Karachi, Pakistan; Johannesburg, South Africa; Salisbury, Southern Rhodesia

Creed and Company, Limited, Croydon, England

International Marine Radio Company Limited, Croydon, England

Ko ster-Brandes Limited, Sidcup, England

Standard Telephones and Cab es Pty. Limited, Sydney, Australia

Branch Offices: Melbourne, Australia; Wellington, New Zealand

Silovac Electrical Products Pty. Limited, Sydney, Australia

Austral Standar l Cables Pty. Limited, Melbourne, Australia

New Zealand Electric Totalisators Limited, Wel ington, New Zealand

Federal Electric Manufacturing Company, Ltd., Montreal, Canada

South America

Compañía Standard Electric Argentina, Sociedad Anónima, Industria y Comercial, Buenos Aires, Argentina

Standard Electrica, S.A., Rio de Janeiro, Brazil

Compañía Standard Electric, S.A.C., Santiago, Chile

Europe and Far East

Vereinigte Telephon- und Telegraphenfabriks Aktien-Gesellschaft Czeija, Nissl & Company, Vienna, Austria

Bell Telephone Manufacturing Company, Antwerp, Belgium

China Electric Company, Limited, Shanghai, China

Standard Electric Aktieselskab, Copenhagen, Denmark

Compagnie Générale de Constructions Téléphoniques, Paris, France

Le Matériel Téléphonique, Paris, France

Les Téléimprimeurs, Paris, France

C. Lorenz, A.G. and Subsidiaries, Berlin, Germany

Mix & Genest Aktiengesellschaft and Subsidiaries, Berlin, Germany

Süddeutsche Apparatefabrik Gesellschaft m.b.H., Nuremberg, Germany

Telephonfabrik Berliner A.G. and Subsidiaries, Berlin, Germany

Nederlandsche Standard Electric Maatschappij N.V., The Hague, Netherlands

Fabbrica Apparecchiature per Comunicazioni Elettriche, Milan, Italy

Standard Telefon-og Kabelfabrik A/S, Oslo, Norway

Standard Electrica, Lisbon, Portugal

Compañía Radio Aérea Marítima Española, Madrid, Spain

Standard Eléctrica, S.A., Madrid, Spain

Aktiebolaget Standard Radiofabrik, Stockholm, Sweden

Standard Telephone et Radio S.A., Zurich, Switzerland

Telephone Operating Systems

Compañía Telefónica Argentina, Buenos Aires, Argentina

Compañía Telegráfico-Telefónica Comercial, Buenos Aires, Argentina

Compañía Telegráfico-Telefónica del Plata, Buenos Aires, Argentina

Companhia Telefonica Paranaense S.A., Curitiba, Brazil

Companhia Telefonica Rio Grandense, Porto Alegre, Brazil

Compañía de Teléfonos de Chile, Santiago, Chile

Compañía Telefónica de Magallanes S.A., Punta Arenas, Chile

Cuban American Telephone and Telegraph Company, Havana, Cuba

Cuban Telephone Company, Havana, Cuba

Mexican Telephone and Telegraph Company, Mexico City, Mexico

Compañía Peruana de Teléfonos Limitada, Lima, Peru

Porto Rico Telephone Company, San Juan, Puerto Rico

Shanghai Telephone Company, Federal Inc. U.S.A., Shanghai, China

Radiotelephone and Radiotelegraph Operating Companies

Compañía Internacional de Radio, Buenos Aires, Argentina

Co pañía Internacional de Radio Boliviana, La Paz, Bolivia

Companhia Radio Internacional do Brasil, Rio de Janeiro, Brazil

Compañía Internacional de Radio, S.A., Santiago, Chile

Radio Corporation of Cuba, Havana, Cuba

Radio Corporation of Porto Rico, San Juan, Puerto Rico

Cable and Radiotelegraph Operating Companies

(Controlled by American Cable & Radio Corporation, New York, New York)

The Commercial Cable Company, New York, New York[1]

Mackay Radio and Telegraph Company, New York, New York[2]

All America Cables and Radio, Inc., New York, New York[3]

Sociedad Anónima Radio Argentina, Buenos Aires, Argen ina[4]

[1] Cable service. [2] International and marine radiotelegraph services.
[3] Cable and radiotel graph services. [4] Radiotelegraph service.

Laboratories

Federal Telecommunication Laboratories, Inc., Nutley, New Jersey

Standard Telecommunication Laboratories, Limited, London, England

Laboratoire Central de Télécommunications, Paris, France